From: richardsevers@lowerchurchillproject.ca
To: Nikolay Argirov
Cc: pharrington@lowerchurchillproject.ca; Steve Pellerin; Frank Gillespie; Scott O"Brien
Subject: Re: Items for further observation, identified by the IE
Date: Tuesday, April 7, 2015 8:27:35 AM
Attachments: _.png
_.png
_.png
MFA-AH-SD-3410-ME-H12-0001-01.pdf
MFA-AH-SD-3410-ME-H27-0001-01_C1 ..Stay Ring Calculation and Fatique Analysis Reports.pdf
Response to IE Questions.docx

MFA-AH-SD-3410-ME-H12-0001-01.pdf

MFA-AH-SD-3410-ME-H27-0001-01_C1 ..Stay Ring Calculation and Fatique Analysis Reports.pdf

Response to IE Questions.docx

Hello Nik,

Attached are the responses to your questions along with the calculation reports for the stay ring (Von Karman) and discharge ring.

Let me know if you need anything else.

Regards,

Richard Severs P.Eng.
Package Lead – Turbines and Generators
PROJECT DELIVERY TEAM
Lower Churchill Project
t. **709 733-5218**
e. **RichardSevers@lowerchurchillproject.ca**
w. **muskratfalls.nalcorenergy.com**

Nikolay Argirov ---03/23/2015 03:15:01 AM---Richard, As per our final discussion at the Tian Bao factory this is a summary of items that the IE

From: Nikolay Argirov <Nikolay.V.Argirov@mwhglobal.com>

To: "RichardSevers@lowerchurchillproject.ca" <RichardSevers@lowerchurchillproject.ca>,

Cc: "Joanne.raddatz@andritz-hydro.com" <Joanne.raddatz@andritz-hydro.com>,
"PHarrington@lowerchurchillproject.ca" <PHarrington@lowerchurchillproject.ca>

Date: 03/23/2015 03:15 AM

Subject: Items for further observation, identified by the IE

Richard,

As per our final discussion at the Tian Bao factory this is a summary of items that the IE identified to be further addressed, monitored and/or discussed:

1. Cleaning of Ferritic contamination of stainless steel surfaces. It is normal practice when using or working with stainless steel/ martensitic

components care should be taken to avoid contamination with Ferritic materials as this can cause corrosion pitting later on during operation.

A water test (using copper sulfate solution) is normally recommended to establish any possibility of contamination. Any such

Contamination should be removed either by grinding/polishing with uncontaminated stone or sand belts. Ideally if there is severe contamination,

stainless steel should be cleaned by passivating gels. These gels should not be used on the martensitic 410 Grades. It is recommended these to be

cleaned with citric acid fluids.

2. Runner blades to hub gaps. It was observed that some of the runner blades are rubbing tight against the hub surface (scratched marks on the paint).

The IE recognizes that this is not the final assembly however it is important to point out that the proper gap dimensions should be achieved and gaps should measure within the allowable design tolerances. Those should be verified at FAT.

3. Runner blades to discharge ring gaps. Verification of the gap between the runner blades and the discharge ring surface should be considered in light of blades deflection due to operating pressures on the blades and the resulting potential bridging of the gap in closed or open position of the blades.

4. IE requested a design report on Von Karman vortices at stave vain locations, indicating the natural frequencies of the veins and the effect of these vortices on the veins. The concern is related to possible resonance oscillation of the veins induced by vortex frequencies closed to the natural frequencies of the stay veins. Apparently such a report exist and Andritz is to make it (if not already) available to NALCOR.

5. IE requested also a verification of the discharge ring operational fatigue stresses and potential fracture issues particularly at the junction of the vertical ribs at top and bottom flanges of the ring.

6. IE inquired if the unit will be able to start in case there is no oil film between the trust bearing contact surface, e.g. high pressure oil pumps malfunctioning concurrently with no compressed air availability for activation of generator brakes.

I discussed the first five items with several people from Andritz team, nevertheless I copied Joanne here so she will be aware of this summary too.

Careful attention should be given to the aforementioned items as to avoid potential commissioning

complications and to insure long term normal operations of the unit(s). In no way however should this summary be construed as criticism to the recently observed and commendable Andritz's performance, quality of work and teams cooperation.

Regards,

Nik

MWH Canada, Inc

Nik Argirov, M.Eng., P.Eng., PMP

VP, Regional Manager, BC

Dams and Hydro Canadian Practice Leader

tel. 604 648 6162

cell. 604 340 7968

fax 604 648 6181

740-1185 W. Georgia Street

Vancouver, BC, V6E 4E6

[attachment "image001.png" deleted by Richard Severs/NLHydro]

Document Front Sheet

SNC·LAVALIN

nalcor energy
LOWER CHURCHILL PROJECT

NE-LCP Contractor/Supplier

Contract or Purchase Number and Description:	Contractor/Supplier Name:
CH0030	Andritz Hydro Canada Inc.

Document Title:	Total Number of Pages Incl. Front Sheet
Discharge Ring Calculation and Fatigue Analysis	66
Contractor/ Supplier Document Number: CAL0200500050	Revision Number: 01
EPC(M) Document Number: Not Applicable	Issue Number: Not Applicable

NE-LCP Document Number:	NE-LCP Issue Number:
MFA-AH-SD-3410-ME-H12-0001-01	C1

Approver's Signature:	Date (dd-mmm-yyyy):	Review Class:
MG Balazs	20-Aug-2013	
Comments:		Equipment Tag or Model Number:

NE-LCP or EPC(M)

REVIEW DOES NOT CONSTITUTE APPROVAL OF DESIGN DETAILS, CALCULATIONS, TEST METHODS OR MATERIAL DEVELOPED AND/OR SELECTED BY THE CONTRACTOR, NOR DOES IT RELIEVE THE CONTRACTOR FROM FULL COMPLIANCE WITH CONTRACTUAL OR OTHER OBLIGATIONS.

- ☑ 01 – REVIEWED AND ACCEPTED – NO COMMENTS
- ☐ 02 – REVIEWED – INCORPORATE COMMENTS, REVISE AND RESUBMIT
- ☐ 03 – REVIEWED - NOT ACCEPTED
- ☐ 04 – INFORMATION ONLY
- ☐ 05 – NOT REVIEWED

Lead Reviewer:	Date (dd-mmm-yyyy):	Project Manager:	Date (dd-mmm-yyyy):
CA	3 Sep 2013		
NE-LCP or EPC(M) Management:	Date (dd-mmm-yyyy):		

General Comments:

MD

PROVINCE OF NEWFOUNDLAND AND LABRADOR
PEGNL Newfoundland and Labrador
PERMIT HOLDER
This Permit Allows
ANDRITZ HYDRO LTD
To practice Professional Engineering in Newfoundland and Labrador.
Permit No. as issued by PEGNL No 602
which is valid for the year 2013

C1	01	According to comments on 13-Nov-2012	20-Aug-2013	HA	
A1	00	Initial release	30-Oct-2012	HA	
Nalcor Doc. Rev.	Andritz Doc. Rev.	Modification	Date	Prepared / Préparé	Appr.

Title / Titre

DISCHARGE RING CALCULATION AND FATIGUE ANALYSIS

HCM	Date	Name / Nom
Prepared by:	30-Oct-2012	Huijun Li
Approved by:	30-Oct-2012	André Coutu, Eng., M. Eng., MBA

Contract / Contrat No.: 0200-183001 to 0200-183004

Part Bill / Nomenclature No.: 050

Andritz Doc. No.	Rev.	Sheet / Feuille	1
CAL0200500050	01	of / de	65

ANDRITZ Hydro

Professional Engineer's Stamp

REGISTERED PROFESSIONAL ENGINEER
PEGNL Newfoundland and Labrador
ANDRÉ COUTU
SIGNATURE
30/08/2013
DATE
NEWFOUNDLAND & LABRADOR

Client

nalcor energy
LOWER CHURCHILL PROJECT

Project

LOWER CHURCHILL PROJECT

MUSKRAT FALLS HYDROELECTRIC DEVELOPMENT

SNC·LAVALIN

NE Doc. No.	Rev.
MFA-AH-SD-3410-ME-H12-0001-01	C1

TABLE OF CONTENT

APPENDICES

TABLES LIST

FIGURES LIST

1. INTRODUCTION

This report presents the results of a finite element analysis performed on the discharge ring for the Muskrat Falls Project. The stress results are used for a fatigue analysis. The blade passing pressure loads are applied. The bottom ring and draft tube liner upper flange are added for more accurate boundary conditions.

2. DISCHARGE RING

2.1 GEOMETRY

The dimensions and the geometry of the discharge ring, bottom ring and draft tube liner are those indicated on the drawings listed in Table 1.

Table 1 – Drawing

Title	drawings
Bottom ring - machining	226045609
Discharge ring - machining	226045605
Draft tube liner	226045604

2.2 MATERIAL

The material of the water passing face barrel is ASTM A240M UNS S30403. The material of flanges and ribs is ASTM A 516M grade 485. The metal of weld is E49xx in accordance with CSA W59 -03 for carbon steel. The filler metal of E-309L is used for stainless steel plate UNS S30403. The mechanical properties are listed in Table 2.

Table 2 – Material Properties

Material	components	Yield Strength Sy [MPa]	Tensile Strength Su [MPa]
ASTM A516M Grade 485	**Flange and ribs**	**260**	**485**
ASTM A 240M UNS S30403	**Discharge ring barrel plate**	**170**	**485**
ASTM A 240M UNS S30400	**Draft tube liner upper barrel plate**	**205**	**515**
E49xx	**Metal of weld for carbon steel**	**400**	**490**
E309L	**Metal of weld for stainless steel**	**410**	**555**

2.3 ALLOWABLE STRESS

2.3.1 ALLOWABLE STRESS FOR PLATE AND RIB

As specified by the contract clause 1.2.6, the primary stresses for stainless steel plate must not exceed 20% of the minimum ultimate tensile strength or 33% of the yield strength. The limit for stress categories as defined by the ASME Code Section VIII Division 2 is evaluated with this contract general membrane limit. The allowable stresses are listed in Table 3.

Table 3 – Allowable stress for plate and rib

Material	Primary membrane stress	Primary bending stress	secondary bending stress
ASTM A516M Grade 485 on normal operating condition	S_m = min [2/3 Sy; 1/3.5 Su] = **139MPa**	1.5* S_m =1.5 x138= **208MPa**	3* S_m =3 x138= **416MPa**
ASTM A516M Grade 485 on extreme condition	S_m = 2/3 Sy = **174 MPa**	1.5* S_m =1.5 x174= **260 MPa**	3* S_m =3 x174= **520 MPa**
ASTM A 240M UNS S30403 on normal operating condition	S_m= min [0.33 Sy; 0.20 Su] = **56MPa**	1.5* S_m =56x1.5= **84MPa**	3 *S_m =56x1.5= **168MPa**
ASTM A 240M UNS S30403 on extreme condition	S_m = 2/3 Sy = **113 MPa**	1.5* S_m =1.5 x113= **170 MPa**	3* S_m =3 x113= **340 MPa**
ASTM A 240M UNS S30400 on normal operating condition	S_m= min [0.33 Sy; 0.20 Su] = **68MPa**	1.5* S_m =56x1.5= **101MPa**	3 *S_m =56x1.5= **203MPa**
ASTM A 240M UNS S30400 on extreme condition	S_m = 2/3 Sy = **137 MPa**	1.5* S_m =1.5 x113= **206 MPa**	3* S_m =3 x113= **412MPa**

2.3.2 ALLOWABLE STRESS FOR WELD

In this report the fillet weld analysis is done according to the welded steel construction standard – CSA W59-03.

Welding material will have as good or better mechanical properties than the base material. As specified in the CSA W59-03 for fillet welds, the shear limit is the lowest of 0.3xSu for

weld metal or 0.4xSy for base metal. The shear must be evaluated in the effective area of the weld using the combination of axial and transverse force on the weld.

Table 4 – Allowable stress for fillet weld

Material	Shear stress
ASTM A516M Grade 485	S = min [0.4 Sy; 0.3 Su] = **104MPa**
ASTM A 240M UNS S30403	S= min [0.4 Sy; 0.3 Su] = **68MPa**
ASTM A 240M UNS S30400	S= min [0.4 Sy; 0.3 Su] = **82MPa**

3. FINITE ELEMENT ANALYSIS

3.1 MODEL

To cover one blade, the discharge ring is modeled as a 72 degree segment together with the corresponding bottom ring and draft daft tube liner upper flange segments. The thickness in the model for the stainless barrel plate is 42 mm. The 16mm fillet weld is used for static stress of the rib weld. Five ribs have been modeled, the center one with finer mesh being used for evaluation. Cyclic symmetry is assumed on the 72 degree segment. Stress results will be significant at the center rib.

The elements used are solid parabolic tetrahedrons elements (CTETRA10). The FE model contains 71015 elements and 144874 nodes. The 16mm fillet welds are not modeled at the junction of the ribs with the barrel and flange but the mesh is refined with 8mm elements (two elements on the 16mm fillet leg). The model and mesh are shown in Appendix A.

The software used for the finite element analysis is NX6 from Siemens Product Lifecycle management Software Inc. The solver is NX Nastran 6.1.

3.2 PRESSURE LOADS

Design static pressures through the flow channel of the turbine are calculated using Andritz Hydro's proprietary empirical rules developed and validated by pressure measurements on similar machines. Flow channel is discretized in six regions, as shown in Figure 1. Head losses are neglected within regions and water level is only considered for pressures at standstill. Muskrat Falls design static pressures for stationary components are given in Table 5 at different operation regimes.

From measurements on existing runners, it was observed that static pressures at runaway and full power are similar and are therefore considered the same. During a load rejection event, the generator loses the grid, the turbine goes in over-speed, the pressure in the casing rises, the overpressure occurs in the casing: the wicket gates are closed or in the process of closing and suction occurs behind the wicket gates to bring the pressure close to atmospheric pressure under the head cover.

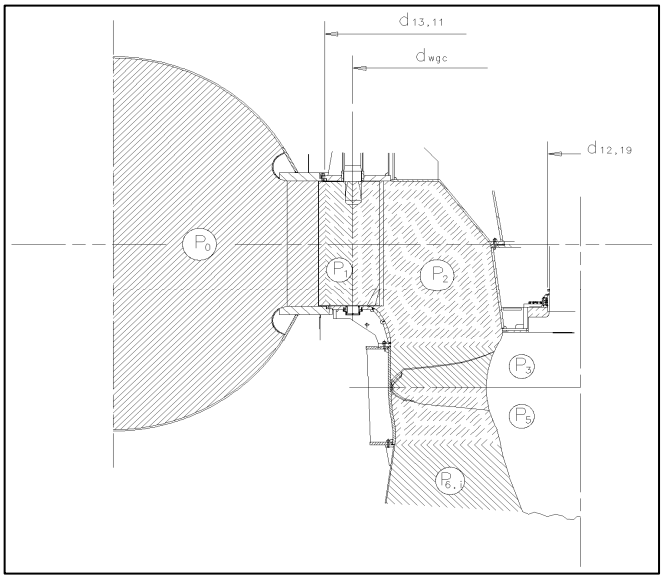

Figure 1 – Pressure applied regions

Table 5 – Design static pressures for stationary components

Operation regime	Pressure in spiral case (P_0)	Pressure upstream of guide vanes (P_1)	Pressure downstream of guide vanes (P_2)	Discharge ring pressure upstream blade axis (P_3)	Discharge ring pressure downstream blade axis (P_5)
	kPa	kPa	kPa	kPa	kPa
Standstill	439	439	117	Hydrostatic variation	Hydrostatic variation
Load rejection	504	504	0	0	0
Full power	439	439	374	374	374
Runaway	439	439	374	374	374
PMF levels Standstill	499	499	177	Hydrostatic variation	Hydrostatic variation

3.3 LOAD CASES

The load components in the models are the pressures and reaction force from guide vanes at bottom ring. The constant pressures for the static stress analysis are listed in Table 6.

Table 6 – Discharge Ring Loads

Load cases	P1 (MPa)	P2 (MPa)	P3 (MPa)	P5 (MPa)	Radial force for one GV [kN]*	Vertical force for one GV [kN]***	Gravity
Standstill	0.439	0.117	Hydro static	Hydro static	-833*	-37.5	g
Load rejection	0.504	0	0	0	-1140	-37.5	g
Full power or runaway	0.439	0.374	0.374	0.374	0	-37.5	g
Seismic on full power	0.439	0.374	0.374	0.374	0	-37.5	1.091g
PMF levels standstill	0.499	0.177	Hydro static	Hydro static	-833*	-37.5	g

*Radial forces in minus sign indicate the direction is toward the center of the machine.
** The radial loads calculation for the wicket gate is presented in Appendix B
***Vertical forces in minus sign indicate the direction is downward.

In the case of a seismic event, the acceleration can be either horizontal or vertical. For horizontal acceleration, stresses introduced into the discharge ring would be negligible as the discharge ring with bottom ring are fixed in all directions at the draft tube cone and stay ring flange. The analysis for seismic load is only done for the case of full power which is the most severe normal operation condition. The maximum vertical acceleration of 1.091g is added.
The operating condition used to calculate the blade passing variable pressures with CFD is summarized in Table 7.

Table 7 – Turbine data

Number of blades	5
Rotating speed	85.714 RPM
Max Head	37.49 m
Max Power	220 MW
Max Tail water level	6.27m

The variable pressure from CFD at the full power condition, as shown in Table 6, is used for the blade passing loads. The pressure field for a single blade is repeated to cover the entire shell inner surface and then rotated 12 times by 6 degree increment to simulate a blade passing cycle. The pressure distribution is presented in Figure 2.

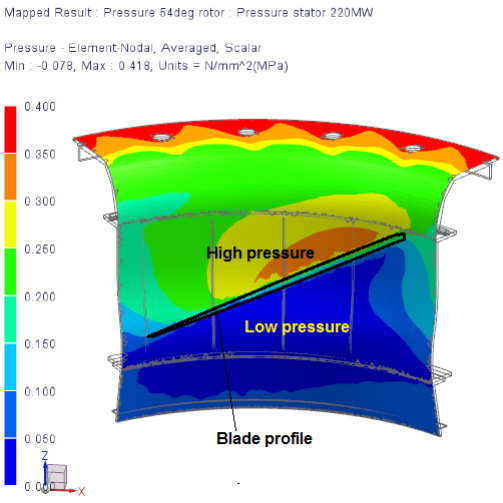

Figure 2 – Variable CFD Pressure

3.4 BOUNDARY CONDITIONS

The nodes on the external side surface of the 72° segment are coupled to simulate the cyclic symmetry condition. One vertex is fixed in the tangential direction (θ direction) to eliminate spinning of the structure (rigid body motion).

Displacements are set to zero in the axial direction (z direction) and in the radial direction at the bolt circle of the bottom ring with the stay ring.

Displacements are set to zero in the all directions at the bottom face of the draft tube liner upper stainless steel section.

The nodes at the interface between the bottom ring and the discharge ring are coupled in the bolt circle and center line of barrel. The lower flange of discharge ring and draft tube cone upper flange are coupled as a same way.

The boundary conditions are represented in Appendix A.

3.5 CALCULATION RESULTS

3.5.1 STRESSES AT PLATE AND RIBS

The stresses at discharge ring and draft tube liner upper cone are checked. The primary membrane stresses are presented in Table 8. The peak or secondary bending von Mises stresses are listed in Table 9 and Table 10. The stress locations are shown in Figure 3.

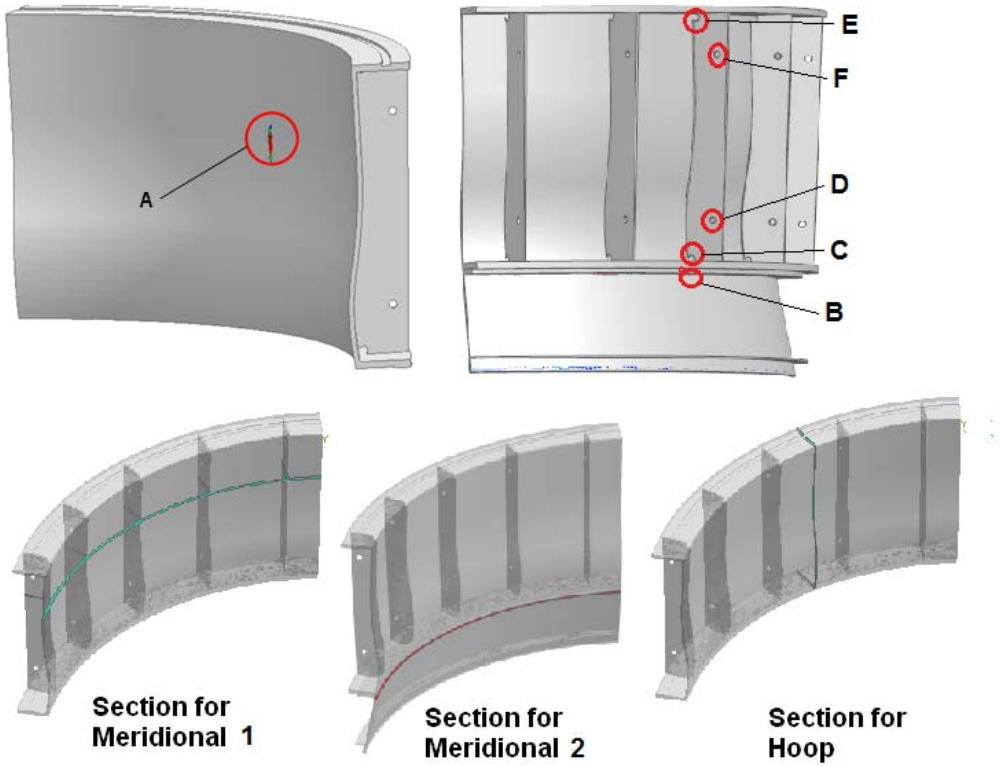

Figure 3 – Stress locations

Table 8 – Primary membrane stresses with constant pressure

Load cases	description	Membrane stresses[MPa]		
		Meridional 1	**Meridional 2**	**Hoop**
1	Standstill	-3.7	-9.4	10.3
2	Load rejection	-1.2	-2.6	-0.7
3	Full power or runaway	-8.7	-21.6	27.0
4	Seismic on Full power	-8.8	-21.7	27.1
5	PMF standstill	-3.7	-9.4	10.3

Table 9 – Peak or secondary stresses with constant pressure

Load cases	description	Primary bending von Mises stress [MPa]		Peak or secondary bending von Mises stress [MPa]			
		A. inside stainless plate at rib center of discharge ring	**B**. outside of stainless plate at weld toe of draft tube upper cone	**C**. lower mouse hole of discharge ring	**D**. lower lifting hole of discharge ring	**E**.upper mouse hole of discharge ring	**F**.upper lifting hole of discharge ring
1	Standstill	33	(33)	(18)*	(6)	(33)	10
2	Load rejection	4	(6)	(6)	(2)	(8)	2
3	Full power or runaway	80	(74)	(44)	(16)	(77)	15
4	Seismic on Full power	80	(75)	(45)	(16)	(77)	25
5	PMF standstill	45	(43)	(25)	(9)	(44)	14

*Stresses in parenthesis are in compression.

Table 10 – Peak or secondary stresses with variable CFD pressure for blade passing

Location of blade	Degree of blade passing [degree]	Primary bending von Mises stress [MPa]		Peak or secondary bending von Mises stress [MPa]			
		A. inside stainless plate at rib center of discharge ring	**B**. outside of stainless plate at weld toe of draft tube upper cone	**C**. lower mouse hole of discharge ring	**D**. lower lifting hole of discharge ring	**E**. upper mouse hole of discharge ring	**F**. upper lifting hole of discharge ring
1	0	55	(36)	(30)	13	(50)	33
2	6	52	(36)	(28)	15	(52)	27
3	12	47	(36)	(27)	(12)	(52)	19
4	18	42	(38)	(30)	(13)	(47)	13
5	24	35	(37)	(33)	(21)	(39)	(12)
6	30	31	(37)	(38)	(33)	(33)	(10)
7	36	33	(37)	(42)	(42)	(32)	7
8	42	44	(36)	(44)	(45)	(30)	20
9	48	54	(36)	(43)	(44)	(34)	34
10	54	58	(36)	(41)	(37)	(38)	41
11	60	60	(36)	(36)	(27)	(42)	41
12	66	58	(36)	(32)	(17)	(47)	38

*Stresses in parenthesis are in compression.

3.5.2 STRESSES AT FILLET WELDS

The analysed weld locations are presented in Figure 4. Welds 1, 2 and 3 have a 16 mm leg and are fillet welds.

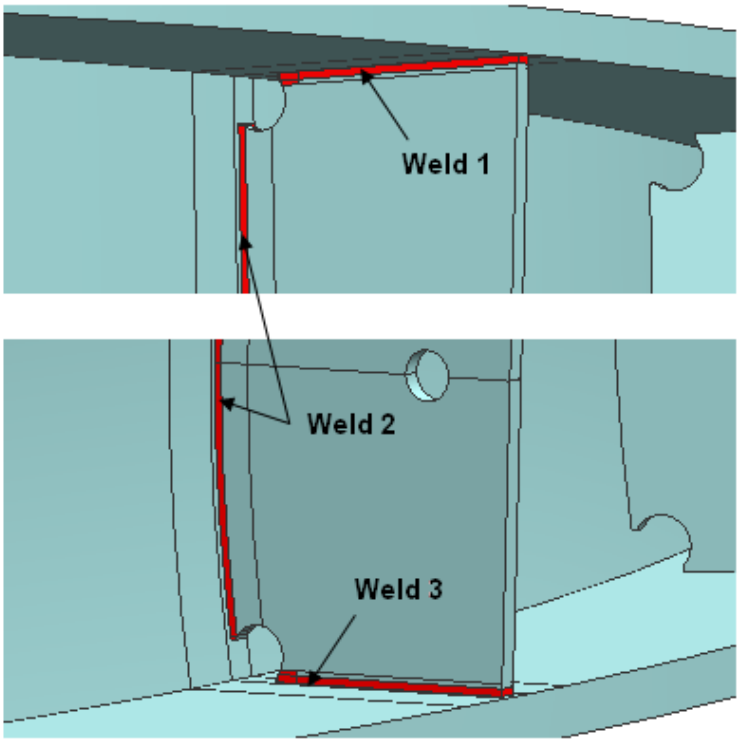

Figure 4 – Identification of the analysed fillet welds

Table 11 presents a summary of the maximum stress with conservatively constant pressure calculated in the welds. Even if the maximum values of the two components occur at different location, the total maximum shear is conservatively calculated by combining them. **Detailed weld stress calculation procedure is presented in Appendix C, showing how the finite element results are processed to obtain the fillet weld average stresses suiting the CSA W59-03**.

Table 11 – Stress results summary for welds with constant pressure

Load cases	Welds	Max shear [MPa] *(parallel to the weld)*	Max shear [MPa] *(normal to the weld)*	Total Max Shear [MPa] *(from normal and parallel loads combined)*
Standstill	1	-2.3	-14.6	14.6
	2	-11.8	-2.8	12.3
	3	-2.7	-10.3	10.5
Load rejection	1	0.7	-3.7	3.8
	2	-2.2	-1.1	2.3
	3	0.7	-2.9	3.0
Full power	1	-6.6	-33.9	33.9
	2	-29.2	-6.8	29.7
	3	-6.2	-24.4	24.8
Seismic on full power	1	-6.6	-34.1	34.1
	2	-29.3	-6.8	29.8
	3	-6.2	-24.5	24.9
PMF standstill	1	-3.3	-19.5	19.5
	2	-16.3	-3.8	16.6
	3	-3.6	-13.7	14.0

The weld 2 is considered as the base material ASTM A240M ss30403. The material ASTM A516M Gr485 is applied for weld 1 and weld3.

3.5.3 DISPLACEMENTS

The maximum radial displacements are presented in Table 12; the location is at runner center line between two ribs. Those values are obtained from constant pressure.

Table 12 – The maximum radial displacements

Load cases	Description	Radial displacements [mm]
1	Standstill	**0.477**
2	Load rejection	**0.032**
3	Full power or runaway	**1.178**
4	Seismic on full power	**1.180**
5	PMF standstill	**0.654**

3.5.4 REACTION FORCES

The total vertical reaction forces for 360 degree model at the coupling face in the stay ring and lower cone are listed in Table 13.

Table 13 – The total vertical reaction forces

Load cases	description	Total vertical reaction force at stay ring [kN]	Total vertical reaction force at lower cone [kN]
1	Standstill	8402*	6330
2	Load rejection	9509	2202
3	Full power or runaway	8056	14500
4	Seismic on full power	9389	8345
5	PMF standstill	8125	14602

* Positive means upward force on the bottom ring and bottom face of discharge ring.

3.6 STRESS ANALYSIS DISCUSSION

The stress results are analysed using two distinct methods. The plates and ribs are analysed following the ASME Boilers and Pressure Vessels Code Section VIII Division 2 stress classification method. The fillet welds are calculated following the CSA W59-03 standard.

The primary stresses in Table 8 and bending or secondary stresses in Table 9 and Table 10 are lower than their respective limit on Table 3.

All stresses found on the 16 mm welds in Table 11 are lower than the total shear stress limit on Table 4.

Comparing the stress results of full power with seismic load and without seismic load, the increase stress for seismic load is only 1MPa, and is therefore negligible..

4. FATIGUE ANALYSIS

4.1 METHOD

In performing fatigue analysis, the cumulative linear damage relationship (Miner's rule) is the usual method to establish fatigue resistance of components subject to various load cycles. In addition, we have also calculated a safety factor on stress for each load cycle. The peak stress specified for fatigue analysis is the von Mises stress, as specified in ASME Boiler and Vessel Code, Section VIII, Division 2, Part 5 (see Appendix E).

The fatigue analyses for fillet welds are performed in accordance with CSA W59-03. The specified fatigue resistance limit is used (see Appendix C).

4.2 LOAD CYCLES

With the addition of dewatered, the load conditions used for fatigue analysis are the same than the ones used for static analysis. The runaway condition is included in the full power condition. The stress range of seismic is only 1 MPa and is therefore, negligible for fatigue analysis. Table 14 gives a summary of these load conditions.

Table 14 – Load conditions for fatigue analysis

Load case	Operating Conditions	Explanation
A	dewatered	Machine dewatered
B	Standstill	Machine stopped
C	Load rejection	Transient condition
D	Full power (or runaway)	Most severe regular operating condition

Four load cycles have been identified and are presented in table 15.

Table 15 – Load cycles for fatigue analysis

Load Cycle	Load cases	Description	# cycles in 75 years	Contract clause
#1	B-D-B	Start / Stop	54750	2 times per day
#2	B-D-C-B	Load rejection	900	once per month
#3	A-B-D-C-A	Dewatered	75	once per year
#4	D	Blade passing	1.7e10	75*365*24*60*85.714x5 =1.7e10

4.2.1 ALTERNATING STRESS

Stress ranges are extracted from the stress tensor subtraction directly in NX6 from the FEA results to take account for possible stress reversal. The maximum stress ranges of plate and rib are listed in Table 16. The stress ranges at the toe of 16 mm fillet weld are shown in Table 17. We use the regular and exceptional condition giving the highest stress range from **shaded cells of Table 16** for plate and rib and **Table 17** for welds.

Table 16 – Maximum stress range at plate and rib

Load cycles	Von Mises stress [MPa]					
	A. inside stainless plate at rib center of discharge ring	**B**. outside of stainless plate at weld toe of draft tube upper cone	**C**. lower mouse hole of discharge ring	**D**. lower lifting hole of discharge ring	**E**. upper mouse hole of discharge ring	**F**. upper lifting hole of discharge ring
#1, max at full power - Standstill	**47**	**15**	**26**	**9**	**44**	**15**
#2, max at full power - Load rejection	**76**	**25**	**40**	**14**	**69**	**25**
#3, max at full power- dewatered	**80**	**25**	**44**	**16**	**77**	**25**
#4 Blade passing	**36**	**12**	**10**	**48**	**29**	**47**

Table 17 – Maximum stress range at toe of welds

Load cycles	Stress category	Principal stress [MPa]		
		1. Upper welds of rib to flange at bolts circle	**2**. vertical welds of rib to barrel	**3**. lower welds of rib to flange at bolt circle
#1, max at full power - Standstill	Shear	**4**	**16**	**7**
	Normal	**18**	**18**	**14**
#2, max at full power - Load rejection	Shear	**6**	**25**	**13**
	Normal	**29**	**28**	**21**
#3, max at full power- dewatered	Shear	**7**	**27**	**12**
	Normal	**32**	**31**	**25**
#4 Blade passing	Shear	**6**	**10**	**5**
	Normal	**23**	**17**	**17**

Table 18 – Stress amplitudes used for fatigue analysis of rib and plate

Load Cycle	locations	Stress Range (Mpa)	Stress amplitude (Mpa)	# Cycles in 75 years
#1	**A**. inside stainless plate at rib center of discharge ring	47	24	54750
#2	**A**. inside stainless plate at rib center of discharge ring	76	38	900
#3	**A**. inside stainless plate at rib center of discharge ring	80	40	75
#4	**D**. lower lifting hole of discharge ring	48	24	1.7e10

4.3 FATIGUE CURVES

The fatigue curve of ASME code 2010 is used for plate and ribs. The fatigue curve of CSA W59-03 is applied for analysis of fillet weld.

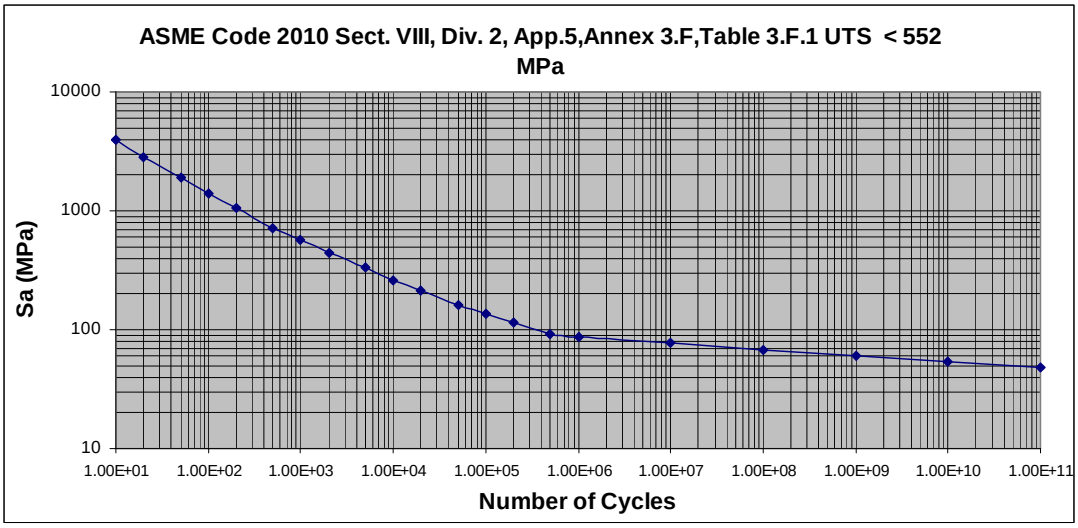

Figure 5 – Fatigue curve of ASME Code 2010

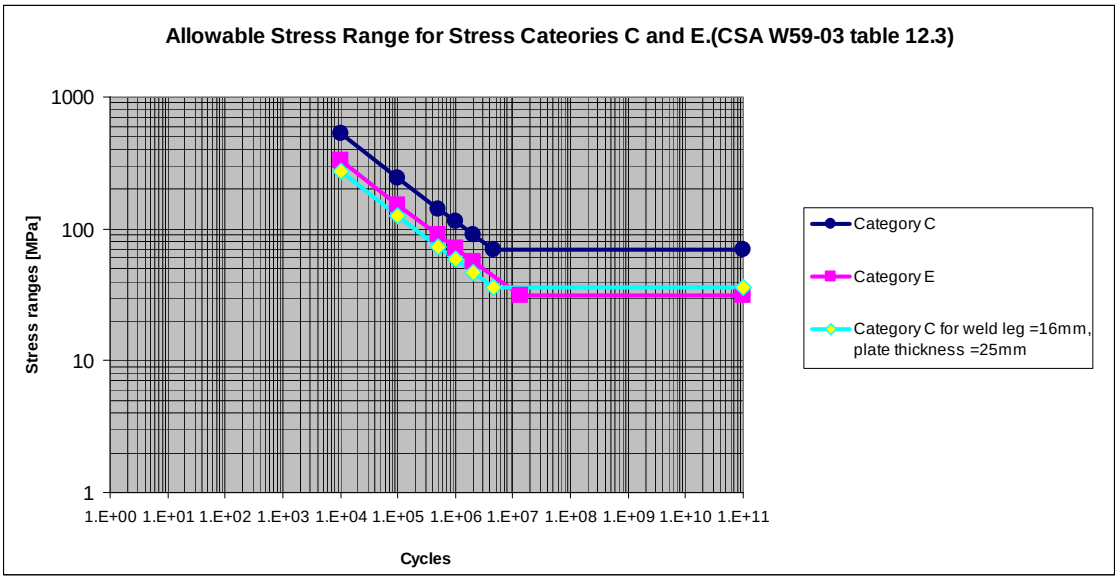

Figure 6 – Fatigue curves of CSA W59-03

4.4 ALLOWABLE ALTERNATING STRESS

4.4.1 ALLOWABLE ALTERNATING STRESS FOR PLATE AND RIB

Load Cycle #1, start /stop: 54750 cycles

Refer to the ASME Boiler and Pressure Vessel Code 2010, Section VIII, Division 2, Table 3.F.1 for Fatigue Curve110.1 (see Appendix E for copy). The allowable stress amplitude for 54750 cycles is 155 MPa. The allowable number of cycles is unlimited for Sa = 23 MPa. The effect of mean stress is already included.

Load Cycle #2, Load rejection: 900 cycles

Refer to the ASME Boiler and Pressure Vessel Code 2010, Section VIII, Division 2, table 3.F.1 for Fatigue Curve110.1 (see Appendix E for copy). The allowable stress amplitude for 900 cycles is 590 MPa. The allowable number of cycles is 8.4 e12 for Sa = 38 MPa. The effect of mean stress is already included.

Load Cycle #3, Dewatered: 75 cycles

Refer to the ASME Boiler and Pressure Vessel Code 2010, Section VIII, Division 2, Table 3.F.1 for Fatigue Curve110.1 (see Appendix E for copy). The allowable stress amplitude

for 60 cycles is 1590 MPa. The allowable number of cycles is 5.2e12 for Sa = 39 MPa. The effect of mean stress is already included.

Load Cycle #4, Blade passing: 1.7e10 cycles
Refer to the ASME Boiler and Pressure Vessel Code 2010, Section VIII, Division 2, Table 3.F.1 for Fatigue Curve110.1 (see Appendix E for copy). The allowable stress amplitude for 1.7e10 cycles is 53 MPa. The allowable number of cycles is infinity for Sa = 19 MPa. The effect of mean stress is already included.

4.4.2 ALLOWABLE ALTERNATING STRESS FOR FILLET WELD

Refer to the CSA W59-03 Code, Table 12.3 the stress range for fatigue life (see Appendix D, examples 16 and 19 for copy).
The normal stress used is category C and shear stress is category E. For Category C, the fatigue resistance of fillet welds transversely loads F_{sr} is a function of the effective throat and plate thickness. The fillet weld leg size is 16mm. The rib plate thickness is 25 mm. The follow equation is given by CSA W59-03 Table 12.4.

$$F_{sr}= F^{c}_{sr} ((0.06+0.79(H/t_p))/(0.64\ t_p^{1/6}))= F^{c}_{sr} ((0.06+0.79*(16/25))/(0.64\ *25^{1/6}))=0.517\ F^{c}_{sr}$$

F_{sr}= the fatigue resistance of fillet welds with transversely load.
F^{c}_{sr} = the fatigue resistance for Category C as determined in the CSA W59-03 Code, Table 12.3.
H = weld leg size (mm)
t_p = plate thickness (mm)

The adjusted fatigue curve Category C for 16mm weld leg and 25 mm plate thickness is used for welds fatigue analysis (see Figure 6).

The allowable stress range on fillet weld from CSA W59-03 Code is presented in Table19.

Table 19 – Allowable stress range for welds

Load cycles	# Cycles in 75 years	Stress types	Category	Allowable stress range Fsr [MPa]
Full power – Standstill	54750	Shear stress	E	187
		Normal stress	C for 16mm weld leg and 25 mm plate	153
Full power – Load	900	Shear stress	E	737
		Normal stress	C for 16mm weld leg and 25 mm plate	603
Full power-dewatered	75	Shear stress	E	1690
		Normal stress	C for 16 mm weld leg and 25mm plate	1380
Blade passing	1.7e10	Shear stress	E	31
		Normal stress	C for 16 mm weld leg and 25mm plate	36

4.5 FATIGUE FACTORS OF SAFETY

4.5.1 FATIGUE FACTORS OF SAFETY FOR PLATE AND RIB

Table 20 – Factors of safety on stress amplitude for plate and rib

Load cycle	Description	Location	Stress amplitude Sa(Mpa)	Allowable stress amplitude Sa(Mpa)	Safety factor
#1	Start / Stop	**A**. inside stainless plate at rib center of discharge ring	23	155	6.7
#2	Load rejection	**A**. inside stainless plate at rib center of discharge ring	38	590	15.5
#3	Dewatered	**A**. inside stainless plate at rib center of discharge ring	40	1590	39.8
#4	Blade passing	**D**. lower lifting hole of discharge ring	24	53	2.2

Note: The stress amplitudes in Table 20 are not all at the same location but rather are the highest for the load cycles given. Assuming that they are all at the same location results in a conservative calculation.

Table 21 – Cumulative damage of fatigue analysis for rib lower mouse hole

Load Cycle	Description	Number of cycles n_i	Allowable number of cycles N_i	Ratio n_i / N_i
#1	Start / Stop	54750	infinite	0
#2	Load rejection	900	8.4e12	1.1e-10
#3	Dewatered	75	5.2.e12	1.4e-11
#4	Blade passing	1.7e10	infinite	0
#1+#2+#3+#4	Accumulation			<1.0e-9

4.5.2 FATIGUE FACTORS OF SAFETY FOR WELDS

We use the highest stress range from the shaded cells of Table 16 for fillet welds.

Table 22 – Factors of safety on stress range for fillet welds

Load cycles	Description	Stress type	location	Stress range [Mpa]	Allowable stress range [Mpa]	Safety factor
#1	Start / Stop	Shear	Center of weld 2	16	187	11.7
		Normal	Bolt circle of weld 1	18	153	8.5
#2	Load rejection	Shear	Center of weld 2	25	737	29.5
		Normal	Bolt circle of weld1	29	603	20.8
#3	Dewatered	Shear	Center of weld 2	27	1690	62.6
		Normal	Bolt circle of weld1	32	1380	43.1
#4	Blade passing	Shear	Center of weld 2	10	31	3.1
		Normal	Bolt circle of weld1	23	36	1.6

Table 23 – Cumulative damage of fatigue analysis for fillet welds

Load cycles	Description	Stress type	Number of cycles n_i	Allowable number of cycles N_i	Ratio n_i / N_i
#1	Start / Stop	Shear	54750	infinity	0
		Normal	54750	infinity	0
#2	Load rejection	Shear	900	infinity	0
		Normal	900	infinity	0
#3	Dewatered	Shear	75	infinity	0
		Normal	75	infinity	0
#4	Blade passing	Shear	1.7e10	infinity	0
		Normal	1.7e10	infinity	0
#1+#2+#3+#4	Accumulation				0

4.6 FATIGUE ANALYSIS DISCUSSION

The safety factors and the cumulative damage exceed the requirements for reliable operation over a period of 75 years. Those calculated factors of safety indicate a robust design, tolerant even to minor non-conformances.

5. MODAL ANALYSIS

5.1 THE MODEL AND BOUNDARY CONDITIONS

The model for modal analysis covers the whole discharge ring; the boundary conditions are the same as the static analysis.

5.2 THE NATURAL FREQUENCIES OF DISCHARGE RING

The natural frequencies of the first four modes are list in Table 24. The mode shape is presented in Appendix D.

Table 24 – Natural frequencies of discharge ring

Modes	Frequencies in air [Hz]
Mode1	82.70
Mode2	85.52
Mode3	96.67
Mode4	99.79

5.3 MODAL ANALYSIS DISCUSSION

The exciting source is the blade passing frequency F=5x85.714/60=7.1Hz. Even considering conservative water added mass effect with 50% deduction factor on the natural frequency in water, the natural frequencies are still far away from the exciting frequency.

6. CONCLUSION

A static analysis has been performed on the Muskrat Falls Discharge Ring. The level of nominal and secondary bending stress are less than the allowable and less than the stress found in many other discharge rings which have given trouble free service for many years.

Fatigue analysis indicates that the plate, rib and welds have low damage.

The modal analysis indicates no resonance on the Discharge Ring.

All requirements for the Discharge Ring according to the contract and to the internal guidelines of Andritz Hydro are fulfilled.

APPENDIX A : The model

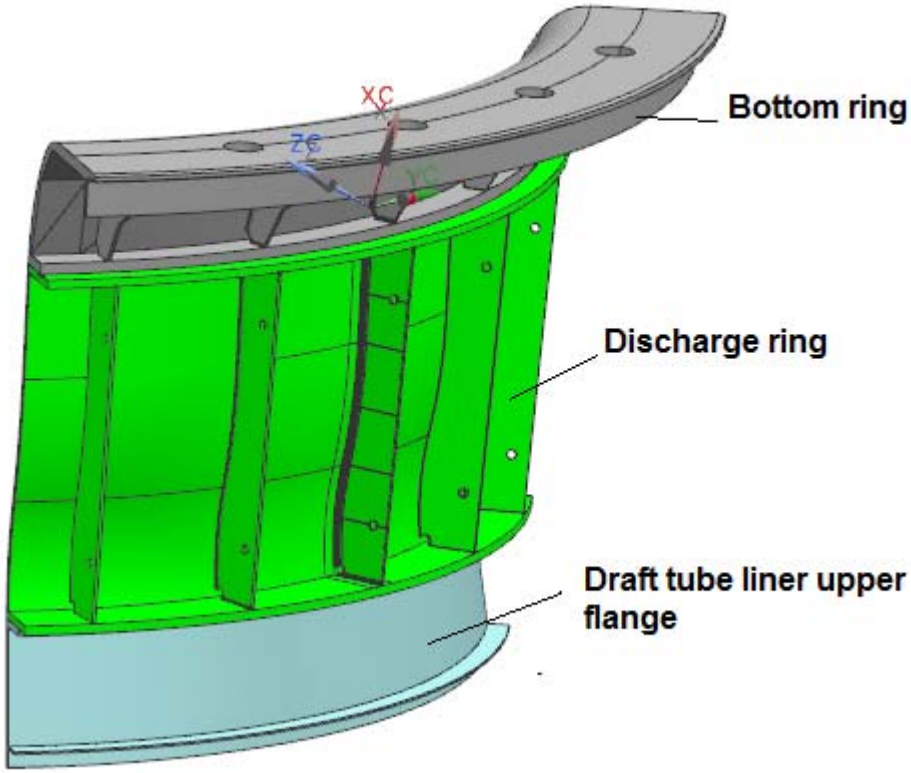

The model

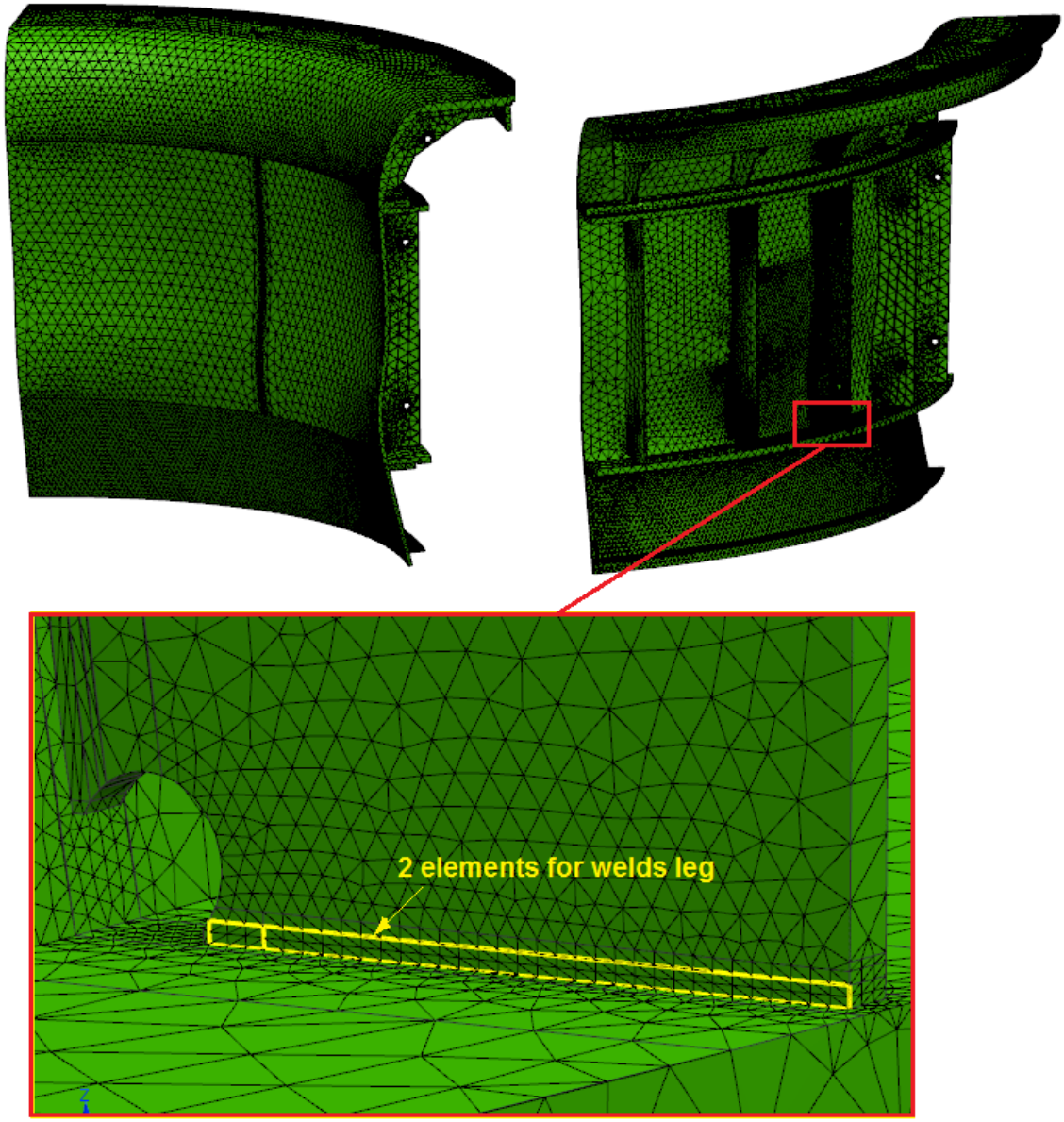

The mesh

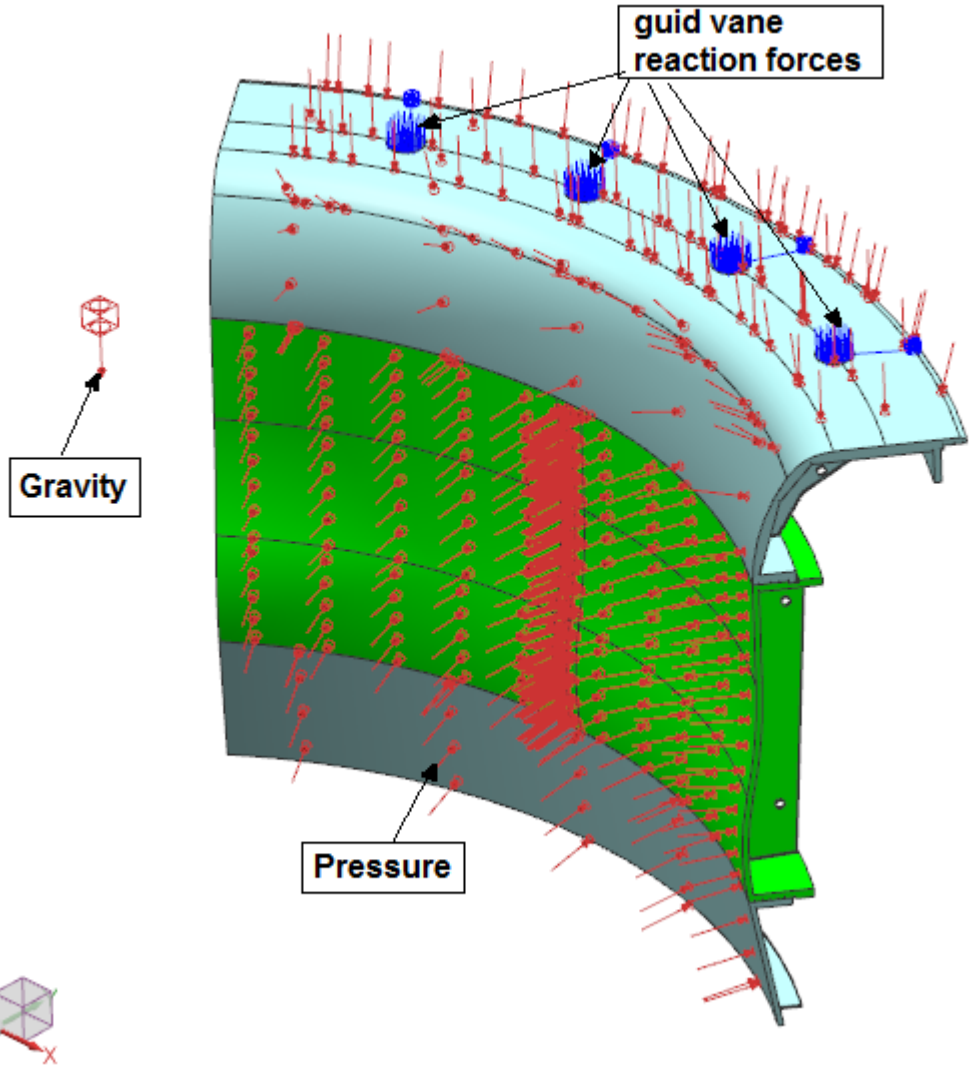

The loads

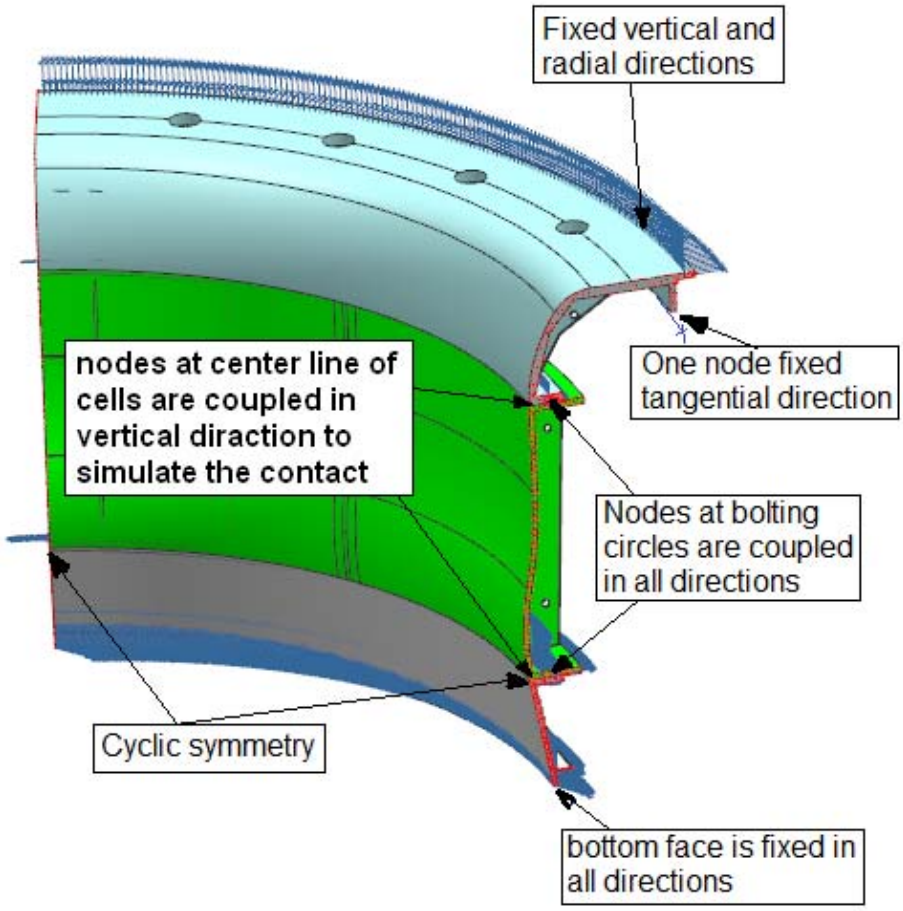

Boundary conditions

APPENDIX B : The stress results

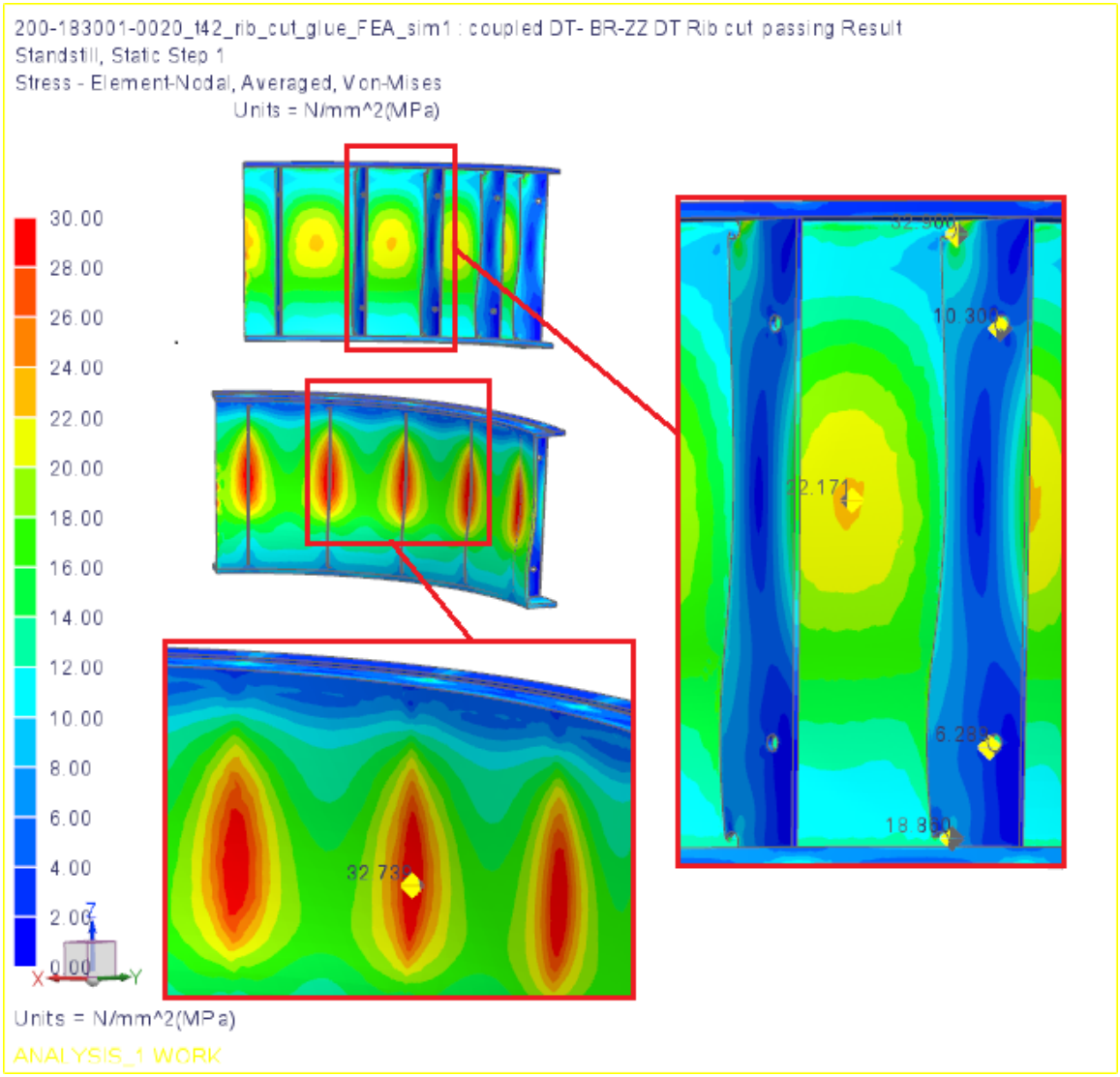

Von Mises stress [Mpa] at the standstill condition

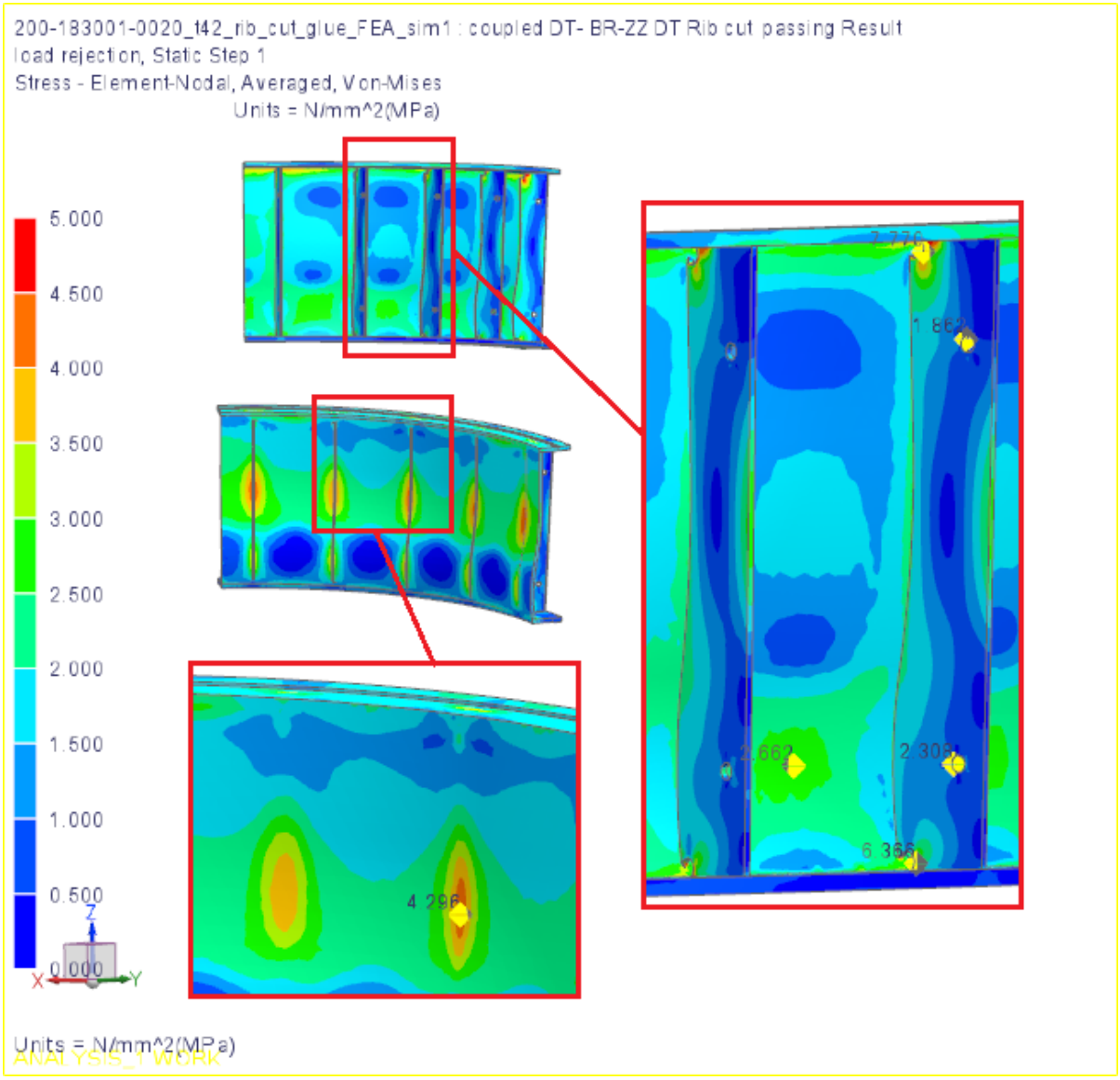

Von Mises stress [Mpa] at the load rejection condition

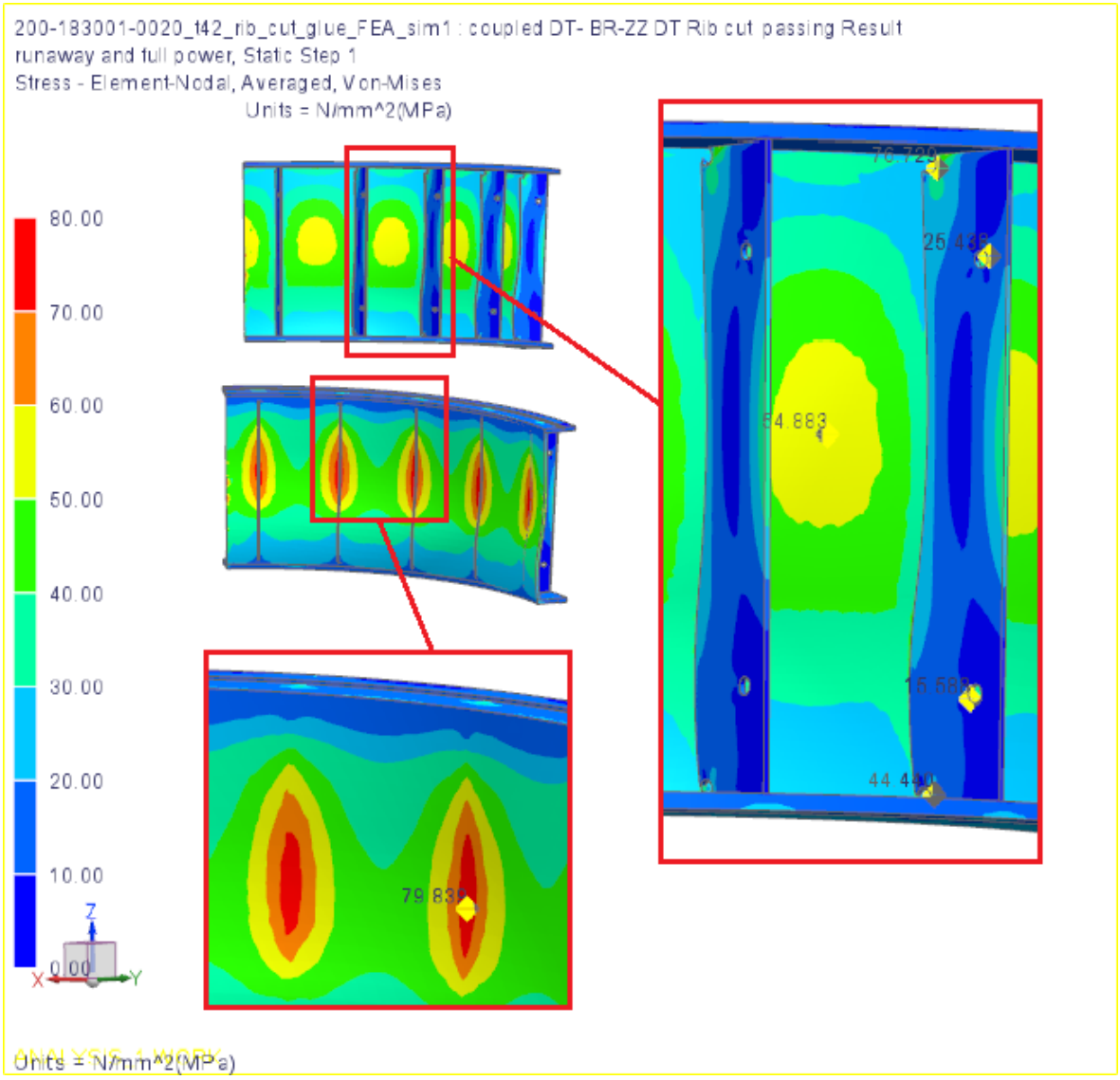

Von Mises stress [Mpa] at the full power condition

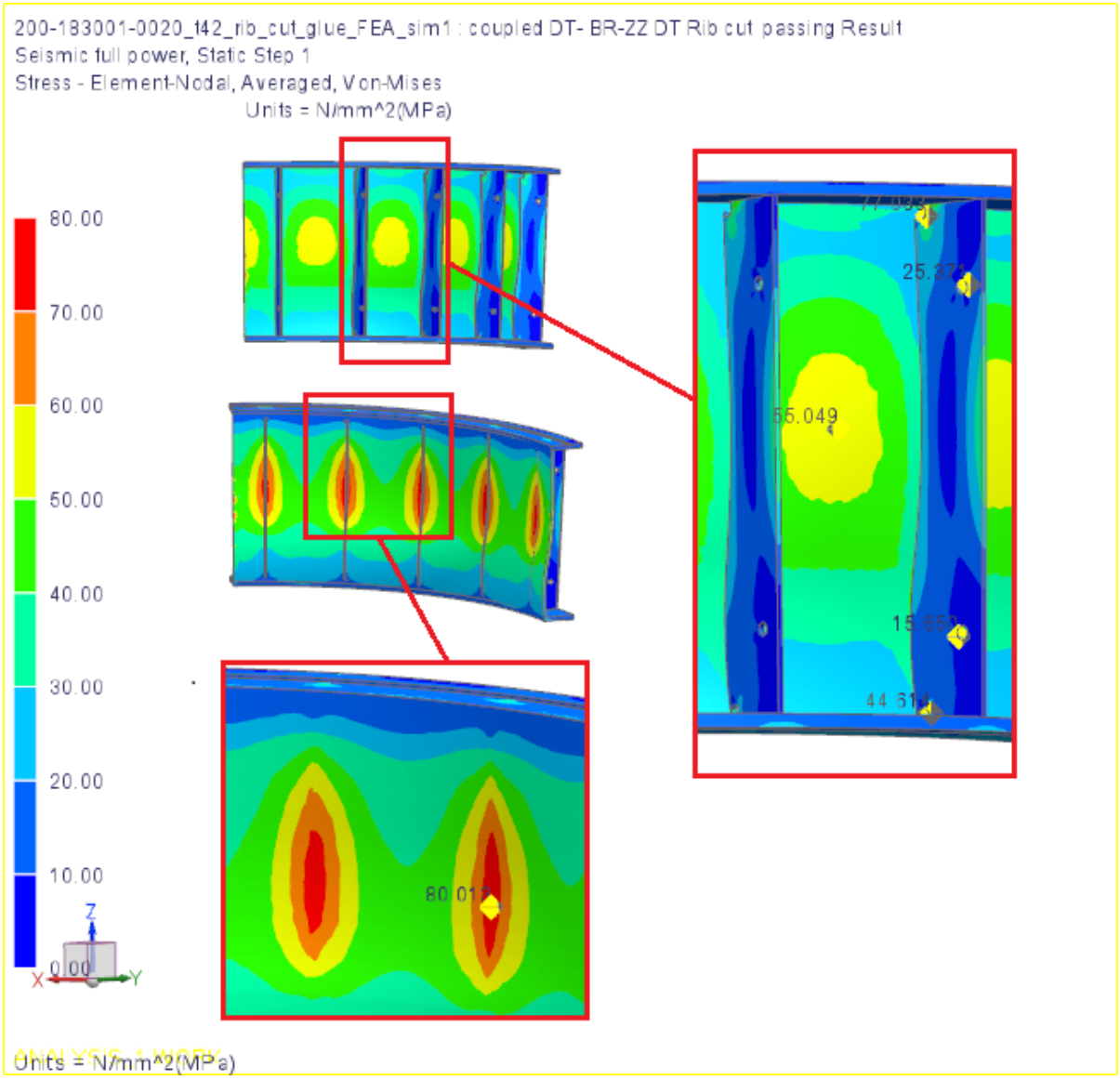

Von Mises stress [Mpa] at the seismic on full power condition

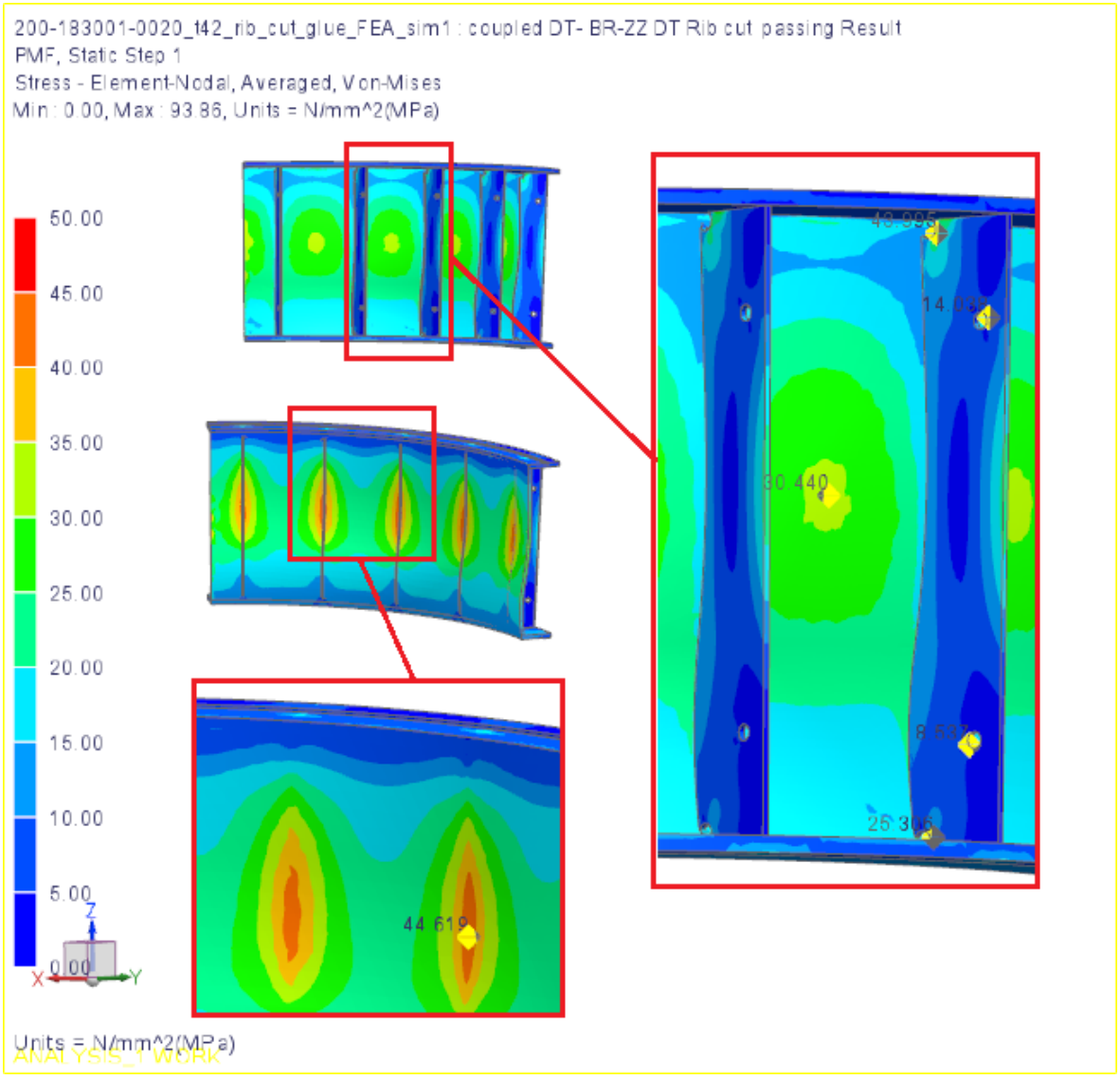

Von Mises stress [Mpa] at the PMF standstill condition

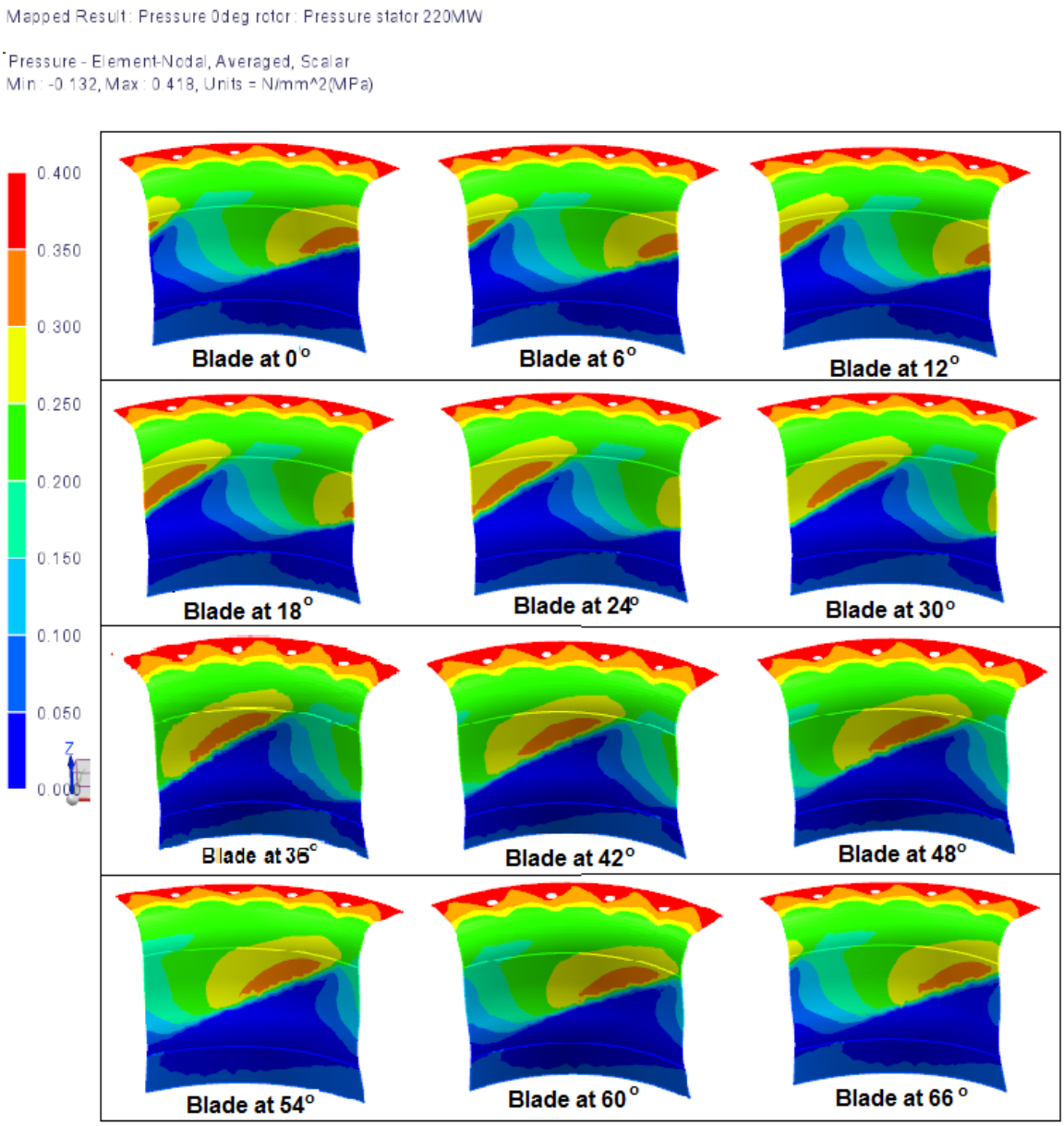

CFD pressures [Mpa] when blade passing in different angles on full power condition

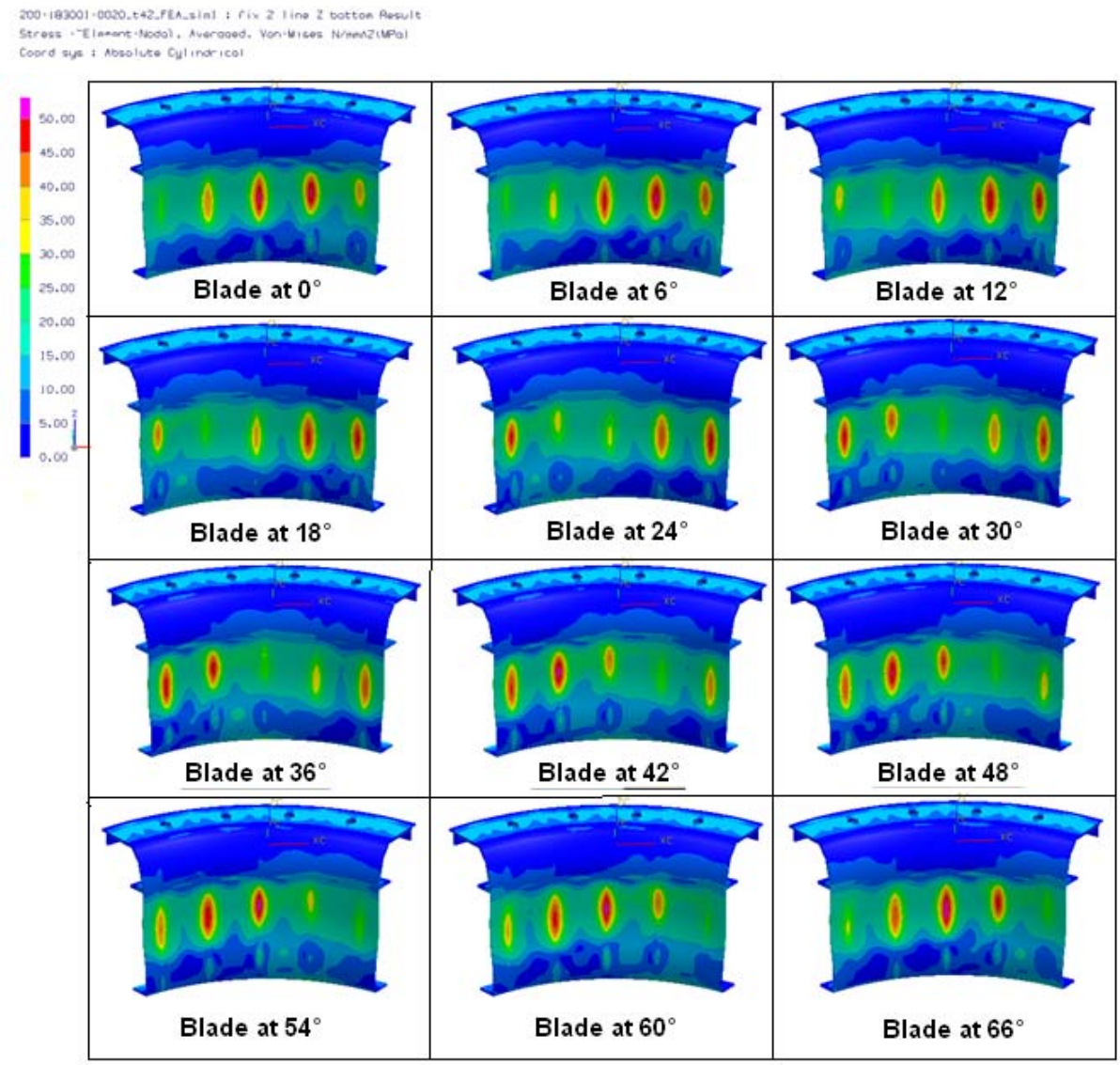

Von Mises stress [Mpa] when blade passing in different angles on full power condition

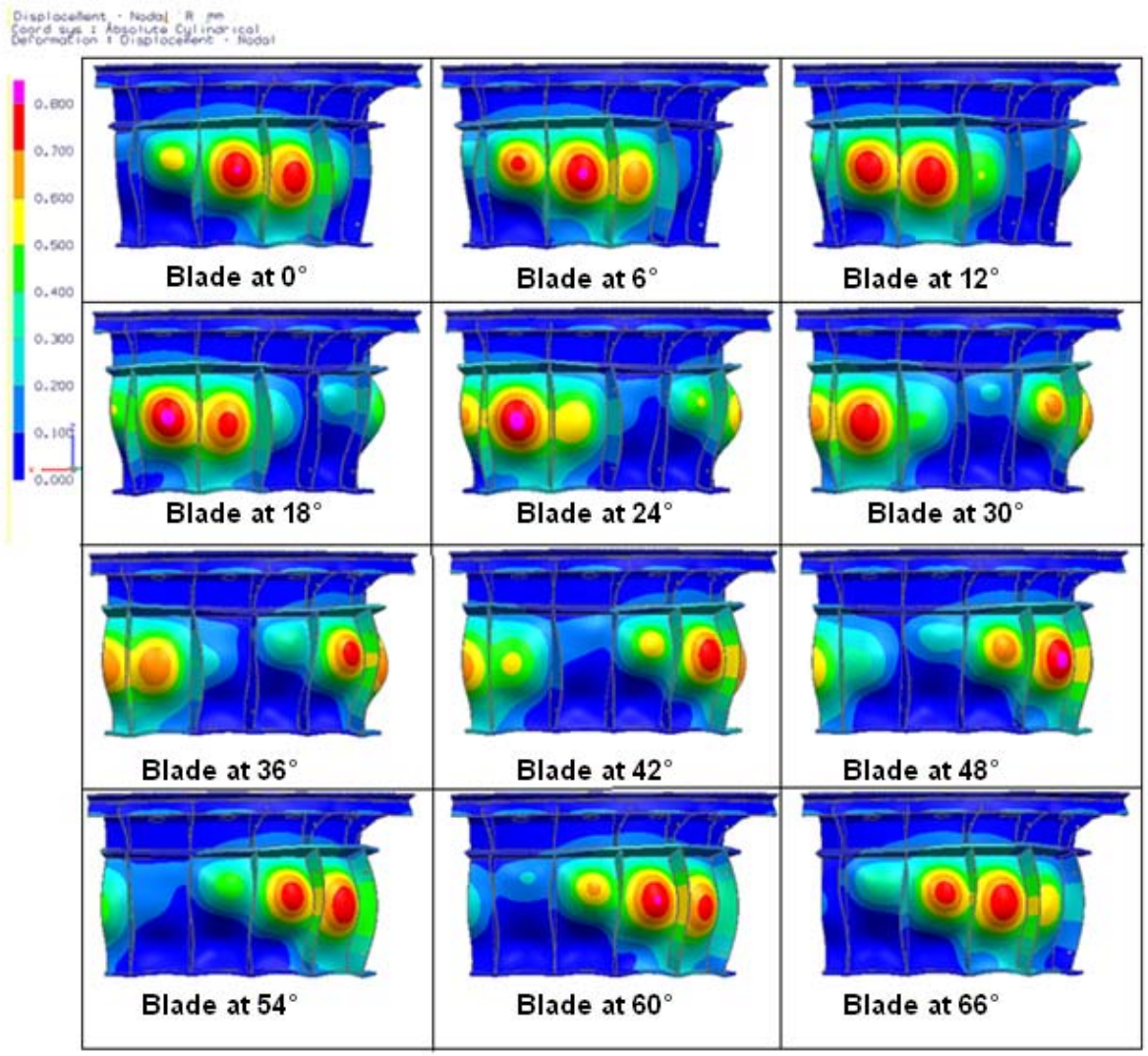

Radial displacement [mm] when blade passing in different angles on full power condition

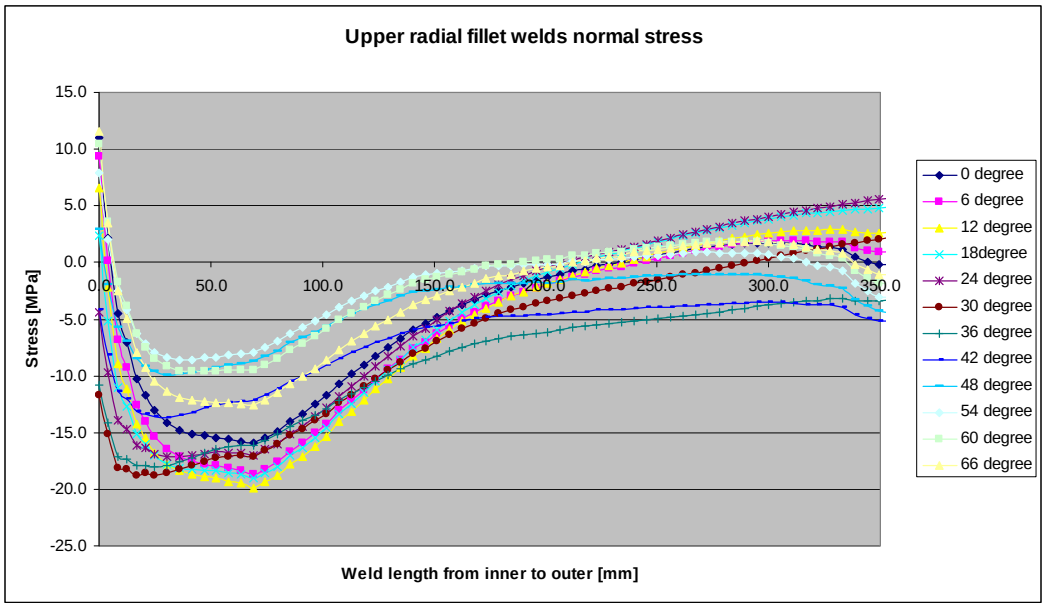

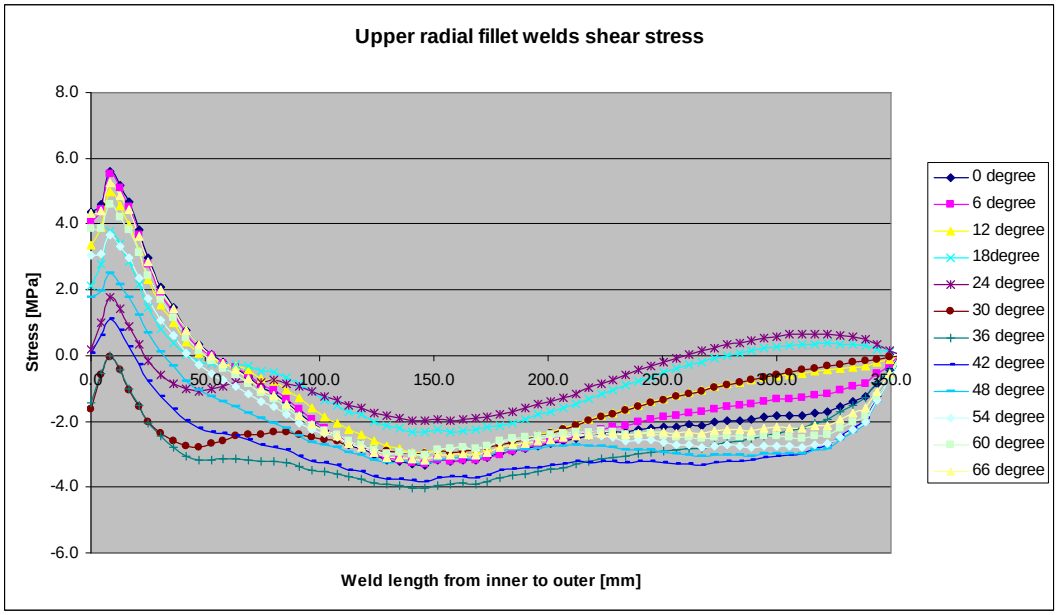

The normal and shear stresses at upper radial weld for blade passing

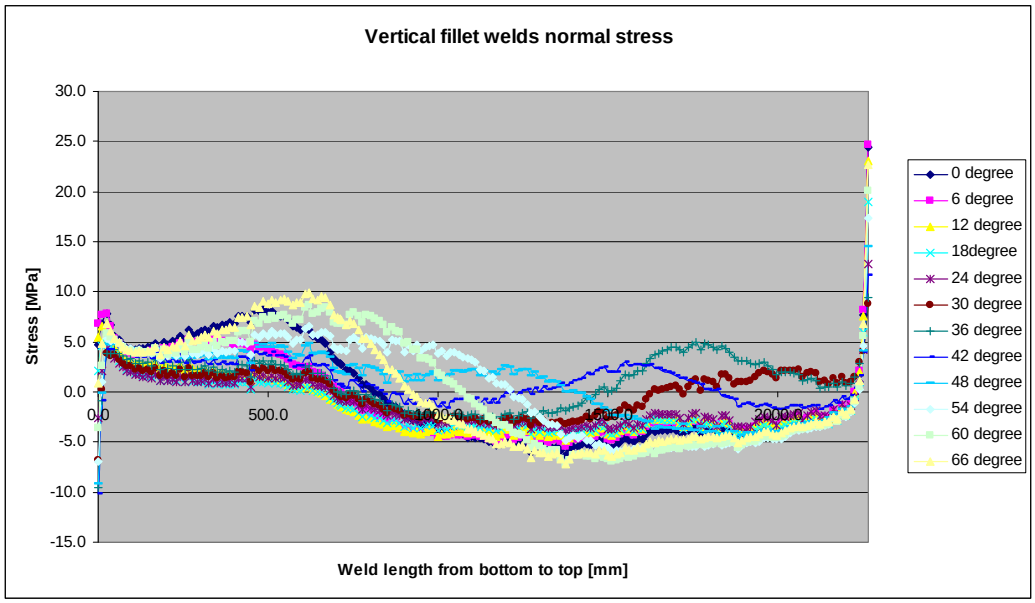

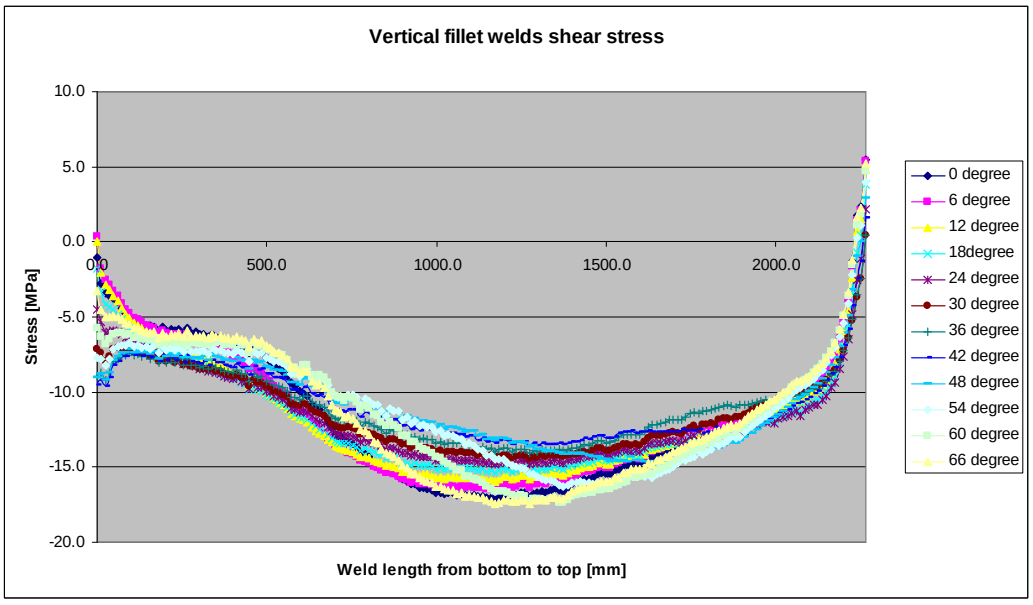

The normal and shear stresses at vertical weld for blade passing

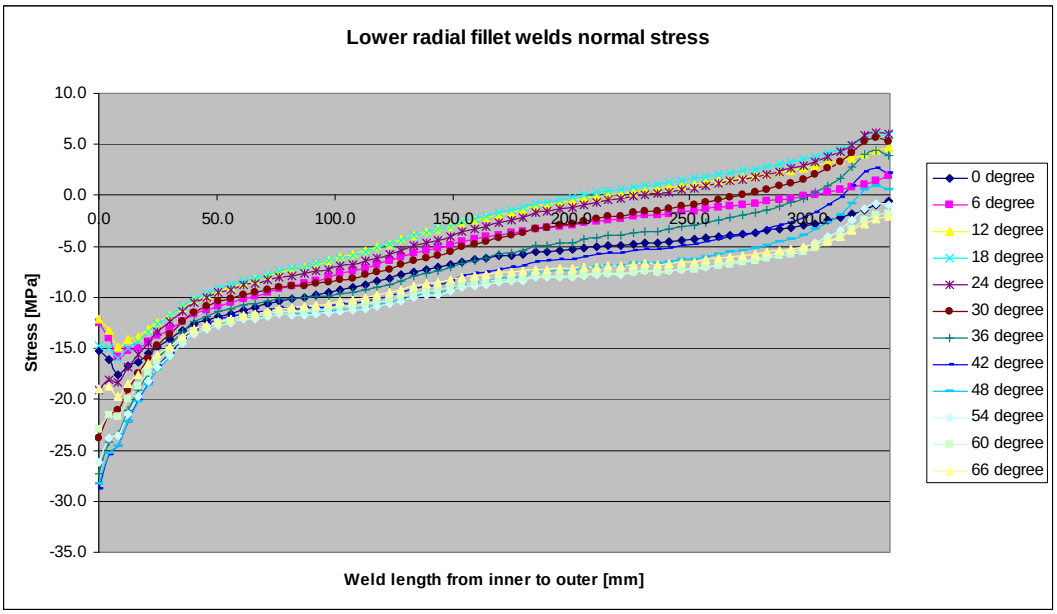

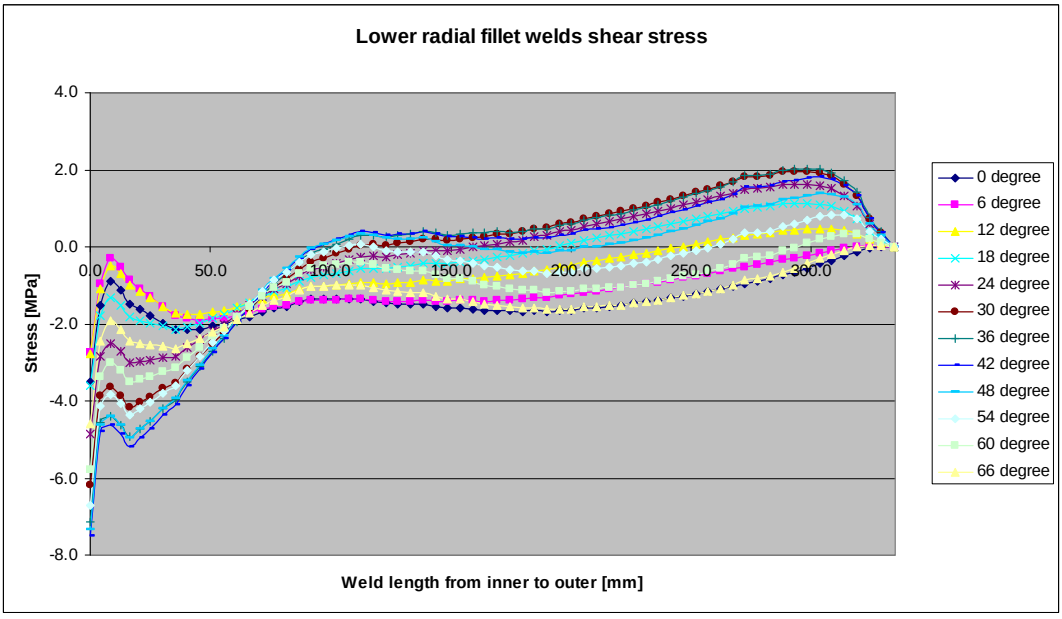

The normal and shear stresses at lower radial weld for blade passing

APPENDIX C : Fillet weld stress calculation

Allowable stress calculation

This appendix presents the calculation method of weld stresses calculated from the finite element results. The stress results at the weld toe, located 2 elements on the weld leg, are used to calculate the force applied on the fillet welds.

A calculation window, that has a length of twice the plate thickness, is swept over the length of the weld. In the calculation tables, the position of the window is identified by the x coordinate of the beginning of the window. The data at the end of the tables is extended by the length of the calculation window. In this report the contribution of the weld end is considered only within the window length. The zones where the end weld is considered are in gray and the transition is identified by a double horizontal line.

The figure below presents an example of the areas used to calculate the forces transmitted to the weld. The example shown is for Node 3, the third line in the calculation tables below.

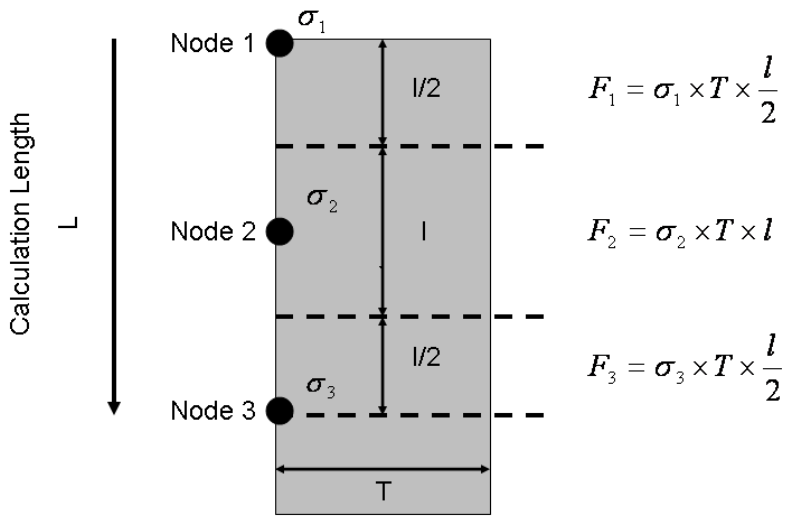

$$F_1 = \sigma_1 \times T \times \frac{l}{2}$$

$$F_2 = \sigma_2 \times T \times l$$

$$F_3 = \sigma_3 \times T \times \frac{l}{2}$$

$$F_L = F_1 + F_2 + F_3$$

$$A_L = T \times L$$

Fillet weld stress calculation

The fillet weld shear stress is evaluated at the effective throat of the weld, which is at 45 degrees.

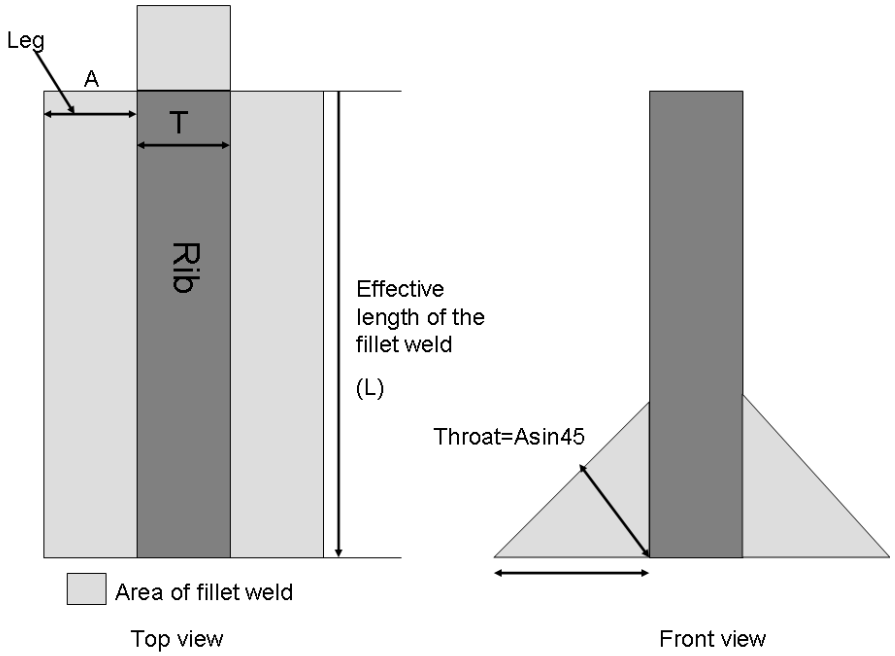

Effective area of the fillet weld

The effective area is then length of the weld times the throat:
(A_{eff}=A x sin45 x (T+2xL)).

The longitudinal stress is: $\sum_{0}^{N}(Fxx_i)/A_{eff}$.

The transverse stress is: $\sum_{0}^{N}(Fzz_i)/A_{eff}$

The total shear is the total stress is the vectorial vector sum of both stress components. ($\sigma_{total} = \sqrt{\sigma_{xx}^2 + \sigma_{zz}^2}$).

PJP weld stress calculation

The PJP weld shear stress is evaluated at the effective area of the weld, which is the shortest distance from the root of the weld to the surface of the reinforcing filet. A length penalty must by applied to this distance to consider unequal filling of the weld preparation.

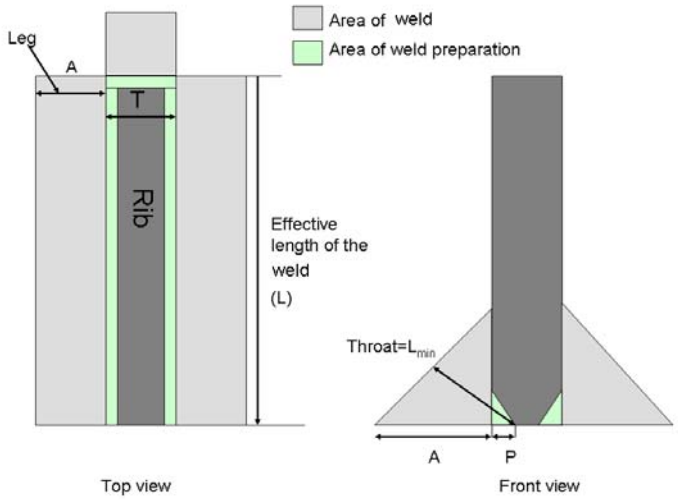

The effective area is then length of the weld times the throat:
(A_{eff}=(L_{min}– 3mm)x (T+2xL)).

<u>For a compression loaded PJP joint</u>

The shear stress is then: $\sum_{0}^{N}(Fxx_i)/A_{eff}$.

Stress induced by compression loads is not combined with shear loads induced stress.

<u>For a tension loaded PJP joint</u>

The longitudinal stress is: $\sum_{0}^{N}(Fxx_i)/A_{eff}$.

The transverse compression stress is: $\sum_{0}^{N}(Fzz_i)/A_{eff}$

The total shear is the total stress is the vectorial vector sum of both stress components. ($\sigma_{total} = \sqrt{\sigma_{xx}^2 + \sigma_{zz}^2}$).

CJP weld stress calculation

The CJP weld shear stress is evaluated at the effective area of the weld, which is the width of the thinner par joined.

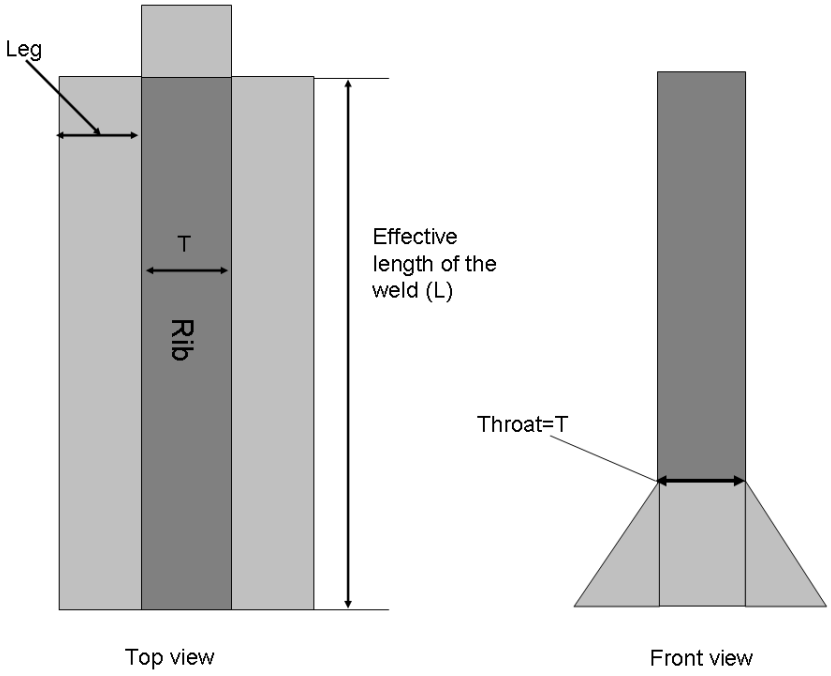

The effective area is (A_{eff}=(Tx (T+2xL)).

The stress is then: $\sum_{0}^{N}(Fzz_i)/A_{eff}$.

The shear stress is then: $\sum_{0}^{N}(Fxx_i)/A_{eff}$.

Compression and tension are evaluated independently.

Allowable stress limits (1 of 2)

Table 12.2(a)
Allowable Stresses for Welds and Joint Capacities for Cyclically Loaded Structures
(See Clauses 5.2.1.2, 12.3.3, and 12.3.4.)

		Matching conditions			Nonmatching conditions		
Type of weld	Type of load and its direction respective to line of weld	Requirements for matching (1)	Allowable stress on throat of weld	Resulting capacity of joint (7)	Extent of nonmatching	Allowable stress on throat of weld	Resulting capacity of joint
1	2	3	4	5	6	7	8
Complete joint penetration groove welds (2)	Tension or compression parallel to axis of weld (3)	Not mandatory, but if matching electrode classification used, see Col. 4 For nonmatching, see Cols. 6, 7, and 8	Same as for base metal	Same as calculated for base metal	Electrode classification lower or higher than matching	Same as for base metal (3)	Same as calculated for base metal (3)
	Compression normal to axis of weld	Mandatory					
	Tension normal to axis of weld	Mandatory			Electrode classification lower than matching	$0.3X_u$ of electrode classification used	Lesser of: (a) base metal $V=0.4A_{wn}F_y$ or (b) weld metal $V=0.3A_wX_u$
	Shear	Mandatory (for exception see Note (2) and Cols. 6, 7, and 8)					
Partial joint penetration groove welds (4)	Tension or compression parallel to axis of weld (3)	Not mandatory, but if matching electrode used, see Col. 4. For nonmatching, see Cols. 6, 7, and 8	Same as for base metal	Same as calculated for base metal	Electrode classification lower or higher than matching	Same as for base metal (3)	Same as calculated for base metal (3)
	Compression normal to axis of weld	Mandatory		See Note (5)			
	Tension normal to axis of weld *For restrictions see Clause 12.4.1(b)*	Not mandatory, but if matching electrode classification used, see Col. 4	$0.3X_u$ of matching electrode classification (Clause 11.3.4.2)	Lesser of: (a) base metal $T=0.6A_{wn}F_y$ or (b) weld metal $V=0.3A_wX_u$	Electrode classification lower than matching	$0.3X_u$ of electrode classification used	Lesser of: (a) base metal $T=0.6A_{wn}F_y$ or (b) weld metal $V=0.3A_wX_u$
	Shear	For permitted condition of nonmatching, see Cols. 6, 7, and 8		Lesser of: (a) base metal $V=0.4A_{wn}F_y$ or (b) weld metal $V=0.3A_wX_u$ (6)			Lesser of: (a) base metal $V=0.4A_{wn}F_y$ or (b) weld metal $V=0.3A_wX_u$ (6)

(Continued)

Allowable stress limits (2 of 2)

Table 12.2(a) (Concluded)

Type of weld	Type of load and its direction respective to line of weld	Matching conditions: Requirements for matching (1)	Matching conditions: Allowable stress on throat of weld	Matching conditions: Resulting capacity of joint (7)	Nonmatching conditions: Extent of nonmatching	Nonmatching conditions: Allowable stress on throat of weld	Nonmatching conditions: Resulting capacity of joint
1	2	3	4	5	6	7	8
Fillet welds (8)	Tension or compression parallel to axis of weld (3)	Not mandatory, but if matching electrode used, see Col. 4 For nonmatching, see Cols. 6, 7, and 8	Same as for base metal	Same as calculated for base metal	Electrode classification lower or higher than matching	Same as for base metal (3)	Same as calculated for base metal (3)
	Tension or compression normal to axis of weld						
	Shear	Not mandatory, but if matching electrode classification used, see Col. 4 For permitted condition of nonmatching, see Cols. 6, 7, and 8	0.3X_u of matching electrode classification	Lesser of: (a) base metal $V=0.4A_m F_y$ or (b) weld metal $V=0.3A_w X_u$	(a) Electrode classification lower than matching (b) Electrode classification one classification one designation higher than matching	(a) 0.3X_u of electrode classification used (b) 0.3X_u of matching electrode classification	Lesser of: (a) base metal $V=0.4A_m F_y$ or (b) weld metal $V=0.3A_w X_u$
Plug and slot welds *For restrictions see Clause 12.4.14(g)*	Shear						

Notes:
(1) *For matching materials and electrode classification refer to Table 12.1.*
(2) *Electrodes of strength lower than that shown for the corresponding base metal group of Table 12.1 may be used for complete joint penetration groove welds when approved by the Engineer.*
(3) *If shear is transferred between components, the design value is the smaller of that for the base metal or the weld metal.*
(4) *For hollow structural sections, the provisions of Appendix L may be used.*
(5) *The resulting capacity of the joint = (A_m + area of base metal in contact bearing) x allowable compressive stress in base metal (see Clause 11.3.4.4).*
(6) *Appendix M, Figure M3.*
(7) *The capacity of the member is to be determined independently.*
(8) *For fillet welds in railway bridges use 0.9 of the allowable joint capacity calculated from this Table.*

Weld Fatigue analysis

The welds resistance for cyclic loadings are assessed using the CSA Fatigue curves. The fatigues curves have distinct slopes for low and high cycle fatigue. For all types of weld the stress is identified at the toe of the weld. The maximum local stress is used in the calculations.

Table 12.3
Fatigue Constants and F_{sr} for Various Detail Categories
(See Clause 12.3.6.6)

Detail category	Fatigue life constant γ		Fatigue life constant γ'		Constant amplitude threshold stress range, F_{sr}		Fatigue resistances, F_{sr} [1,2] N-cycles									
							For 10 000 cycles		For 100 000 cycles		For 500 000 cycles		For 1 000 000 cycles		For 2 000 000 cycles	
	Metric	(Imperial)	Metric	(Imperial)	MPa	(ksi)	MPa	(ksi)	MPa	(ksi)	MPa	(ksi)	MPa	(ksi)	MPa	(ksi)
A	8.19E+12	2.5E+10	2.23E+17	1.4E+13	165	24.0	936	136	434	63	254	37	202	29	165[3]	24[3]
B	3.93E+12	1.2E+10	4.76E+16	3.1E+12	110	16.0	732	106	340	49	199	29	158	23	125	18
B1	2.00E+12	6.1E+09	1.38E+16	8.8E+11	83	12.0	585	85	271	39	159	23	126	18	100	15
C	1.44E+12	4.4E+09	6.86E+15	4.4E+11	69	10.0	524	76	243	35	142	21	113	16	90	13
C1	1.44E+12	4.4E+09	9.92E+15	6.4E+11	83	12.0	524	76	243	35	142	21	113	16	90	13
D	7.21E+11	2.2E+09	1.66E+15	1.1E+11	48	7.0	416	60	193	28	113	16	90	13	71	10
E	3.61E+11	1.1E+09	3.47E+14	2.2E+10	31	4.5	330	48	153	22	90	13	71	10	57	8
E1	1.28E+11	3.9E+08	4.15E+13	2.6E+9	18	2.6	234	34	109	16	63	9	50	7	40	6

Notes:
(1) *Fatigue resistances are independent of the strength of the material.*
(2) *The conditions of Clause 12.3.6 shall also be satisfied.*
(3) *Limited by F_{sr}.*

(See Note A)

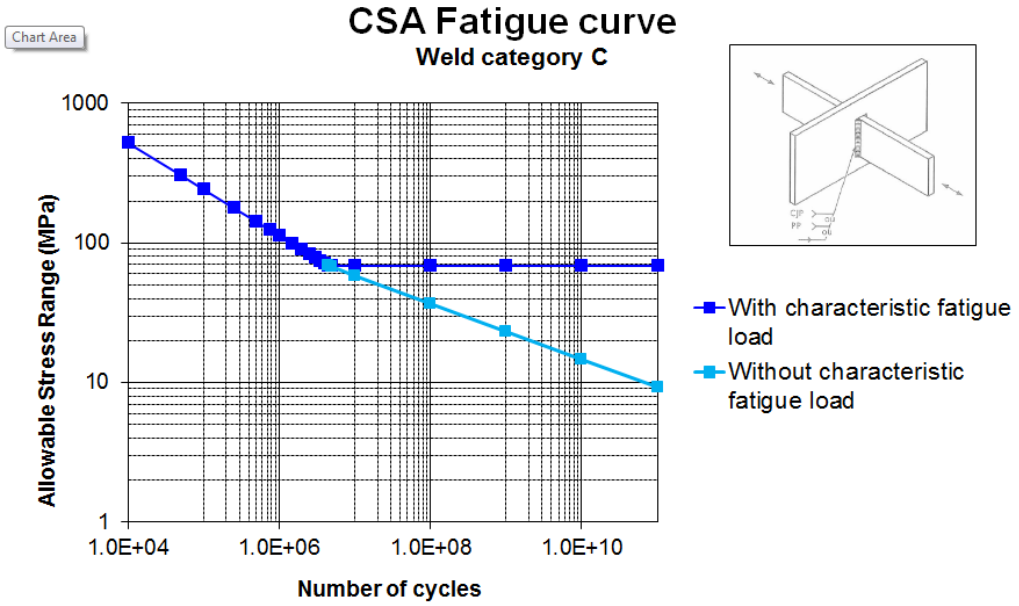

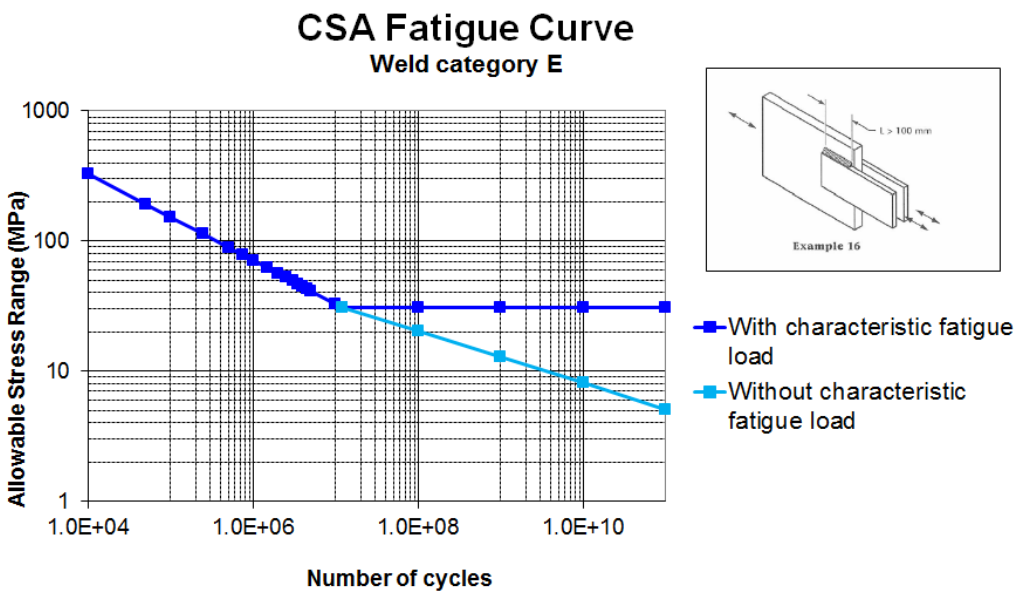

Note A: for C type joint a derating factor must be applied for joints that are not CJP.

Note:
The following notes are based on a paper by Frank and Fisher, "Fatigue Strength of Fillet Welded Cruciform Sections" Journal of the Structural Division ASCE Vol. 105 ST9, September 1979, pp 1727-1740:

In Metric,
(a) *The fatigue resistance of fillet welds transversely loaded is a function of the effective throat and plate thickness.*

$F_{sr} = F^{c}_{sr}\,[(0.06 + 0.79\,(H/t_p))/(0.64\,t_p^{\,1/6})]$

where

F^{c}_{sr} = *the fatigue resistance for Category C as determined in accordance with Clause 12.3.6.6.5. This assumes no penetration at the root of the weld.*

$[(0.06 + 0.79\,(H/t_p))/(0.64\,t_p^{\,1/6})]$ = a reduction factor ≤ 1.0

H = *weld leg size* (mm)
t_p = *plate thickness* (mm)

(b) *The fatigue resistance of PJP groove welds transversely loaded, with or without reinforcing welds, is a function of weld throat, plate thickness, and the length of the unwelded root.*

$F_{sr} = F^{c}_{sr}\,[(0.71 - 0.65\,(2a/t_p) + 0.79\,(H/t_p))/(0.64\,t_p^{\,1/6})]$

where
F^{c}_{sr} = *the fatigue resistance for Category C as determined in accordance with Clause 12.3.6.6.5. This assumes no penetration at the root of the weld.*

$[(0.71 - 0.65\,(2a/t_p) + 0.79\,(H/t_p))/(0.64\,t_p^{\,1/6})]$ = a reduction factor ≤ 1.0

$2a$ = *the length of the unwelded root face* (mm)
t_p = *plate thickness* (mm)
H = *weld leg size* (mm)

In Imperial,
(a) $F_{sr} = F^{c}_{sr}\,[(0.06 + 0.79\,(H/t_p))/(1.1\,t_p^{\,1/6})]$

(b) $F_{sr} = F^{c}_{sr}\,[(0.71 - 0.65\,(2a/t_p) + 0.79\,(H/t_p))/(1.1\,t_p^{\,1/6})]$

where 2a, H and t_p are in inches.

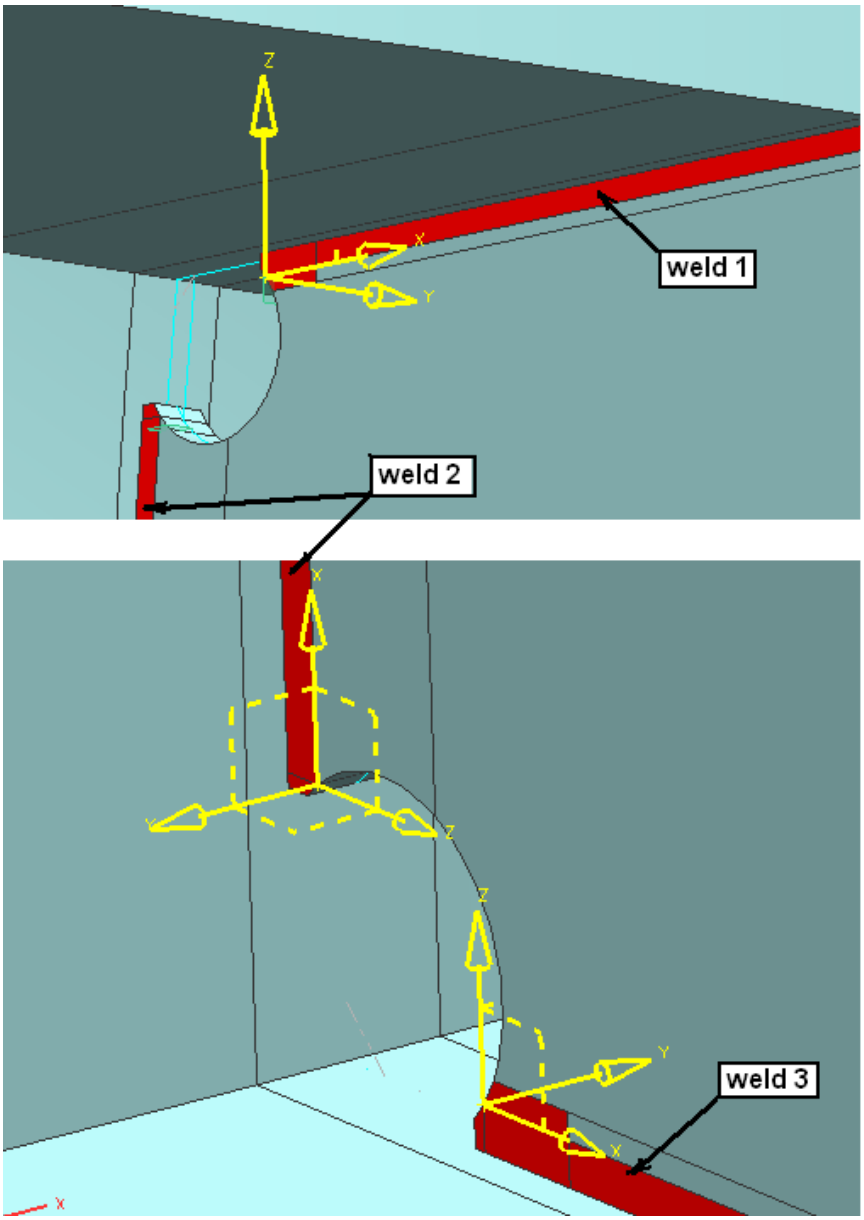

Local coordinate system for welds analysis

stand still

stress at nodes			stress in window		
X Coord	XX	ZZ	Stress XX	Stress ZZ	Total Shear
(mm)	(MPa)	(MPa)	(MPa)	(MPa)	(MPa)
0.0	2.1	3.9	1.9	-9.6	9.8
36.0	0.7	-12.8	-0.1	-14.6	14.6
41.5	0.4	-13.0	-0.2	-14.5	14.5
129.5	-1.9	-7.9	-2.3	-6.0	6.4
355.1	0.0	-0.1	0.0	-0.1	0.1

load rejection

stress at nodes			stress in window		
X Coord	XX	ZZ	Stress XX	Stress ZZ	Total Shear
(mm)	(MPa)	(MPa)	(MPa)	(MPa)	(MPa)
0.0	0.4	0.5	0.7	-2.8	2.9
25.0	0.7	-3.2	0.6	-3.7	3.8
30.5	0.6	-3.4	0.6	-3.7	3.8
355.1	0.0	-0.2	0.0	-0.2	0.2

runaway and full power

stress at nodes			stress in window		
X Coord	XX	ZZ	Stress XX	Stress ZZ	Total Shear
(mm)	(MPa)	(MPa)	(MPa)	(MPa)	(MPa)
0.0	4.8	8.6	3.8	-22.2	22.6
36.0	0.8	-29.4	-1.3	-33.9	33.9
41.5	0.0	-30.0	-1.7	-33.7	33.8
140.6	-5.9	-16.3	-6.6	-12.7	14.3
355.1	0.2	0.3	0.2	0.4	0.4

Seismic on full power

stress at nodes			stress in window		
X Coord	XX	ZZ	Stress XX	Stress ZZ	Total Shear
(mm)	(MPa)	(MPa)	(MPa)	(MPa)	(MPa)
0.0	4.8	8.5	3.8	-22.4	22.7
36.0	0.8	-29.6	-1.3	-34.1	34.1
41.5	0.0	-30.2	-1.7	-33.9	33.9
135.1	-5.7	-17.9	-6.6	-13.8	15.3
355.1	0.2	0.3	0.2	0.4	0.4

PMF

stress at nodes			stress in window		
X Coord	XX	ZZ	Stress XX	Stress ZZ	Total Shear
(mm)	(MPa)	(MPa)	(MPa)	(MPa)	(MPa)
0.0	2.9	5.3	2.5	-12.7	12.9
36.0	0.8	-16.9	-0.3	-19.5	19.5
41.5	0.4	-17.3	-0.5	-19.3	19.4
151.6	-3.0	-7.8	-3.3	-5.9	6.7
355.1	0.1	0.0	0.1	0.0	0.1

Stress Results for weld 1 (16mm leg at upper flange)

stand still

stress at nodes			stress in window		
X Coord	XX	ZZ	Stress XX	Stress ZZ	Total Shear
(mm)	(MPa)	(MPa)	(MPa)	(MPa)	(MPa)
0.0	-1.2	1.9	-4.7	0.9	4.8
1110.1	-10.8	-1.6	-12.0	-2.3	12.3
1272.9	-10.9	-2.7	-11.8	-2.8	12.1
1285.4	-10.7	-2.1	-11.7	-2.8	12.1
2161.9	-5.4	-0.6	-2.3	2.2	3.2

load rejection

stress at nodes			stress in window		
X Coord	XX	ZZ	Stress XX	Stress ZZ	Total Shear
(mm)	(MPa)	(MPa)	(MPa)	(MPa)	(MPa)
0.0	-0.8	-0.3	-1.1	0.7	1.4
1110.1	-2.0	-0.4	-2.2	-0.4	2.3
2149.1	-0.9	0.2	-0.3	1.0	1.1
2161.9	-0.9	0.1	-0.2	1.1	1.1

runaway and full power

stress at nodes			stress in window		
X Coord	XX	ZZ	Stress XX	Stress ZZ	Total Shear
(mm)	(MPa)	(MPa)	(MPa)	(MPa)	(MPa)
0.0	-3.0	4.2	-11.2	2.2	11.4
1110.1	-26.1	-3.8	-29.2	-5.5	29.7
1122.5	-26.7	-5.6	-29.2	-5.5	29.7
1298.0	-26.4	-6.3	-28.6	-6.8	29.4
2161.9	-13.5	-1.8	-6.2	4.3	7.6

Seismic on full power

stress at nodes			stress in window		
X Coord	XX	ZZ	Stress XX	Stress ZZ	Total Shear
(mm)	(MPa)	(MPa)	(MPa)	(MPa)	(MPa)
0.0	-3.0	4.2	-11.2	2.2	11.5
1110.1	-26.2	-3.8	-29.3	-5.5	29.8
1122.5	-26.8	-5.6	-29.3	-5.5	29.8
1298.0	-26.5	-6.3	-28.7	-6.8	29.5
2161.9	-13.5	-1.8	-6.3	4.3	7.6

PMF

stress at nodes			stress in window		
X Coord	XX	ZZ	Stress XX	Stress ZZ	Total Shear
(mm)	(MPa)	(MPa)	(MPa)	(MPa)	(MPa)
0.0	-1.6	2.6	-6.3	1.2	6.4
1110.1	-14.6	-2.2	-16.3	-3.1	16.6
1122.5	-14.9	-3.2	-16.3	-3.1	16.6
1298.0	-14.7	-3.5	-15.9	-3.8	16.3
2161.9	-7.3	-0.9	-3.2	2.8	4.2

Stress Results for weld 2 (16mm leg at vertical barrel)

stand still

stress at nodes			stress in window		
X Coord	XX	ZZ	Stress XX	Stress ZZ	Total Shear
(mm)	(MPa)	(MPa)	(MPa)	(MPa)	(MPa)
0.0	-1.7	-7.9	-1.9	-10.3	10.4
4.2	-0.9	-9.2	-2.0	-10.3	10.5
30.2	-2.1	-9.2	-2.7	-9.0	9.4
35.3	-2.4	-8.8	-2.7	-8.8	9.2
334.5	0.0	1.0	0.0	1.1	1.1

load rejection

stress at nodes			stress in window		
X Coord	XX	ZZ	Stress XX	Stress ZZ	Total Shear
(mm)	(MPa)	(MPa)	(MPa)	(MPa)	(MPa)
0.0	-1.0	-4.0	-0.7	-3.2	3.2
4.2	-0.6	-3.7	-0.6	-2.9	3.0
8.3	-0.5	-3.7	-0.6	-2.7	2.8
334.5	0.0	0.9	0.0	0.9	0.9

runaway and full power

stress at nodes			stress in window		
X Coord	XX	ZZ	Stress XX	Stress ZZ	Total Shear
(mm)	(MPa)	(MPa)	(MPa)	(MPa)	(MPa)
0.0	-3.9	-18.6	-4.4	-24.3	24.7
4.2	-2.1	-21.6	-4.6	-24.4	24.8
8.3	-1.6	-24.7	-5.0	-24.1	24.6
35.3	-5.5	-20.9	-6.2	-20.9	21.8
334.5	0.0	1.8	0.0	2.0	2.0

Seismic on full power

stress at nodes			stress in window		
X Coord	XX	ZZ	Stress XX	Stress ZZ	Total Shear
(mm)	(MPa)	(MPa)	(MPa)	(MPa)	(MPa)
0.0	-4.0	-18.8	-4.4	-24.4	24.8
4.2	-2.1	-21.8	-4.6	-24.5	24.9
8.3	-1.6	-24.9	-5.0	-24.2	24.8
35.3	-5.6	-21.0	-6.2	-21.0	21.9
334.5	0.0	1.8	0.0	2.0	2.0

PMF

stress at nodes			stress in window		
X Coord	XX	ZZ	Stress XX	Stress ZZ	Total Shear
(mm)	(MPa)	(MPa)	(MPa)	(MPa)	(MPa)
0.0	-2.1	-10.3	-2.5	-13.7	13.9
4.2	-1.1	-12.1	-2.6	-13.7	14.0
8.3	-0.9	-13.8	-2.8	-13.6	13.9
35.3	-3.1	-11.8	-3.6	-11.8	12.4
334.5	0.0	1.1	0.0	1.2	1.2

Stress Results for weld 3 (16mm leg at lower flange)

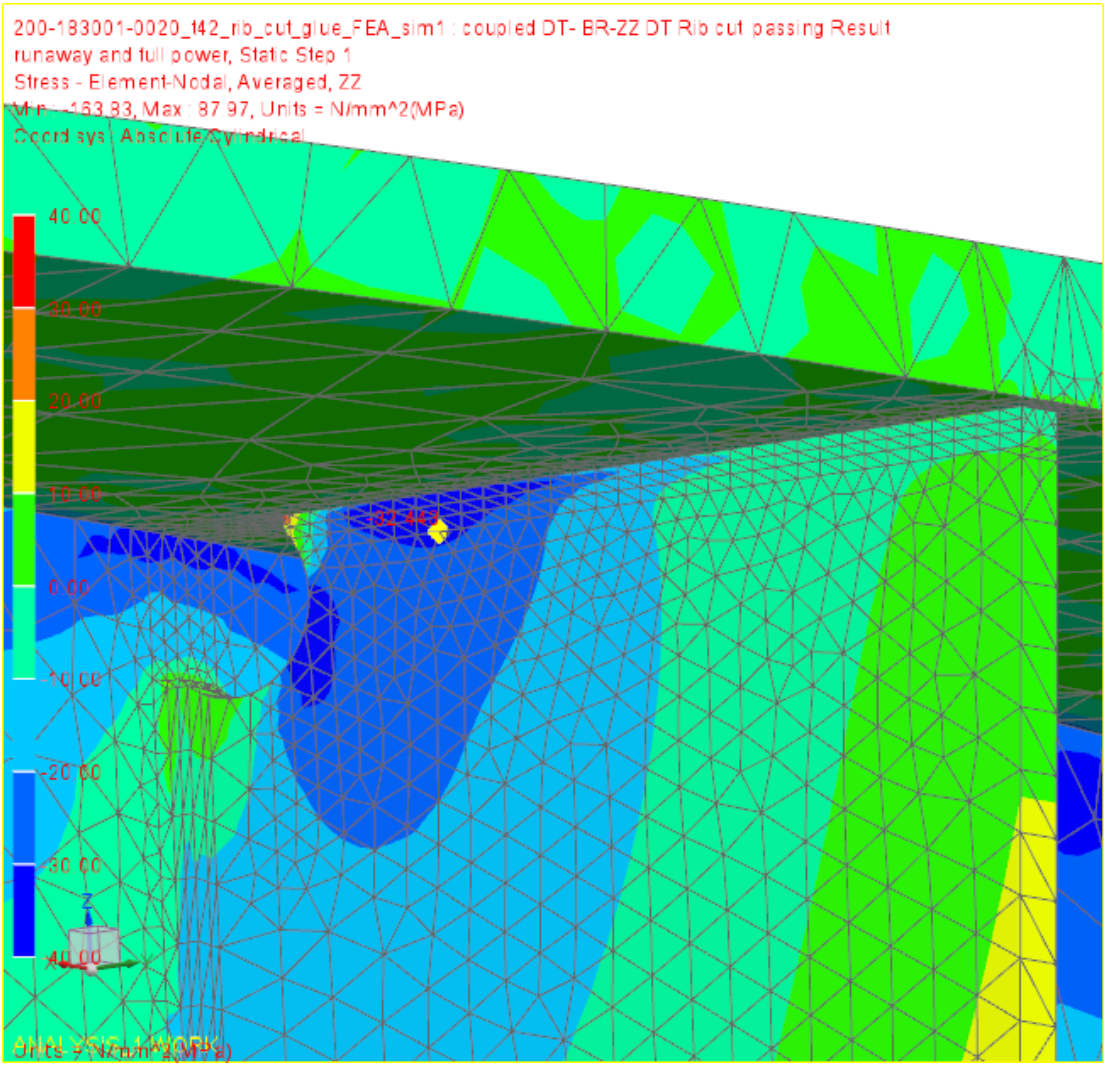

Maximum normal stress at weld toe for weld 1 on full power or runaway condition (16mm leg on upper flange at bolt circle)

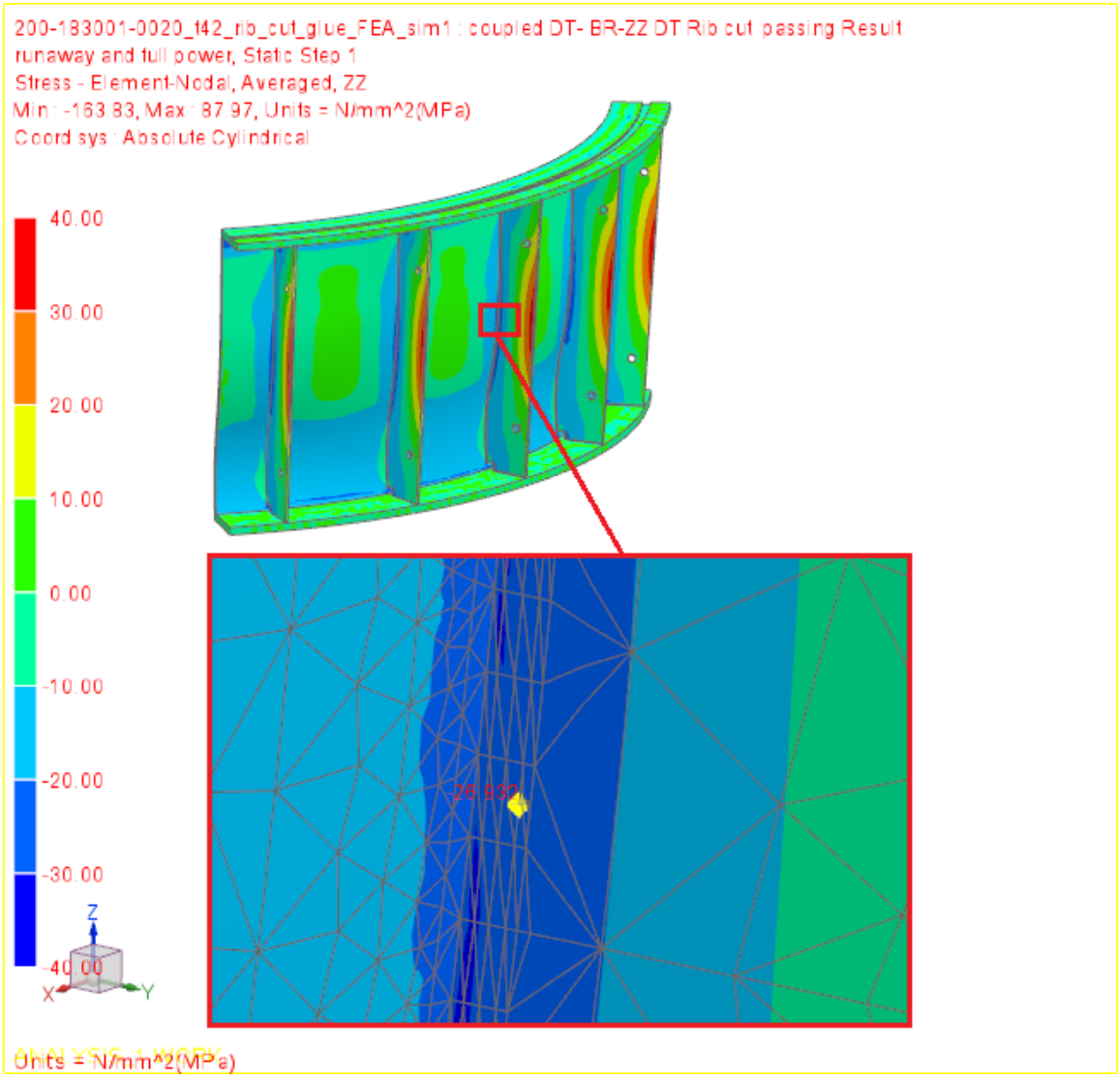

Maximum shear stress at weld toe for weld 2 on full power or runaway condition (16mm leg on weld of rib to barrel at center of weld)

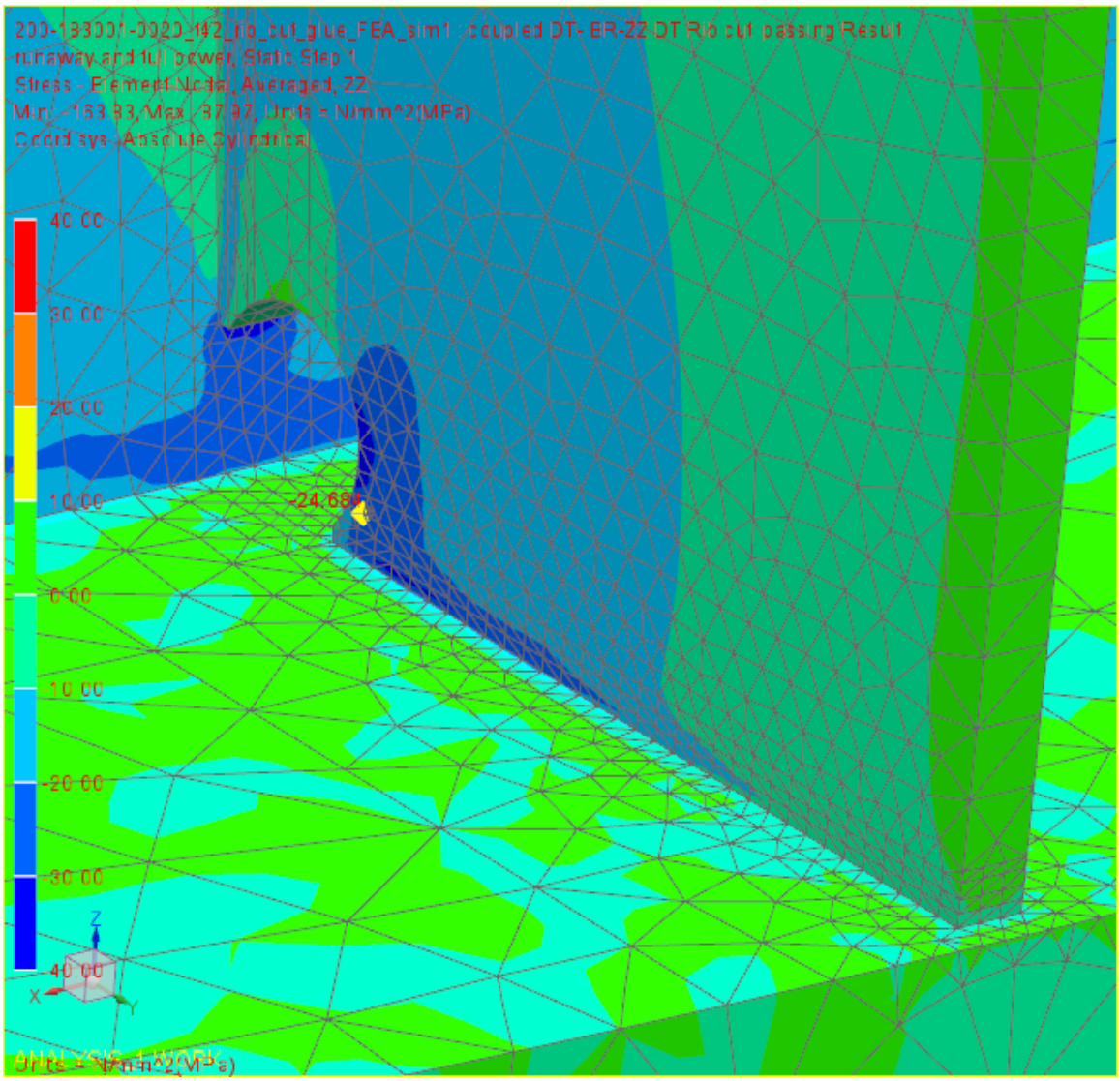

Maximum normal stress at weld toe for weld 3 on full power or runaway condition (16mm leg on lower flange at bolt circle)

APPENDIX D : Modal analysis mode shapes

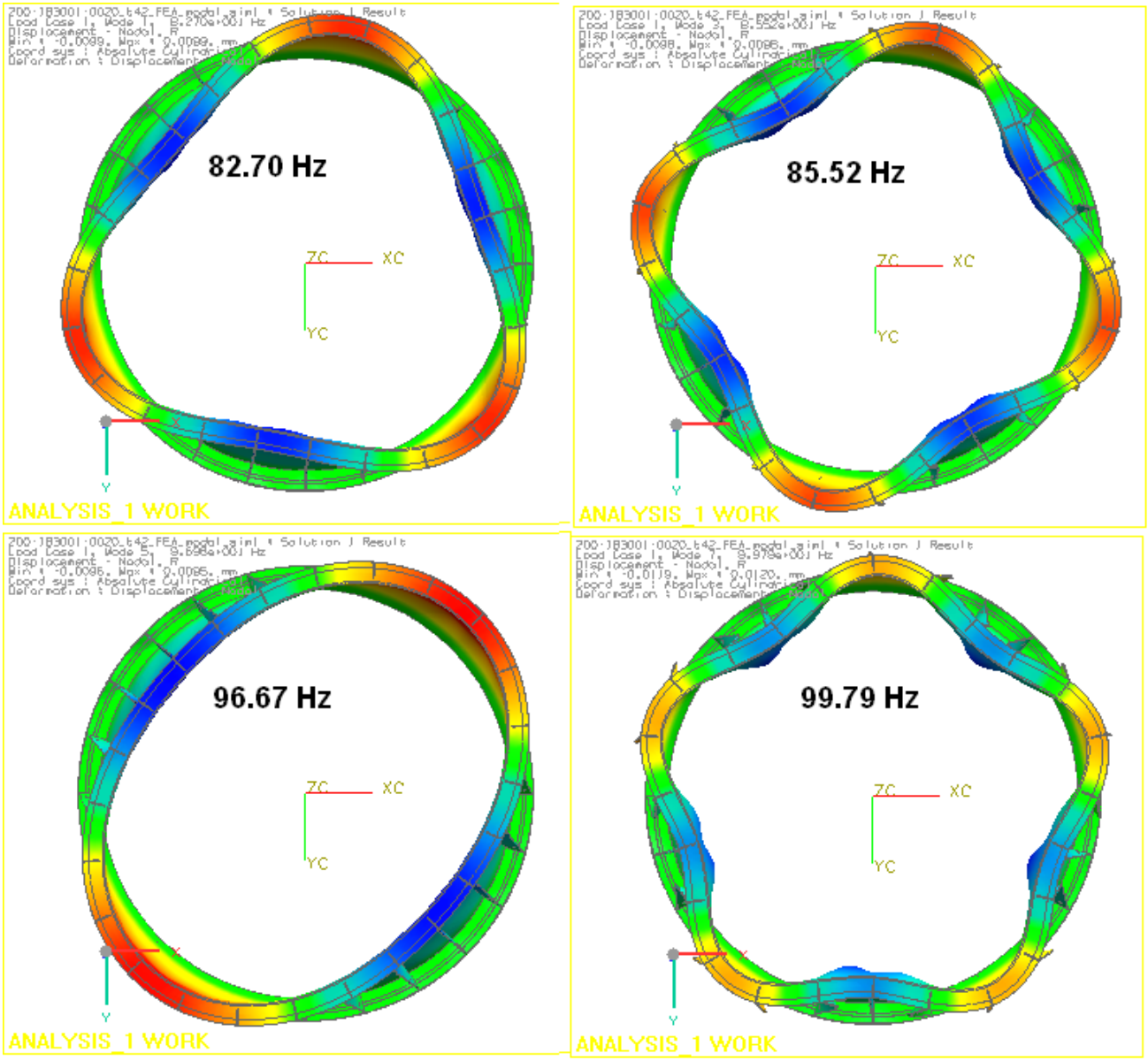

Natural frequency and mode shape

APPENDIX E : Extract of the ASME Boiler and Pressure Vessel Code for fatigue Analysis

2007 SECTION VIII, DIVISION 2

5.15 Figures

Stress Category	Primary			Secondary Membrane plus Bending	Peak
	General Membrane	Local Membrane	Bending		
Description (For examples, see Table 5.2)	Average primary stress across solid section. Excludes discontinuities and concentrations. Produced only by mechanical loads.	Average stress across any solid section. Considers discontinuities but not concentrations. Produced only by mechanical loads.	Component of primary stress proportional to distance from centroid of solid section. Excludes discontinuities and concentrations. Produced only by mechanical loads.	Self-equilibrating stress necessary to satisfy continuity of structure. Occurs at structural discontinuities. Can be caused by mechanical load or by differential thermal expansion. Excludes local stress concentrations.	1. Increment added to primary or secondary stress by a concentration (notch). 2. Certain thermal stresses which may cause fatigue but not distortion of vessel shape.
Symbol	P_m	P_L	P_b	Q	F

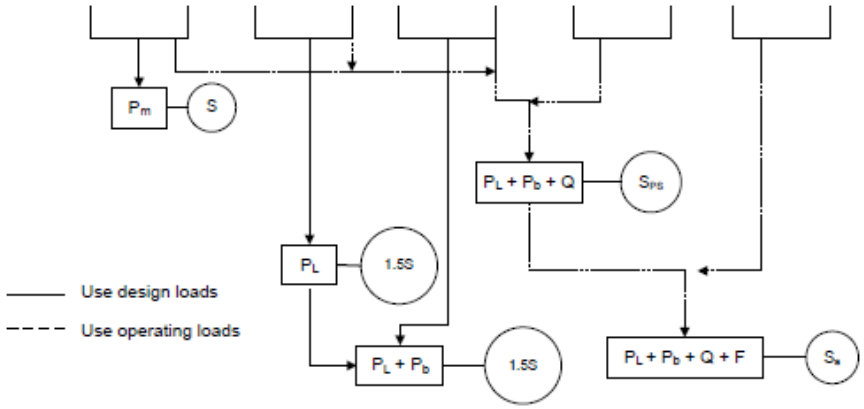

Figure 5.1
Stress Categories and Limits of Equivalent Stress

ANNEX 3.F

DESIGN FATIGUE CURVES

(NORMATIVE)

3.F.1 Smooth Bar Design Fatigue Curves

3.F.1.1 Smooth bar design fatigue curves in paragraph 3.F.1.1 are provided for the following materials in terms of a polynomial function, see Equation (3.F.1). The constants for these functions, C_n, are provided for different fatigue curves as described below.

a) Carbon, Low Alloy, Series 4xx, and High Tensile Strength Steels for temperatures not exceeding 371°C (700°F) where $\sigma_{uts} \leq 552\ MPa\ (80\ ksi)$ (see Table 3.F.1).

b) Carbon, Low Alloy Series 4xx, and High Tensile Strength Steels for temperatures not exceeding 371°C (700°F) where $\sigma_{uts} = 793 - 892\ MPa\ (115 - 130\ ksi)$ (see Table 3.F.2).

c) Series 3xx High Alloy Steels, Nickel-Chromium-Iron Alloy, Nickel-Iron-Chromium Alloy, and Nickel-Copper Alloy for temperatures not exceeding 427°C (800°F) where $S_a > 195\ MPa\ (28.2\ ksi)$ (see Table 3.F.3).

d) Series 3xx High Alloy Steels, Nickel-Chromium-Iron Alloy, Nickel-Iron-Chromium Alloy, and Nickel-Copper Alloy for temperatures not exceeding 427°C (800°F) where $S_a \leq 195\ MPa\ (28.2\ ksi)$ (see Table 3.F.4).

e) Wrought 70-30 Copper-Nickel for temperatures not exceeding 232°C (450°F) (see Tables 3.F.5, 3.F.6, and 3.F.7). These data are applicable only for materials with minimum specified yield strength as shown. These data may be interpolated for intermediate values of minimum specified yield strength.

f) Nickel-Chromium-Molybdenum-Iron, Alloys X, G, C-4, And C-276 for temperatures not exceeding 427°C (800°F) (see Table 3.F.8).

g) High strength bolting for temperatures not exceeding 371°C (700°F) (see Table 3.F.9).

3.F.1.2 The design number of design cycles, N, can be computed from Equation (3.F.1) or Table 3.F.10 based on the stress amplitude, S_a, which is determined in accordance with Part 5 of this Division.

$$N = 10^X \tag{3.F.1}$$

where

$$X = \frac{C_1 + C_3 Y + C_5 Y^2 + C_7 Y^3 + C_9 Y^4 + C_{11} Y^5}{1 + C_2 Y + C_4 Y^2 + C_6 Y^3 + C_8 Y^4 + C_{10} Y^5} \tag{3.F.2}$$

$$Y = \left(\frac{S_a}{C_{uts}}\right) \cdot \left(\frac{E_{FC}}{E_T}\right) \tag{3.F.3}$$

3.F.4 Tables

Table 3.F.1 – Coefficients for Fatigue Curve 110.1 – Carbon, Low Alloy, Series 4XX, High Alloy Steels, And High Tensile Strength Steels For Temperatures not Exceeding 371 °C (700 °F) – $\sigma_{uts} \le 552\,MPA\ (80\,ksi)$

Coefficients C_i	$48 \le S_a < 214 (MPa)$ $7 \le S_a < 31 (ksi)$	$214 \le S_a \le 3999 (MPa)$ $31 \le S_a \le 580 (ksi)$
1	2.254510E+00	7.999502E+00
2	-4.642236E-01	5.832491E-02
3	-8.312745E-01	1.500851E-01
4	8.634660E-02	1.273659E-04
5	2.020834E-01	-5.263661E-05
6	-6.940535E-03	0.0
7	-2.079726E-02	0.0
8	2.010235E-04	0.0
9	7.137717E-04	0.0
10	0.0	0.0
11	0.0	0.0
Note: $E_{FC} = 195E3\ MPa\ (28.3E3\ ksi)$		

Document Front Sheet

SNC·LAVALIN

nalcor energy
LOWER CHURCHILL PROJECT

NE-LCP Contractor/Supplier

Contract or Purchase Number and Description:	Contractor/Supplier Name:
CH0030	Andritz Hydro Canada Inc.

Document Title:	Total Number of Pages Incl. Front Sheet
Stay Ring Calculation and Fatigue Analysis Reports	101
Contractor/ Supplier Document Number:	**Revision Number:**
AH-MUS-SE-0001	01
EPC(M) Document Number: Not Applicable	**Issue Number:** Not Applicable

NE-LCP Document Number:	NE-LCP Issue Number:
MFA-AH-SD-3410-ME-H27-0001-01	C1

Approver's Signature:	Date (dd-mmm-yyyy):	Review Class:
	23-Sep-2013	
Comments:		Equipment Tag or Model Number:

NE-LCP or EPC(M)

REVIEW DOES NOT CONSTITUTE APPROVAL OF DESIGN DETAILS, CALCULATIONS, TEST METHODS OR MATERIAL DEVELOPED AND/OR SELECTED BY THE CONTRACTOR, NOR DOES IT RELIEVE THE CONTRACTOR FROM FULL COMPLIANCE WITH CONTRACTUAL OR OTHER OBLIGATIONS.

- [x] 01 – REVIEWED AND ACCEPTED – NO COMMENTS
- [ ] 02 – REVIEWED – INCORPORATE COMMENTS, REVISE AND RESUBMIT
- [ ] 03 – REVIEWED - NOT ACCEPTED
- [ ] 04 – INFORMATION ONLY
- [ ] 05 – NOT REVIEWED

Lead Reviewer:	Date (dd-mmm-yyyy):	Project Manager:	Date (dd-mmm-yyyy):
CH	15 Oct 2013		
NE-LCP or EPC(M) Management:	Date (dd-mmm-yyyy):		

General Comments:

C1	01	Issue for Construction	23-Sep-2013	LDA	YB
A1	00	Initial release	30-Oct-2012	LD'A	YB
Nalcor Doc. Rev.	Andritz Doc. Rev.	Modification	Date	Prepared / Préparé	Appr.

Title / Titre

STAY RING CALCULATION AND FATIGUE ANALYSIS REPORTS

HCM	Date	Name / Nom
Prepared by:	23-Sep-2012	Lucio D'Alessandro, Eng., M. Eng., MBA
Approved by:	23-Sep-2012	Yves Bergeron, Eng.

Contract / Contrat No.: 0200-183001 to 0200-183004

Part Bill / Nomenclature No.: 060

Andritz Doc. No.	Rev.	Sheet / Feuille	1
AH-MUS-SE-0001	01	of / de	100

Professional Engineer's Stamp

Client

Project

LOWER CHURCHILL PROJECT

MUSKRAT FALLS HYDROELECTRIC DEVELOPMENT

NE Doc. No.	Rev.
MFA-AH-SD-3410-ME-H27-0001-01	C1

TABLE OF CONTENTS

C1	01	General revision according to customer comments and AH replies	21-June-2013		
A1	00	Initial release	26-Oct-2012		
Nalcor Doc. Rev.	Andritz Doc. Rev.	Modification	Date	Prepared / Préparé	Appr.

Title / Titre

STAY RING FINITE ELEMENT ANALYSIS AND FATIGUE ANALYSIS

HCM	Date	Name / Nom
Prepared by:	26-Oct.-2012	Christine Monette, Eng., M. Eng.
Approved by:	26-Oct.-2012	André Coutu, Eng., M. Eng., MBA

Contract / Contrat No.: 0200-183001 to 0200-183004

Part Bill / Nomenclature No.: 060

Andritz Doc. No.	Rev.	Sheet / Feuille	1
CAL0200500060	01	of / de	44

Professional Engineer's Stamp

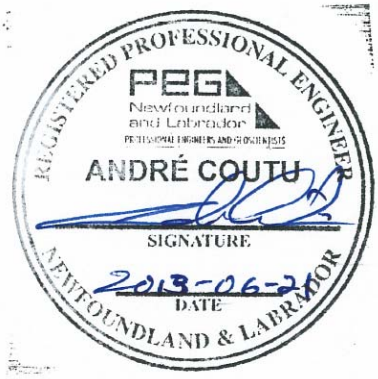

Client

nalcor energy
LOWER CHURCHILL PROJECT

Project

LOWER CHURCHILL PROJECT

MUSKRAT FALLS HYDROELECTRIC DEVELOPMENT

SNC·LAVALIN

NE Doc. No.	Rev.
MFA-AH-SD-3410-ME-H27-0001-01	**C1**

TABLE OF CONTENTS

TABLE OF APPENDICES

TABLES LIST

FIGURES LIST

1. INTRODUCTION

This report presents the static 3D finite element analysis of the Muskrat Falls stay ring for six operating conditions. It also includes a fatigue analysis of the component.

2. STAY RING

2.1 GEOMETRY

The model represents a stay ring 1/24 segment. The stay vane #15 is modeled with its corresponding bolted anchors because it is the most loaded stay vane. Stay ring geometry is as per drawing except that the extensions shown in HDSO 4303 view B-B are not included. The model used for stress calculation has a trailing edge thickness of 10.5 mm. As the extension of 15.87 mm for a trailing edge thickness of 3 mm is not in a high stress area, it was neglected and not included in the model for the stay vane calculation. Drawing numbers are given in Table 1.

Table 1 – Drawing numbers

Drawing Title	Drawing Number
Muskrat Falls Stay Ring Machining	226045606
Muskrat Falls Stay Ring Fabrication	226045706

2.2 MATERIAL

Materials used in the analysis are given in Table 2 with their properties. Welding material will have as good or better mechanical properties than the base material.

Table 2 – Material properties

Material	Yield Strength (S_y) [MPa]	Tensile Strength (S_u) [MPa]	Young Modulus [GPa]	Density [kg/m^3]	Poisson ratio
Stay ring material: ASTM A516M Grade 485	260	485	210	7859	0.3
Concrete	-	-	20	2400	0.2

2.3 ALLOWABLE STRESSES

As per contract clause 1.2.6.1.1, allowable stresses are given in Table 3.

Table 3 – Allowable stresses

	Primary membrane stress	Primary bending stress	Secondary bending stress
ASME Section VIII, Division 1 and Division 2 2010	$S_m = \min(2/3*S_y; 1/3.5*S_u)$	$1.5*S_m$	$3*S_m$
Value	139 MPa	208 MPa	416 MPa

3. FINITE ELEMENT ANALYSIS

3.1 MODEL

The software used for the finite element analysis is NX6 from Siemens Product Lifecycle Management Software Inc. The elements used are their standard 10 nodes parabolic tetrahedron element. Model mesh sizes are given in Table 4. Part of the concrete is included in the models to properly transfer the loads. The model includes details such as fillets at the junctions of the stay vane with the stay ring plates. The mesh in critical locations is fine enough so that the calculated stress is the real stress for the applied loads. See appendix A for model representation.

Table 4 – Model mesh sizes

Stay ring model	Mesh size
Stay ring	130790 nodes 76430 elements
Anchors	17233 nodes 10031 elements
Upper concrete block	8199 nodes 4855 elements
Lower concrete block	9390 nodes 5592 elements

3.2 PRESSURE LOADS

Design static pressures through the flow channel of the turbine are calculated using Andritz Hydro's proprietary empirical rules developed and validated by pressure measurements on similar machines. Flow channel is discretized in six regions shown in Figure 1. Head losses are neglected within regions and water level is only considered for discharge ring pressures at standstill. Muskrat Falls design static pressures for stationary components are given in Table 5 at different operation regimes.

From measurements on existing runners, it was observed that static pressures at runaway and full power are similar and are therefore considered the same. During a load rejection event, the overpressure occurs in the casing: the wicket gates are closed or in the process of closing and suction occurs behind the wicket gates to bring the pressure close to atmospheric pressure under the head cover.

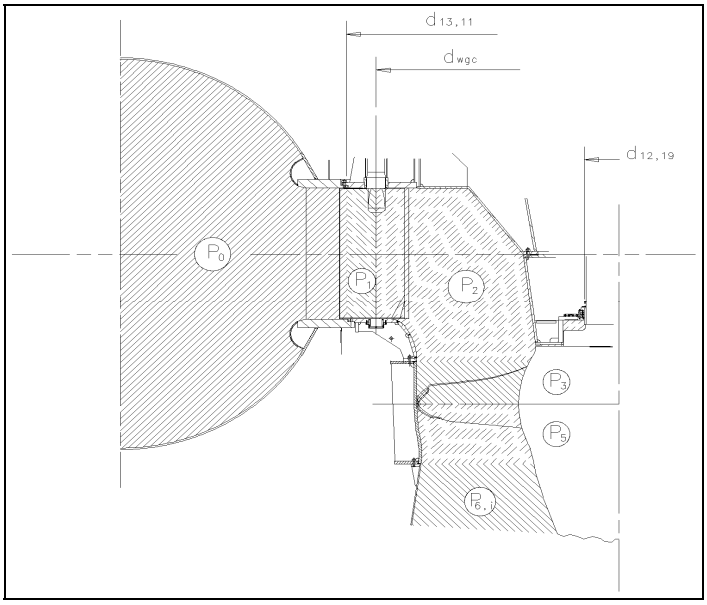

Figure 1 – Flow channel pressure regions

Table 5 – Design static pressures for stationary components

Operation regime	Pressure in spiral case (P_0)	Pressure upstream of guide vanes (P_1)	Pressure downstream of guide vanes (P_2)	Discharge ring pressure upstream blade axis (P_3)	Discharge ring pressure downstream blade axis (P_5)
	kPa	kPa	kPa	kPa	kPa
Standstill	439	439	117	Hydrostatic variation	Hydrostatic variation
Load rejection	504	504	0	0	0
Full power	439	439	374	374	374
Runaway	439	439	374	374	374
PMF standstill	499	499	177	177	177

3.3 LOAD CASES

Loads of stay vane #6 are applied for the dewatered condition while loads of stay vane #15 are applied on the model for all other load cases. It is shown from stay vane loads in Figure 2 that those stay vanes are the most loaded stay vanes.

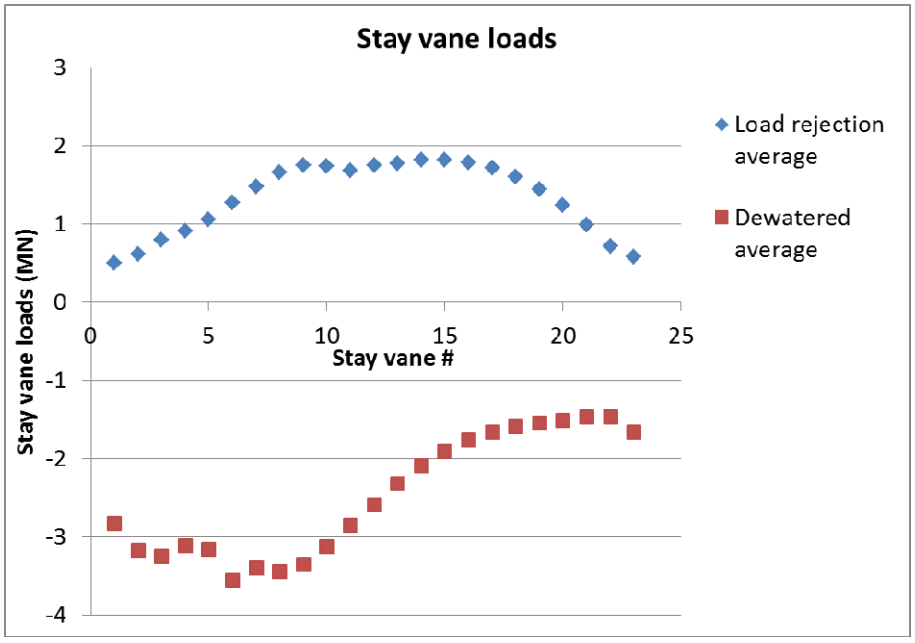

Figure 2 – Stay vane loads

All loads applied on the stay ring model are described in Table 6. Negative loads represent downward loads. Loads for power generation are shown under a graphical form in Appendix A. To take account for the stay ring weight in the analysis, gravity is added to all load cases, but concrete density was changed to a negligible value as its weight was already taken into account in the concrete force described in Table 6. Water is assumed to leak between the stay ring shrouds and the concrete; therefore, no pressure is applied on this part of the shrouds. Pressure is either not applied on the concrete of the casing because all the forces are already included in the concrete force. Concrete force calculation details are as follow.

$F_{c6\text{-}ds}$	Concrete force (upper anchor load) at dewatered standstill for stay vane 6 (Ref [1])	-3000	kN
$F_{c15\text{-}s}$	Concrete force (upper anchor load) during load rejection for stay vane 15 (Ref [1])	1733	kN
$F_{c15\text{-}ds}$	Concrete force (upper anchor load) at dewatered standstill for stay vane 15 (Ref [1])	-1347	kN
F_{c15}	Concrete force at other pressure condition for stay vane 15		

$$F_{c15} = \left(F_{c15-s} - F_{c15-ds}\right)\frac{P_0}{P_{0-s}} + F_{c15-ds}$$

Head cover and bottom ring pressure loads are calculated using the following geometry data and formulas:

D_p	pitch circle diameter (mm)	10682
D_{hi}	inner HC diameter (mm)	1880
D_{hs}	outer HC seal diameter (mm)	11855
D_{bi}	inner BR diameter (mm)	8800
D_{bs}	BR seal diameter (mm)	11726

$$\text{Head cover pressure load per stay vane} = \frac{\frac{\pi(D_{hs}{}^2 - D_p{}^2)}{4}P_1 + \frac{\pi(D_p{}^2 - D_{hi}{}^2)}{4}P_2}{24}$$

$$\text{Bottom ring pressure load per stay vane} = \frac{\frac{\pi(D_{bs}{}^2 - D_p{}^2)}{4} P_1 + \frac{\pi(D_p{}^2 - D_{bi}{}^2)}{4} P_2}{24}$$

Weights of components are taken from [1]:

W_R	Rotor weight per stay vane (-1364210 kg) * (9.81 m/s^2) / (1000 N/kN) / 24	-558 kN
W_{SR}	Stay ring weight (-165000 kg) * (9.81 m/s^2) / (1000 N/kN) / 24	
W_{BR_noSR}	Bottom ring, wicket gates, levers and half of the links weight (-276960 kg + 165000 kg) * (9.81 m/s^2) / (1000 N/kN) / 24	-46 kN

The axial thrust is helping to reduce the head cover load as it acts in the opposite direction than the pressure load. The minimum value of 12.109 MN measured during the model test at P = 112.4 MW and Hp = 32.26 m is therefore taken as a conservative value for the axial thrust at full power. For runaway, the model test has shown that the conservative value to use would be around 6.5 MN at beta = 28.4° and alpha = 44°.

Table 6 – Stay Ring loads per stay vane

Load Case	Stay vane #	Pressure upstream of the guide vanes (P_1)	Head cover axial force (pressure load + W_R - axial thrust)	Bottom ring axial force (-60% pressure load* + $W_{BR\ noSR}$)	Concrete force (Casing pressure load – Stator and concrete weight)
		kPa	kN	kN	kN
1. Standstill, dewatered	6	0	-558 (0-558-0)	-46 (-0.6*0-46)	-3000
2. Standstill	15	439	246 (803-558-0)	-332 (-0.6*476-46)	1336
3. Load rejection	15	504	-122 (436-558-0)	-277 (-0.6*386-46)	1733
4. Full power	15	439	671 (1733-558-505)	-517 (-0.6*785-46)	1336
5. Runaway	15	439	904 (1733-558-271)	-517 (-0.6*785-46)	1336
6. PMF levels standstill	15	499	515 (1072-558-0)	-402 (-0.6*594-46)	1702

* It is conservatively assumed that 60% of the bottom ring axial pressure load is taken by the stay ring connection while 40% is distributed on the discharge ring.

3.4 BOUNDARY CONDITIONS

Following boundary conditions are applied for all load cases:

- Nodes on the side faces of stay ring and concrete segments are coupled in all direction for cyclic symmetry
- Bottom face of the bottom concrete block is fixed in all directions
- Top face of the top concrete block is fixed in radial direction
- All faces of each anchor horizontal plate are coupled to corresponding concrete faces with gluing conditions
- Faces of each anchor vertical plate are fixed tangentially to avoid stay ring rotation
- All nodes on the bottom ring bolting circle are coupled together in the axial direction to conservatively account for bottom ring rigidity
- All nodes on the head cover bolting circle are coupled together in the axial direction to conservatively account for head cover rigidity
- RBE2 rigid elements are created on all bolt surfaces of the anchor and stay ring bolted plates in order to properly distribute the bolt load into the bolted plates. Each RBE2 middle node of the anchor bolted plate is coupled in all direction with the corresponding RBE2 middle node of the stay ring bolted plate.

All boundary conditions are shown on the model in Appendix A.

Contact surfaces are added between concrete blocks and stay ring shroud plates for the dewatered load case in order to properly transfer the loads on the stay ring.

3.5 CALCULATION RESULTS

3.5.1 STAY VANE STRESSES

Stay ring global deformations are shown in Appendix B for dewatered and full power load cases. Primary stresses in stay vanes are given in Table 7. Secondary and peak stresses are presented in Table 8. Stresses in parenthesis are in compression. Pictures of stresses in power generation load case are presented in Appendix B.

Table 7 – Stay vane primary membrane + bending stresses

Load Case	Mid-span trailing edge von Mises Stress (MPa)	Mid-span mid-chord von Mises Stress (MPa)	Mid-span leading edge von Mises Stress (MPa)
1. Standstill, dewatered	(46)	(52)	(59)
2. Standstill	38	28	12
3. Load rejection	22	31	23
4. Full power	65	33	38
5. Runaway	74	37	38
6. PMF levels standstill	53	39	16

Table 8 – Stay vane secondary bending and peak stresses

Load Case	Peak von Mises Stress (MPa)		Peak or secondary bending von Mises stress (MPa)	
	Trailing edge junction with top plate	Trailing edge junction with bottom plate	Stay vane root or nose junction with top plate	Stay vane root or nose junction with bottom plate
1. Standstill, dewatered	(353)	(165)	(285)	(276)
2. Standstill	208	398	65	105
3. Load rejection	(48)	349	(104)	99
4. Full power	492	588	88	140
5. Runaway	650	572	98	159
6. PMF levels standstill	392	453	88	150

In the case of a seismic event, the acceleration can be either horizontal or vertical. For horizontal acceleration, stresses introduced into the stay ring would be negligible as the stay ring is fixed radially and tangentially at every anchor and that only its own mass would contribute. For vertical acceleration, stresses could be higher because the acceleration of all components that are supported by the stay ring must be taken into consideration. Stresses at the dewatered condition are only for weight of components and gravity load. They can then be used to calculate the seismic stresses by scaling them by the ratio of acceleration (0.091g/1g). The maximum seismic peak stress is then 32.1 MPa. Maximum seismic stresses at full power can then be calculated and are given in Table 9.

Table 9 – Stay vane maximum secondary bending and peak stresses during seismic event

Load Case	Peak von Mises Stress (MPa)		Peak or secondary bending von Mises stress (MPa)	
	Trailing edge junction with top plate	Trailing edge junction with bottom plate	Stay vane root or nose junction with top plate	Stay vane root or nose junction with bottom plate
4. Full power + seismic loads	524 (492+32.1)	603 (588+0.091*165)	114 (88+0.091*285)	165 (140+0.091*276)

3.5.2 BOLTED ANCHORS

The anchor bolt labels are presented in the figure 3 and the reaction forces are given in Table 10. The anchor weld stresses given in Table 11 are the maximum values taken at the weld size distance from the bolted plate with two elements on the weld root. Graphical results at full power are given in Appendix B.

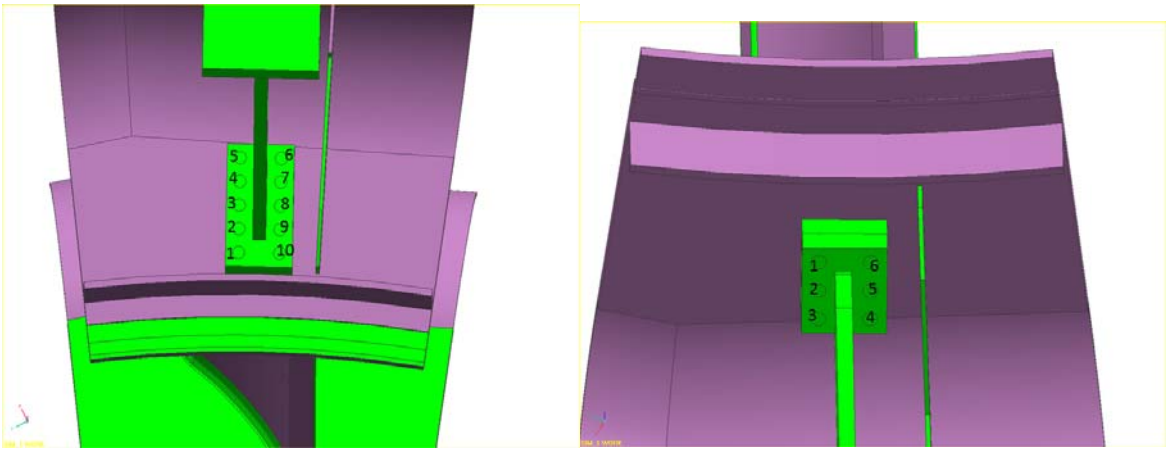

Figure 3 – Upper and lower anchor bolt labels

Table 10 – Anchor bolt reaction forces

	Bolt #	Vertical load (kN)	x load (kN)	y load (kN)	Combine horizontal load (kN)
Upper anchor	1	65	19	-7	20
	2	222	-10	-51	52
	3	275	-29	-79	84
	4	231	-47	-75	89
	5	94	-46	-45	64
	6	42	9	25	26
	7	156	47	30	56
	8	220	95	26	98
	9	238	129	26	132
	10	183	115	36	120
	total	**1726**	282	-114	**304**
Lower anchor	1	178	-10	57	58
	2	323	22	98	100
	3	240	51	90	104
	4	148	-35	-51	62
	5	229	-86	-44	96
	6	197	-104	-35	110
	Total	**1314**	-162	115	**530**

Table 11 – Anchor weld stresses at weld size distance from bolted plate

Load Case	Maximum von Mises Stress (MPa)	
	Upper anchor	Lower anchor
1. Standstill, dewatered	(62)	(55)
2. Standstill	152	193
3. Load rejection	185	219
4. Full power	178	214
5. Runaway	189	261
6. PMF levels standstill	200	299

3.6 STRESS ANALYSIS DISCUSSION

All stay vane primary bending stresses of Table 7 are lower than the corresponding allowable stress (208 MPa) given in Table 3. All stay vane secondary bending stresses of Tables 8 and 9 are lower than the allowable secondary bending stress of 416 MPa given in Table 3 accordingly to stress categorization of ASME code Division 2 (see Extract in Appendix C). Peak and anchor weld stresses will be addressed in the fatigue analysis.

4. FATIGUE ANALYSIS

4.1 METHOD

In performing the fatigue analysis, the cumulative linear damage relationship is the usual method to establish fatigue resistance of components subject to various load cycles. To simplify the calculations we have also calculated a safety factor for each load cycle. In this report, von Mises stress is used as recommended by the ASME code.

4.2 LOAD CYCLES

Five load cycles have been identified and are presented in Table 12 with their stay vane mean stresses and maximum stress amplitudes. Stress amplitudes for load cycles A, B and C are extracted from stress tensor subtraction directly in NX6 from FEA results to take account for possible stress reversal. Mean stress is conservatively taken as the yield strength minus the stress amplitude, with a minimum value of zero.

Table 12 – Load Cycles for Fatigue Analysis

Load Cycle	Load Cases	Description	Stay vane Stress Amplitude (MPa)	Stay vane Mean Stress (MPa)	Number of Cycles n_i
A	2-4-2	Start-Stop	142	118 (260 – 142)	**54750 cycles**: 2 cycles per day for 75 years
B	2-4-3-2	Load Rejection	264	0	**900 cycles**: 1 cycle per month for 75 years
C	2-4-3-5-2	Runaway	344	0	**75 cycles**: 1 cycle per year for 75 years
D	1-2-4-3-5-2-1	Dewatering	502 (650-(-353))/2	0	**75 cycles**: 1 cycle per year for 75 years
E	4	Seismic event	32.1	228	**< 1E11**

4.3 FATIGUE CURVES

For the stay vane peak stresses, fatigue curve from ASME Boiler and Pressure Vessel Code 2010, Section VIII, Division 2, Annex 3.F, fatigue curve 110.1 is used to identify the allowable stresses and cycles. The effect of maximum mean stress is already included in this curve. The fatigue curve is shown in Figure 4 and details are given in Appendix D.

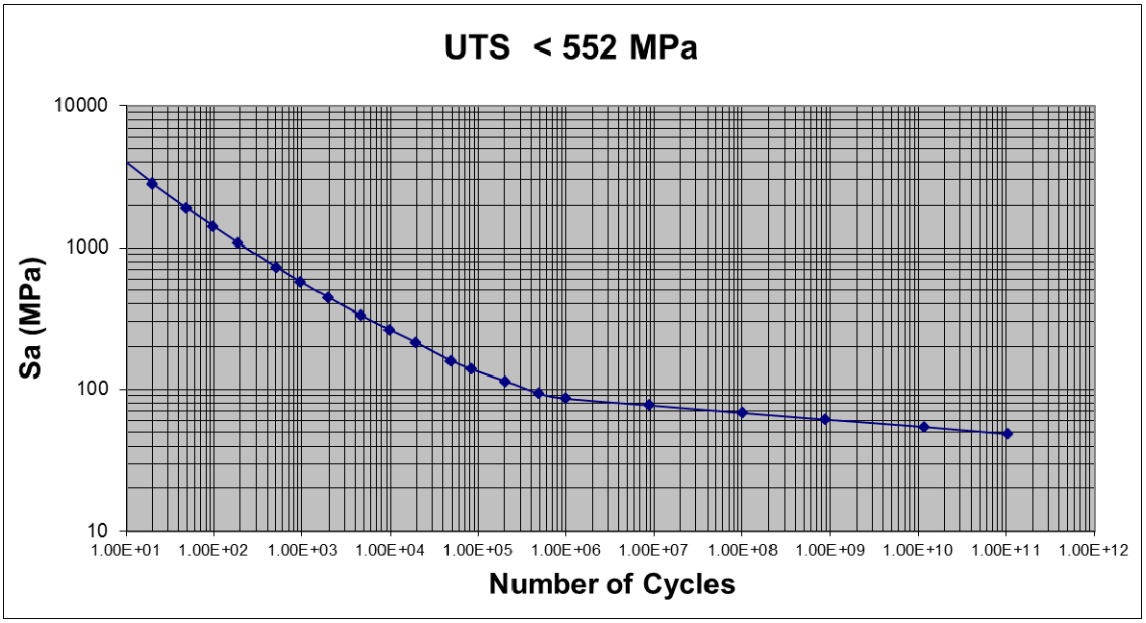

Figure 4 – ASME code fatigue curve

For the anchor weld stresses, fatigue curve from the CSA Standard W59-03 Welded Steel Construction 2003, Table 12.3, Category C, CJP, is used to identify the allowable stresses. The anchor weld fatigue curve is given in Appendix E.

4.4 STAY VANE FATIGUE SAFETY FACTORS AND CUMULATIVE DAMAGE

Table 13 – Factors of Safety on stay vane stresses for Fatigue Analysis

Load Cycle	Description	Stress Amplitude Sa (MPa)	Number of Cycles n_i	Allowable Stress Amplitude (Mpa)	Stress Safety Factor
A	Start-Stop	142	54750	155	**1.09**
B	Load Rejection	264	900	590	**2.23**
C	Runaway	344	75	1590	**4.62**
D	Dewatering	502	75	1590	**3.17**
E	Seismic event	32.1	< 1E11	48*	**1.50**

* Allowable stress for seismic event is given as the fatigue design curve value at 1.08e11 cycles.

Table 14 – Stay vane cumulative damage calculation

Load Cycle	Description	Number of Cycles n_i	Stress Amplitude Sa (MPa)	Allowable Number of Cycles N_i	Ratio n_i / N_i
A	Start-Stop	54750	142	76736	**0.71**
B	Load Rejection	900	264	9927	**0.09**
C	Runaway	75	344	4295	**0.02**
D	Dewatering	75	502	1409	**0.05**
A+B+C+D	Accumulation				**0.87**

4.5 ANCHOR WELD FATIGUE SAFETY FACTORS AND CUMULATIVE DAMAGE

Table 15 – Factors of Safety on anchor weld stresses for Fatigue Analysis

Load Cycle	Description	Stress Amplitude Sa (MPa)	Number of Cycles n_i	Allowable Stress Amplitude (Mpa)	Stress Safety Factor
A	Start-Stop	50	54750	297	**5.9**
B	Load Rejection	130	900	1170	**9.0**
C	Runaway	154	75	2678	**17.4**
D	Dewatering	316	75	2678	**8.5**
E	Seismic event	5.6	< 1E11	9.26	**1.7**

Table 16 – Anchor weld cumulative damage calculation

Load Cycle	Description	Number of Cycles n_i	Stress Amplitude Sa (MPa)	Allowable Number of Cycles N_i	Ratio n_i / N_i
A	Start-Stop	54750	50	21 952 000	**0.002**
B	Load Rejection	900	130	655 439	**0.001**
C	Runaway	75	154	394 276	**0.0002**
D	Dewatering	75	316	45 635	**0.002**
A+B+C+D	Accumulation				**0.0052**

4.6 FATIGUE ANALYSIS DISCUSSION

The safety factors exceed the requirements for reliable operation over a period of 75 years. Those calculated factors of safety indicate a robust design, tolerant even to minor non-conformances. A seismic event would not contribute to the fatigue life of the stay ring.

5. CONCLUSION

This report presents static analysis and fatigue analysis of the Muskrat Falls stay ring. All primary and secondary stresses are lower that allowable stresses while all peak and weld stresses have been considered in the fatigue analysis. The fatigue analysis shows that a reliable operation over a period of 75 years is expected.

6. REFERENCE

[1] CAL0200500030 Muskrat Falls stay vanes and anchors calculation, revision 4, June 2013

Appendix A : Finite Element Models

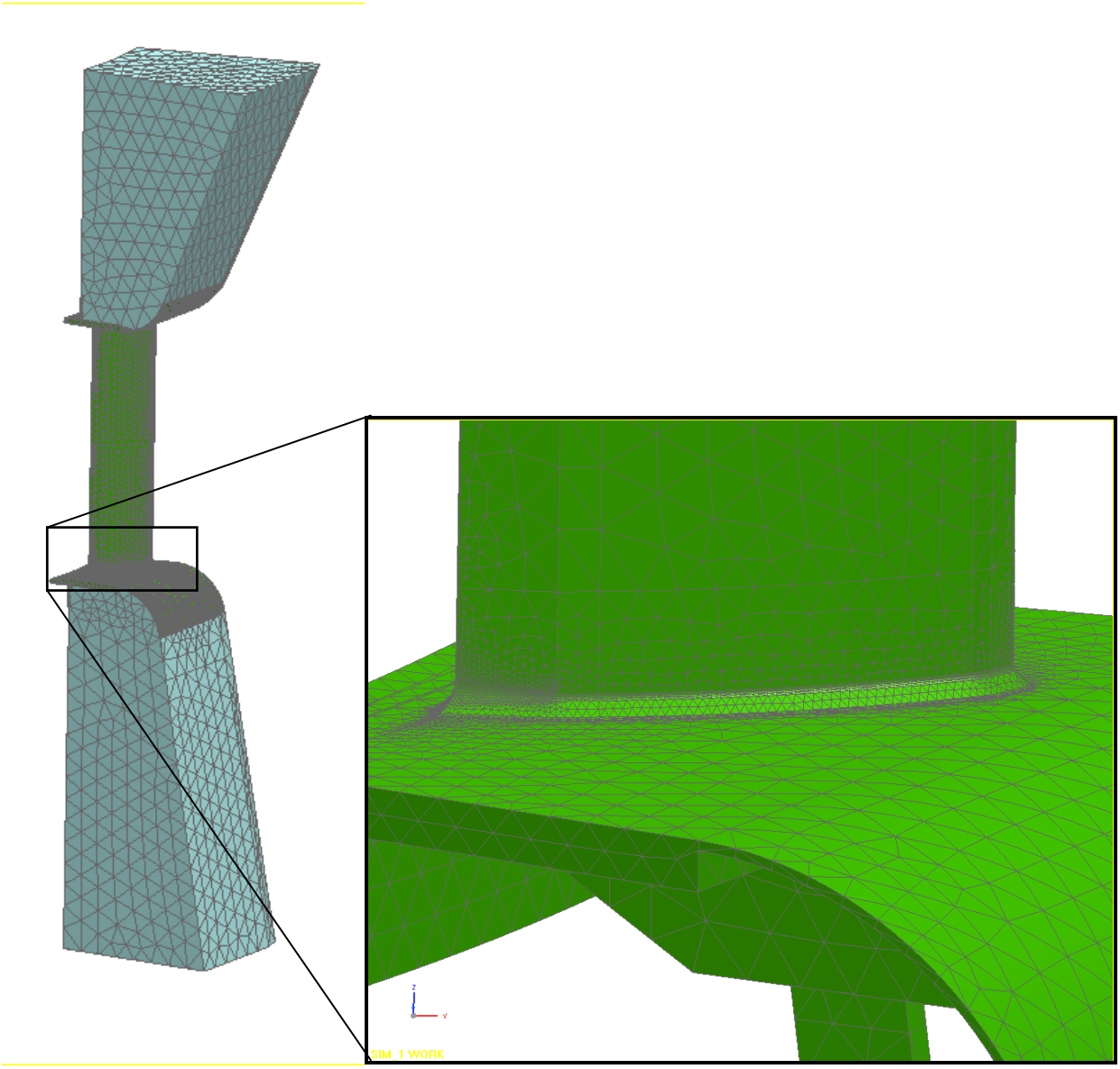

Finite element model

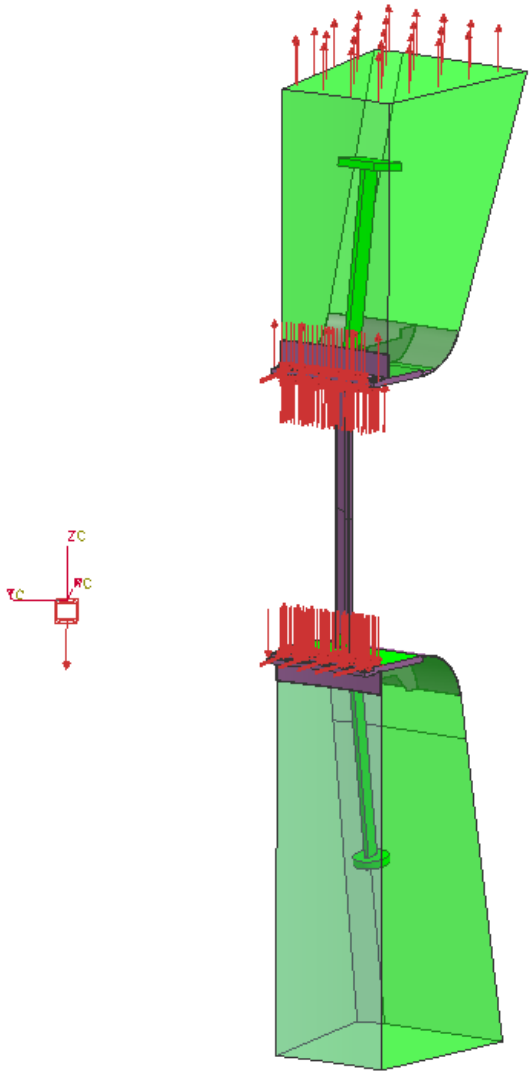

Load case 4, Full Power, applied loads

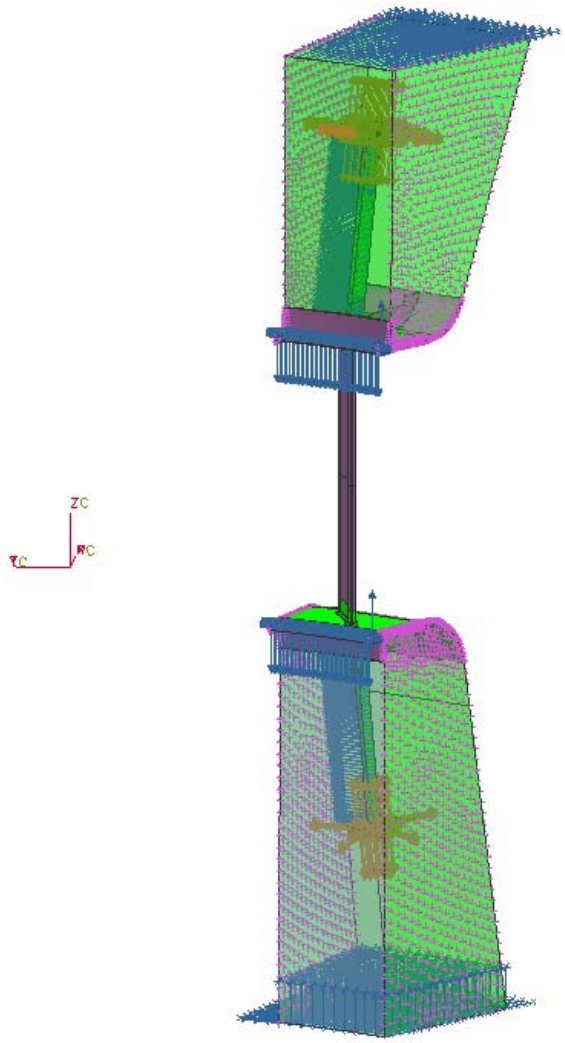

Load cases 2 to 6, boundary conditions

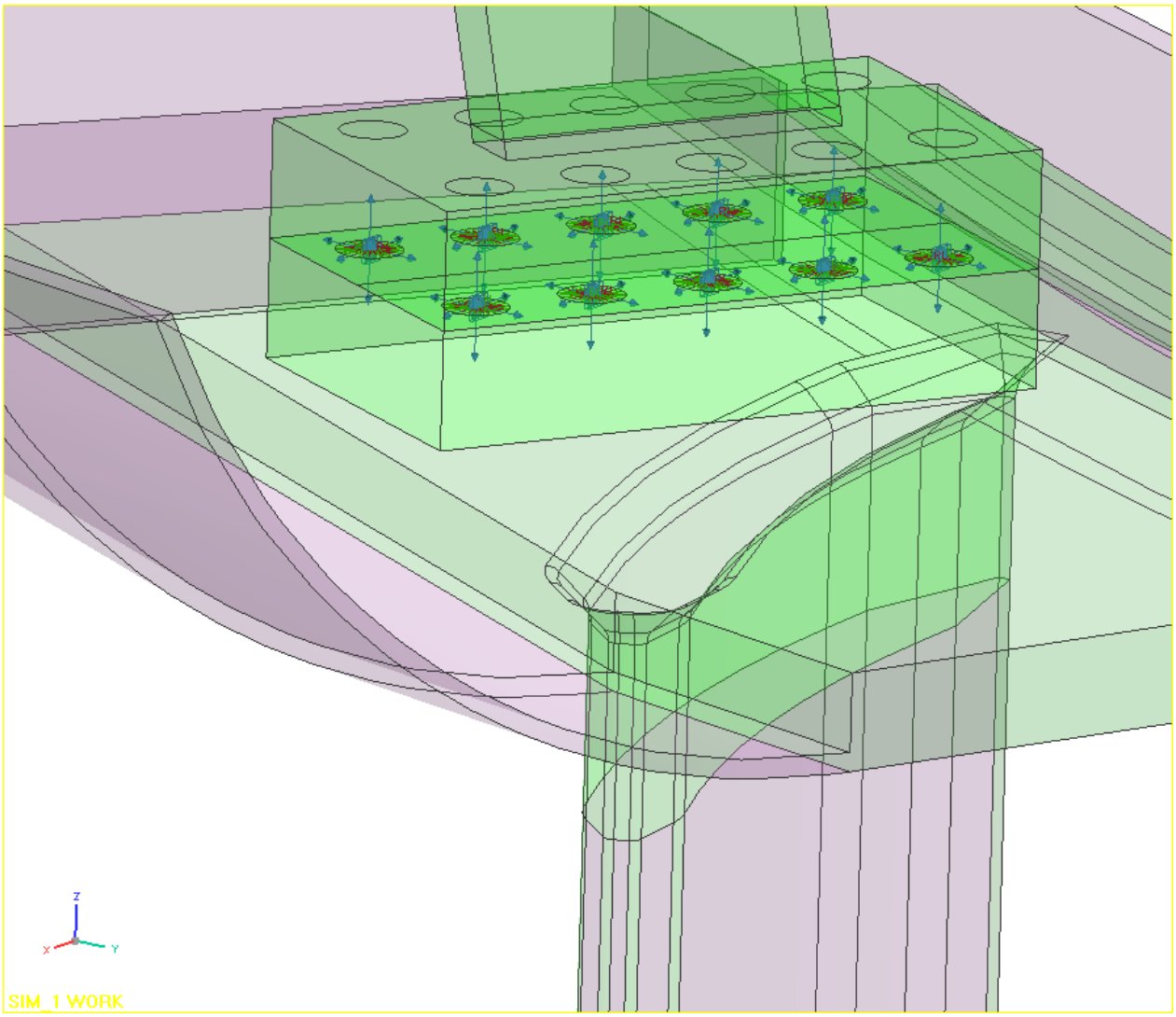

Anchor bolt connections using RBE2 rigid elements and coupled nodes

Appendix B : Stay Ring Calculation Results

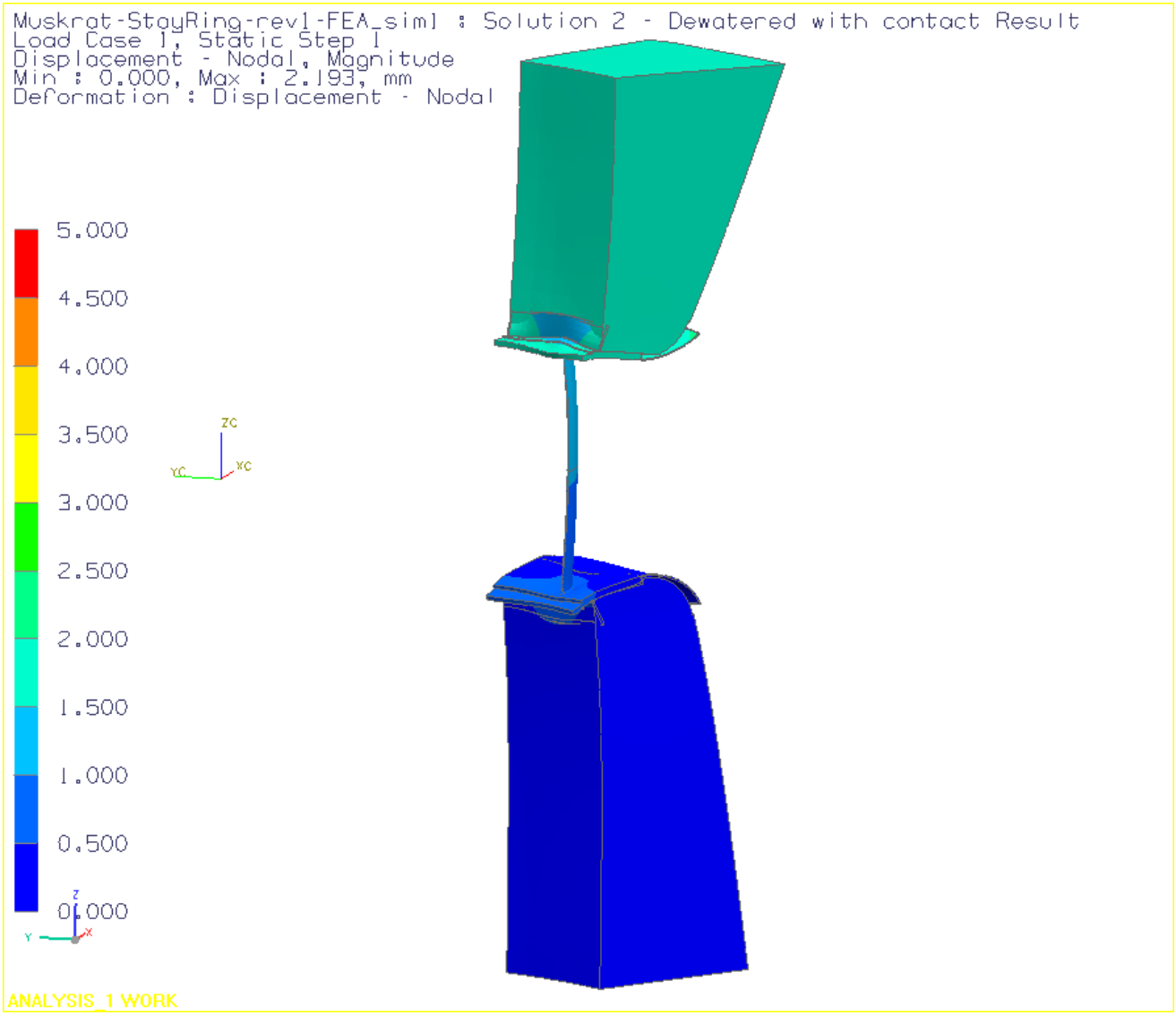

Load case 1, Dewatered, global displacement magnitude (mm)

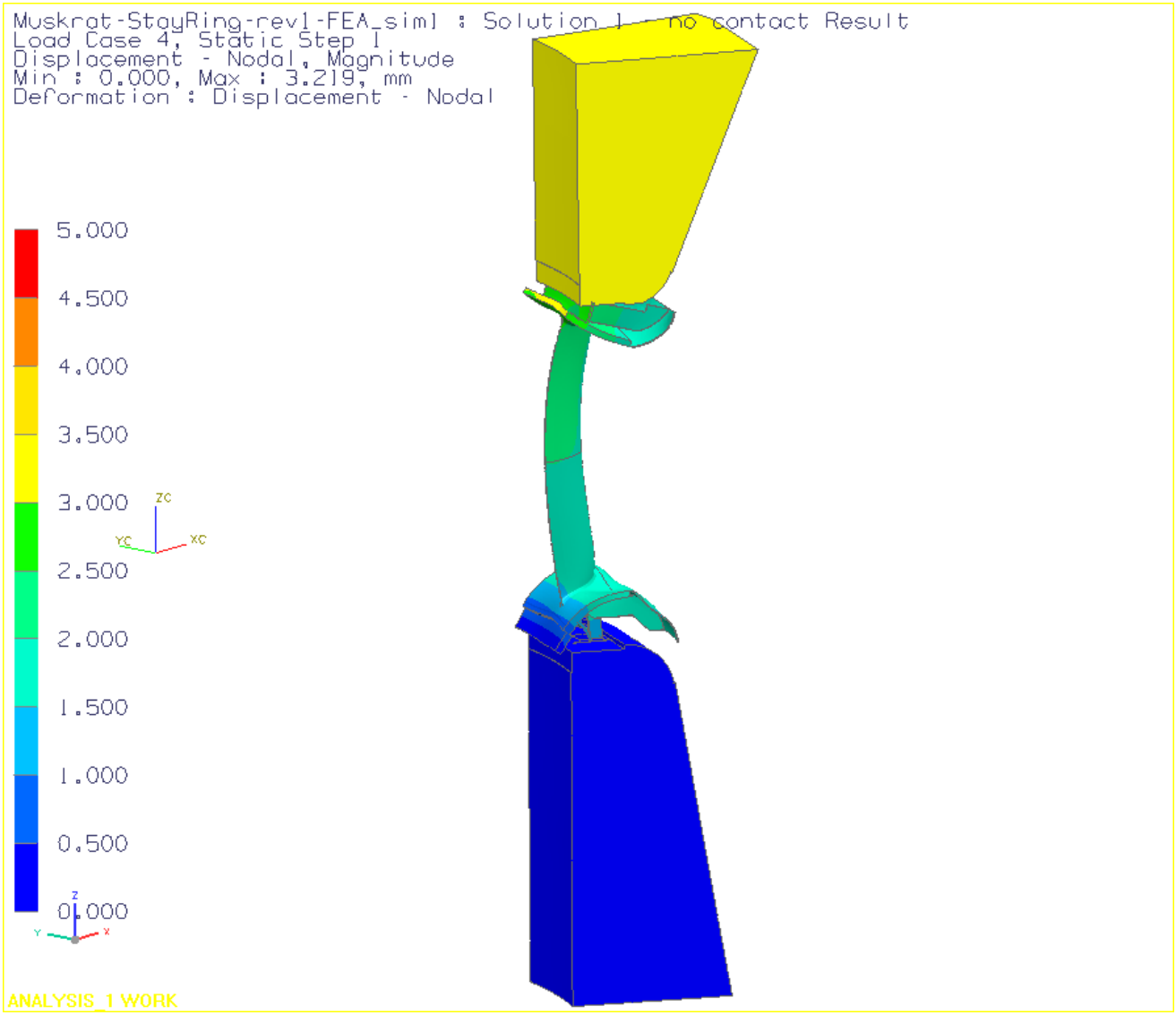

Load case 4, Full Power, global displacement magnitude (mm)

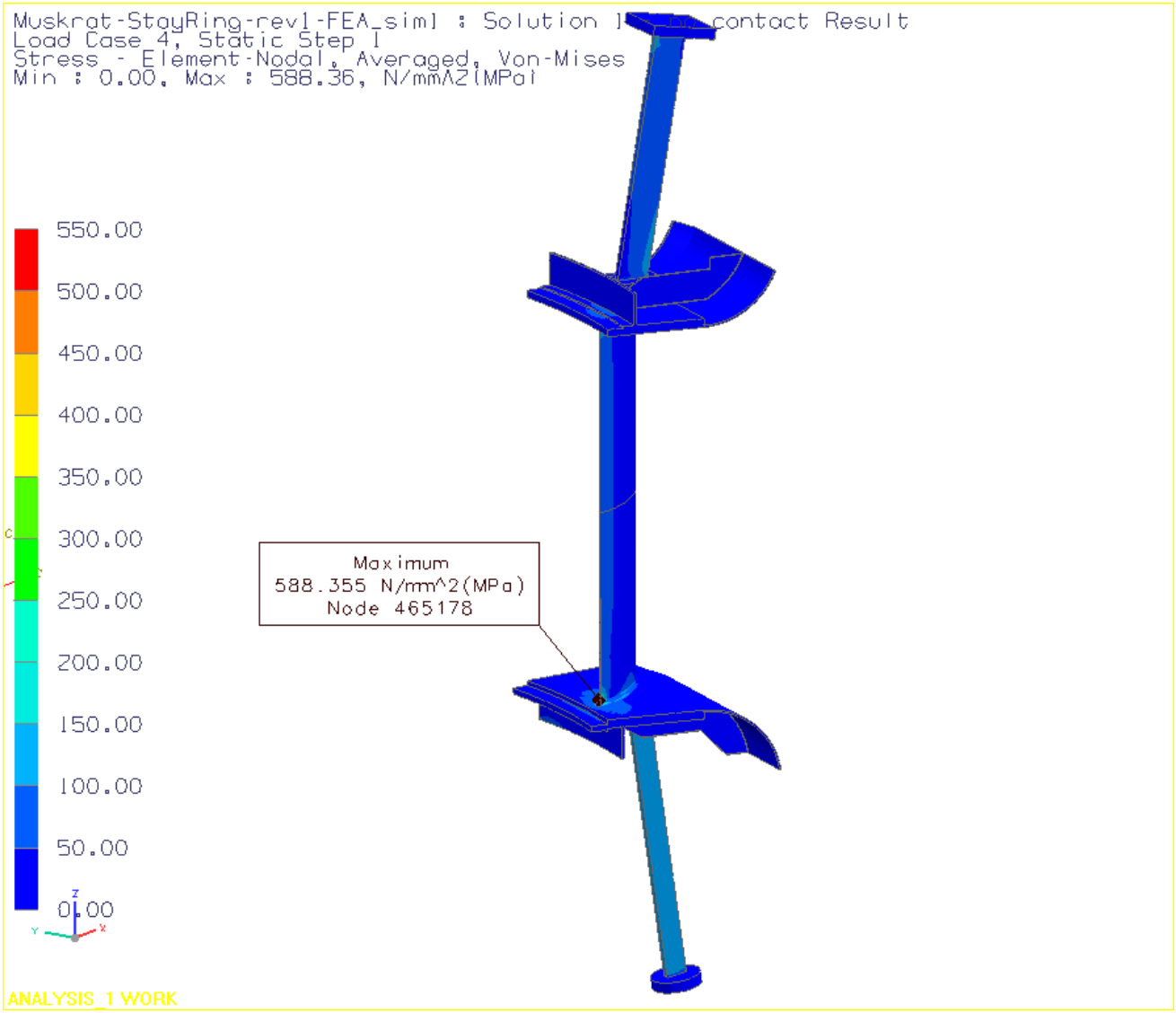

Load case 4, Full Power, global von Mises stresses (MPa)

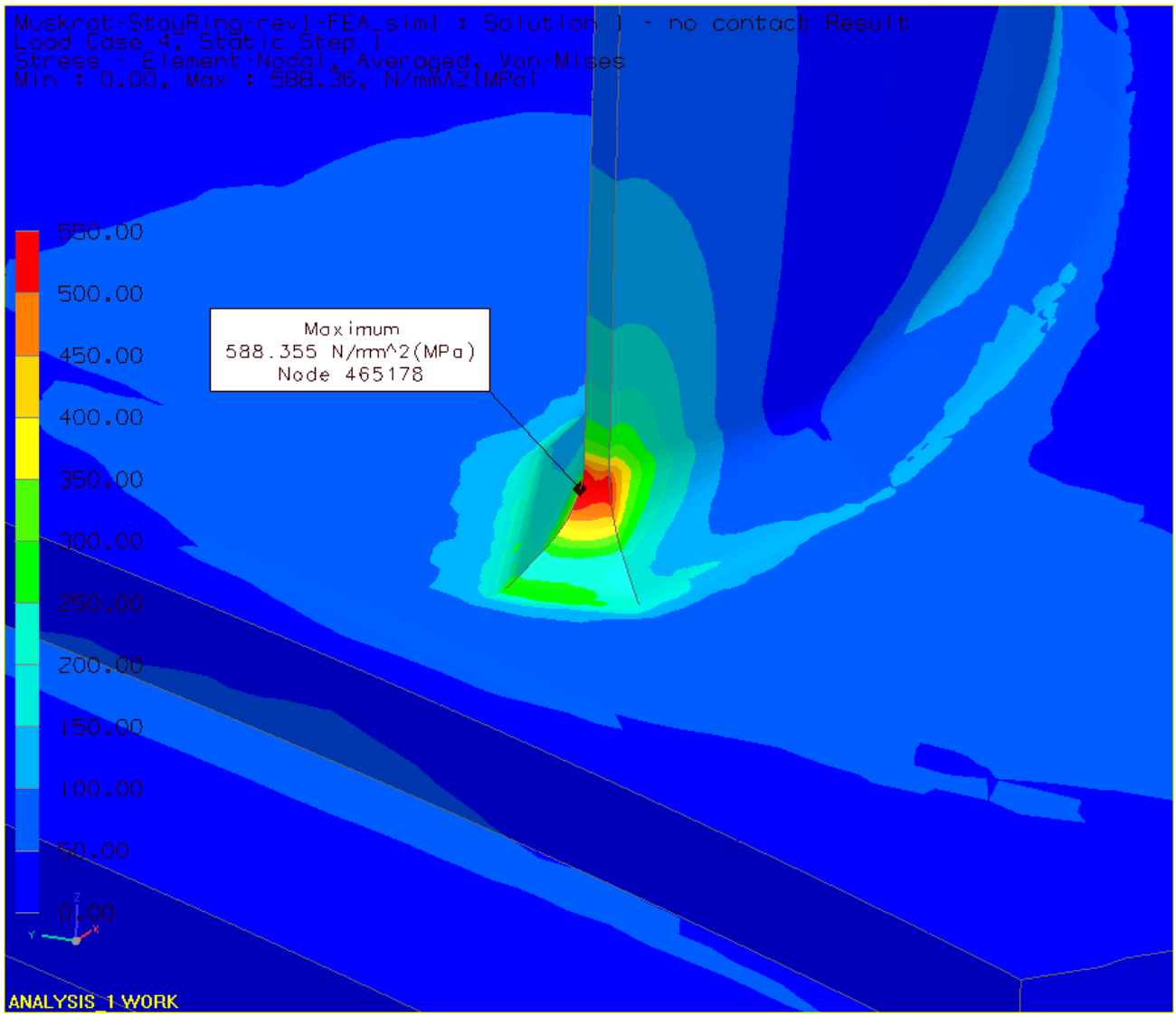

Load case 4, Full Power, local maximum von Mises stresses (MPa)

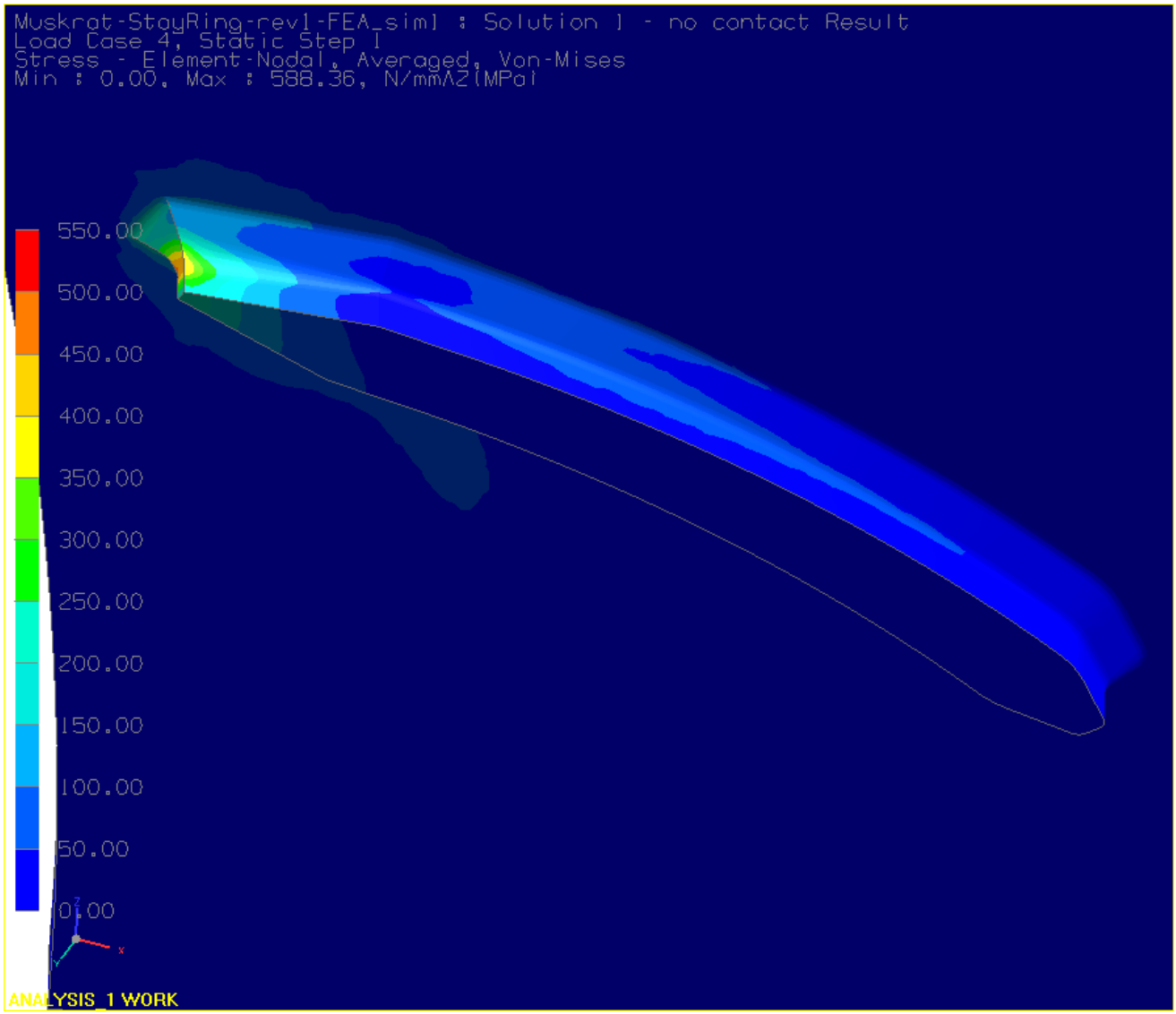

Load case 4, Full Power, von Mises stresses on horizontal section at 60 mm from top plate (MPa)

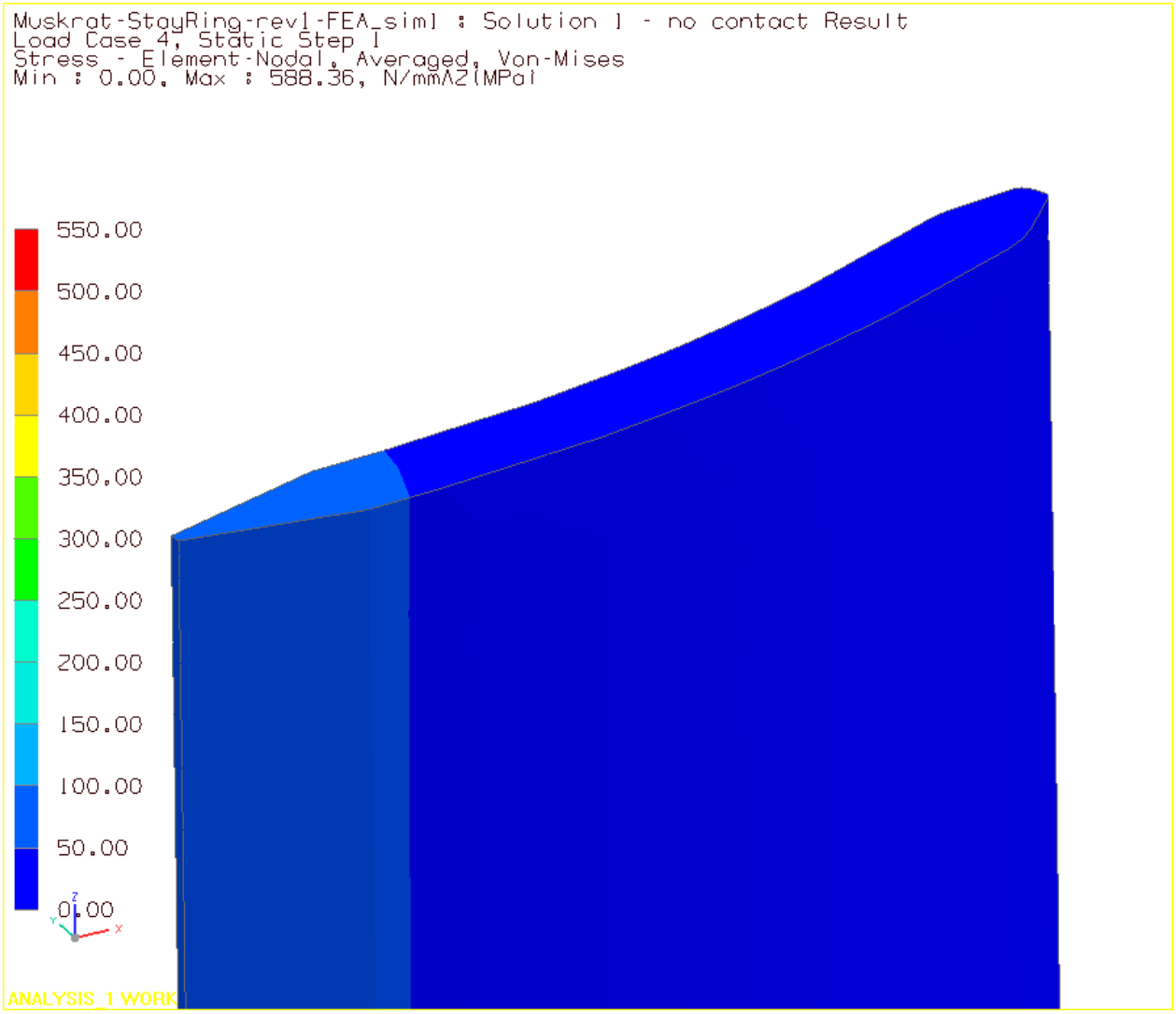

Load case 4, Full Power, von Mises stresses on horizontal section at the center of the stay vane (MPa)

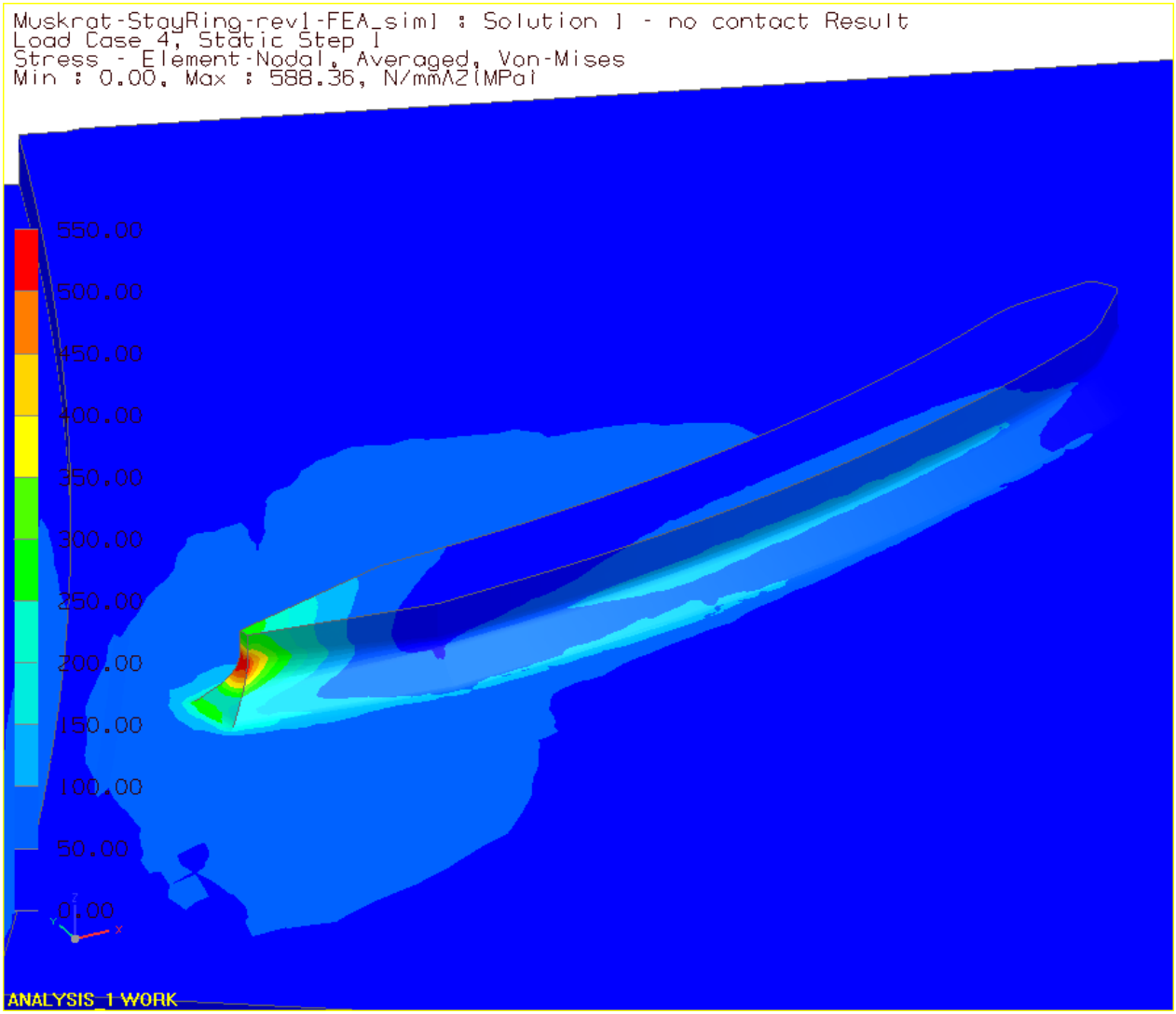

Load case 4, Full Power, von Mises stresses on horizontal section at 60 mm from bottom plate (MPa)

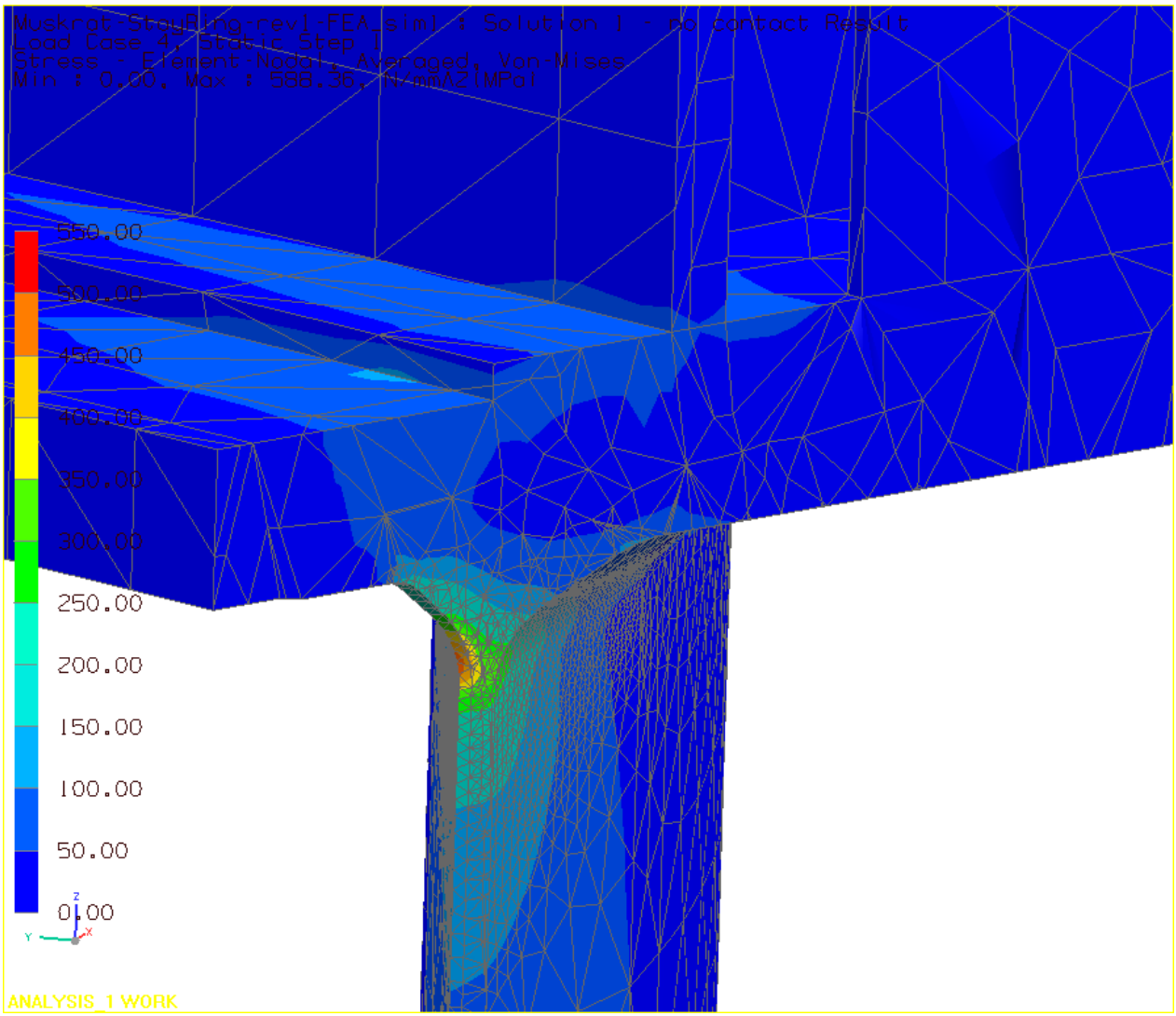

Load case 4, Full Power, von Mises stresses on cross section of the top shroud at the bolting flange to head cover (MPa)

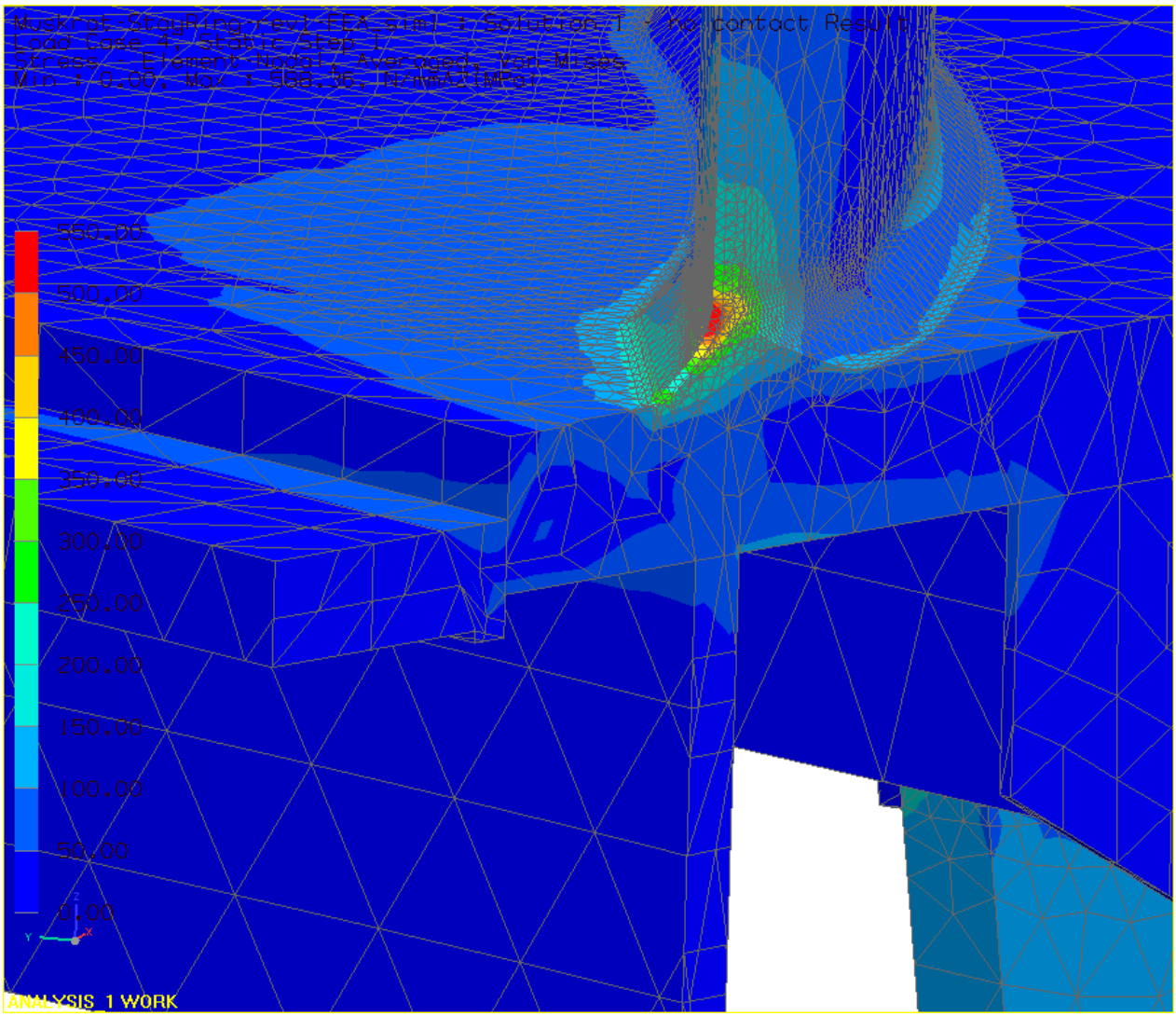

Load case 4, Full Power, von Mises stresses on cross section of the bottom shroud at the bolting flange to bottom ring (MPa)

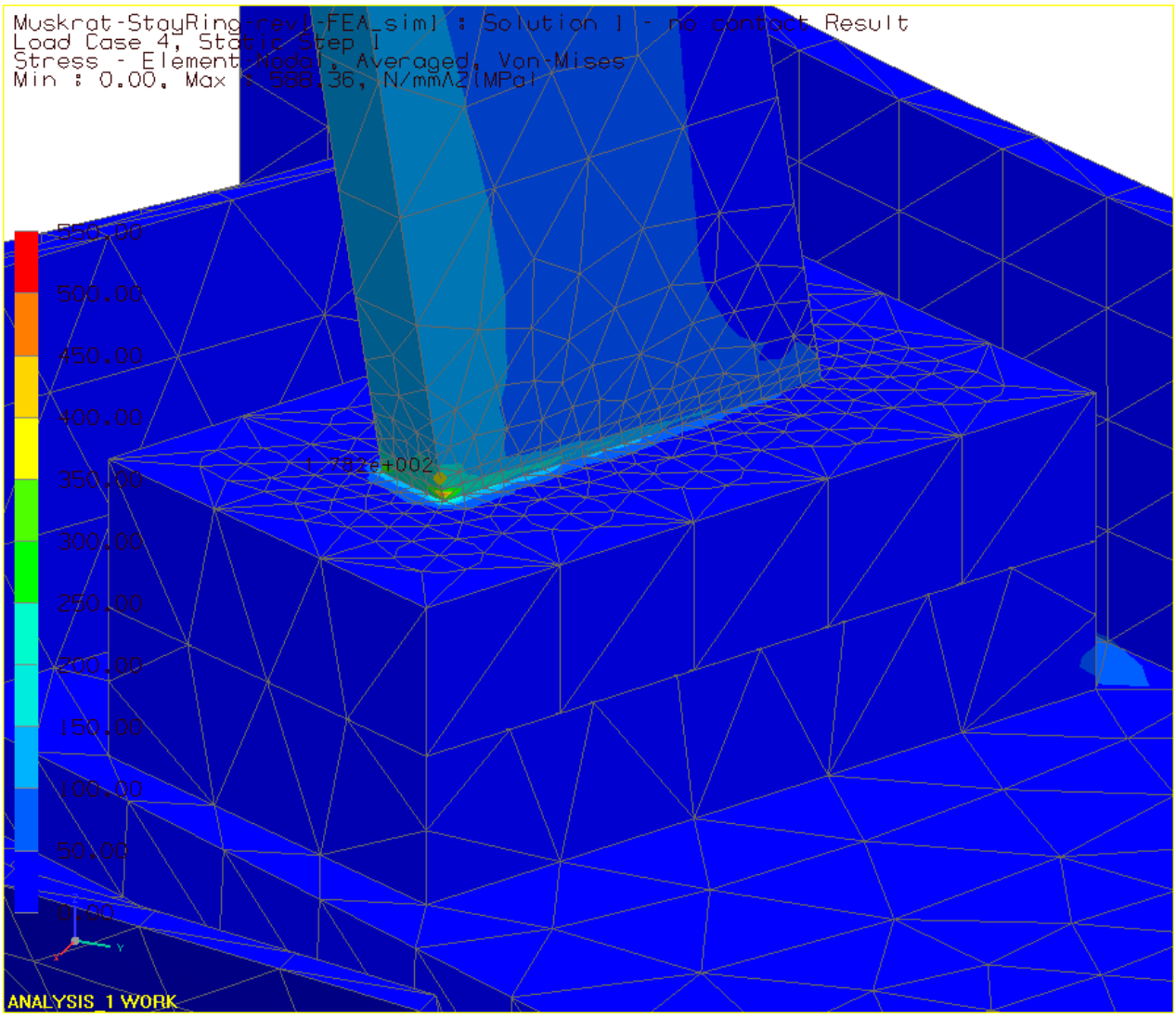

Load case 4, Full Power, von Mises stresses at the upper anchor weld (MPa)

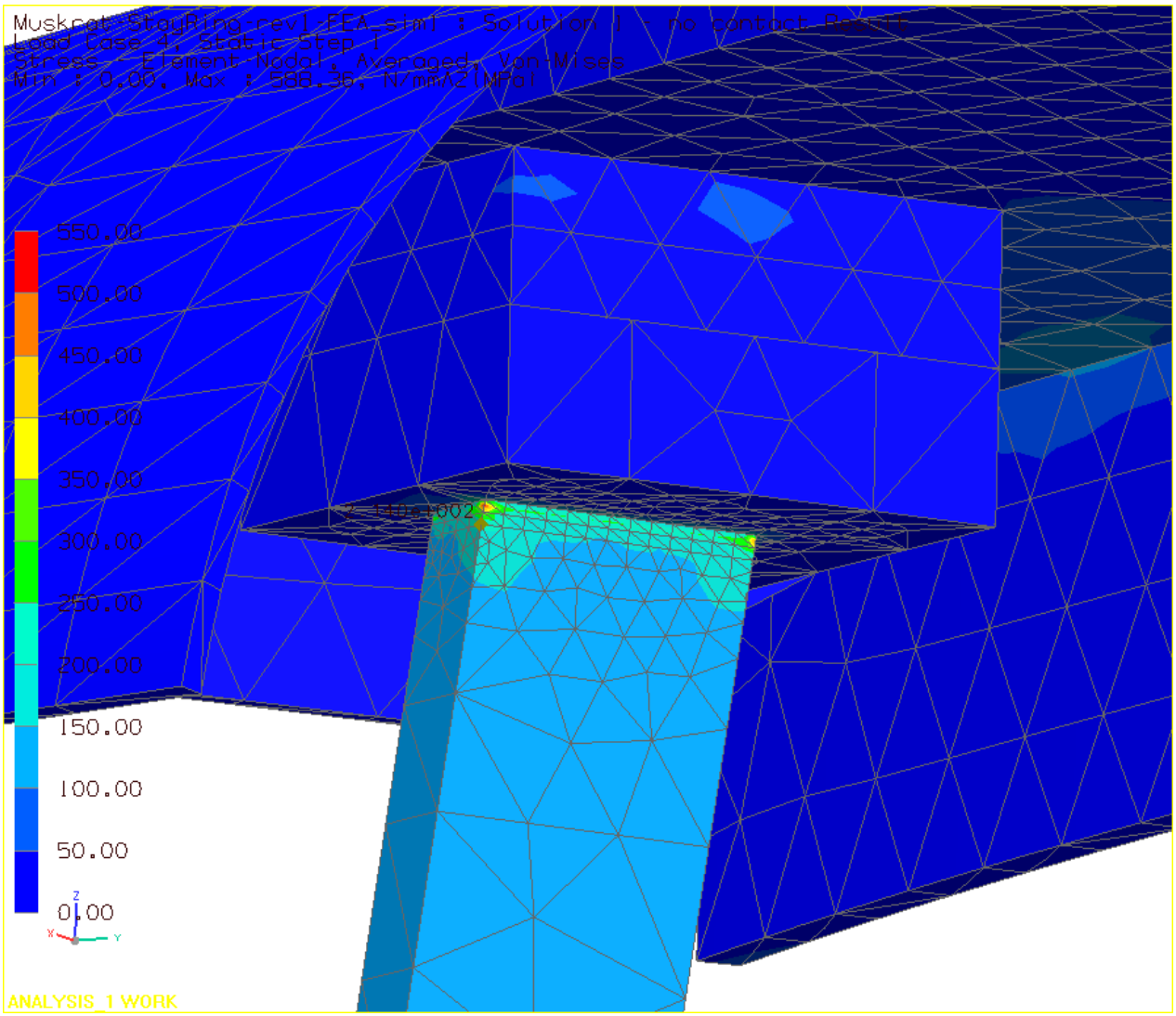

Load case 4, Full Power, von Mises stresses at the lower anchor weld (MPa)

Appendix C : Extract of 2009 ASME Boiler and Pressure Vessel Code Section VIII, Division 2, Annex 5

2007 SECTION VIII, DIVISION 2

5.15 Figures

Stress Category	Primary			Secondary Membrane plus Bending	Peak
	General Membrane	Local Membrane	Bending		
Description (For examples, see Table 5.2)	Average primary stress across solid section. Excludes discontinuities and concentrations. Produced only by mechanical loads.	Average stress across any solid section. Considers discontinuities but not concentrations. Produced only by mechanical loads.	Component of primary stress proportional to distance from centroid of solid section. Excludes discontinuities and concentrations. Produced only by mechanical loads.	Self-equilibrating stress necessary to satisfy continuity of structure. Occurs at structural discontinuities. Can be caused by mechanical load or by differential thermal expansion. Excludes local stress concentrations.	1. Increment added to primary or secondary stress by a concentration (notch). 2. Certain thermal stresses which may cause fatigue but not distortion of vessel shape.
Symbol	P_m	P_L	P_b	Q	F

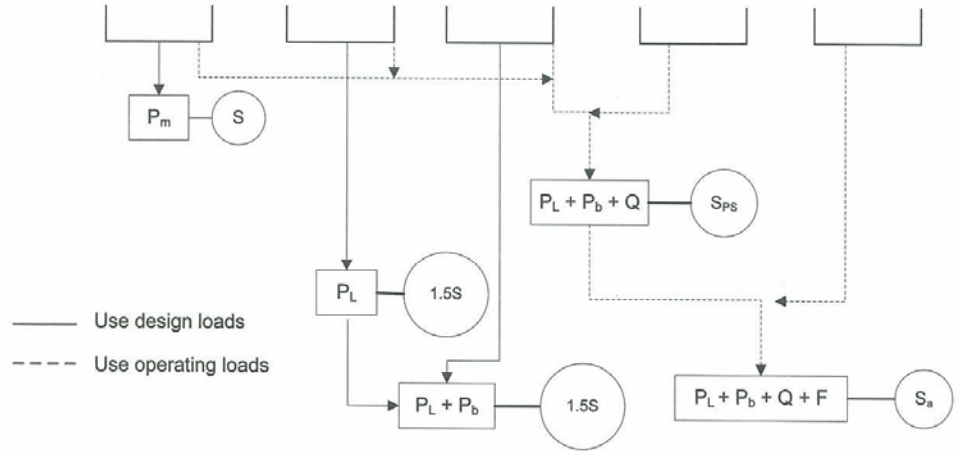

Figure 5.1
Stress Categories and Limits of Equivalent Stress

Appendix D : Extract of 2009 ASME Boiler and Pressure Vessel Code Section VIII, Division 2, Annex 3.F

ANNEX 3.F

DESIGN FATIGUE CURVES

(NORMATIVE)

3.F.1 Smooth Bar Design Fatigue Curves

3.F.1.1 Smooth bar design fatigue curves in paragraph 3.F.1.1 are provided for the following materials in terms of a polynomial function, see Equation (3.F.1). The constants for these functions, C_n, are provided for different fatigue curves as described below.

a) Carbon, Low Alloy, Series 4xx, and High Tensile Strength Steels for temperatures not exceeding 371°C (700°F) where $\sigma_{uts} \le 552\ MPa\ (80\ ksi)$ (see Table 3.F.1).

b) Carbon, Low Alloy Series 4xx, and High Tensile Strength Steels for temperatures not exceeding 371°C (700°F) where $\sigma_{uts} = 793 - 892\ MPa\ (115 - 130\ ksi)$ (see Table 3.F.2).

c) Series 3xx High Alloy Steels, Nickel-Chromium-Iron Alloy, Nickel-Iron-Chromium Alloy, and Nickel-Copper Alloy for temperatures not exceeding 427°C (800°F) where $S_a > 195\ MPa\ (28.2\ ksi)$ (see Table 3.F.3).

d) Series 3xx High Alloy Steels, Nickel-Chromium-Iron Alloy, Nickel-Iron-Chromium Alloy, and Nickel-Copper Alloy for temperatures not exceeding 427°C (800°F) where $S_a \le 195\ MPa\ (28.2\ ksi)$ (see Table 3.F.4).

e) Wrought 70-30 Copper-Nickel for temperatures not exceeding 232°C (450°F) (see Tables 3.F.5, 3.F.6, and 3.F.7). These data are applicable only for materials with minimum specified yield strength as shown. These data may be interpolated for intermediate values of minimum specified yield strength.

f) Nickel-Chromium-Molybdenum-Iron, Alloys X, G, C-4, And C-276 for temperatures not exceeding 427°C (800°F) (see Table 3.F.8).

g) High strength bolting for temperatures not exceeding 371°C (700°F) (see Table 3.F.9).

3.F.1.2 The design number of design cycles, N, can be computed from Equation (3.F.1) or Table 3.F.10 based on the stress amplitude, S_a, which is determined in accordance with Part 5 of this Division.

$$N = 10^X \cdot \left(\frac{E_T}{E_{FC}}\right) \qquad (3.F.1)$$

where

$$X = \frac{C_1 + C_3\left(\frac{S_a}{C_{us}}\right) + C_5\left(\frac{S_a}{C_{us}}\right)^2 + C_7\left(\frac{S_a}{C_{us}}\right)^3 + C_9\left(\frac{S_a}{C_{us}}\right)^4 + C_{11}\left(\frac{S_a}{C_{us}}\right)^5}{1 + C_2\left(\frac{S_a}{C_{us}}\right) + C_4\left(\frac{S_a}{C_{us}}\right)^2 + C_6\left(\frac{S_a}{C_{us}}\right)^3 + C_8\left(\frac{S_a}{C_{us}}\right)^4 + C_{10}\left(\frac{S_a}{C_{us}}\right)^5} \qquad (3.F.2)$$

3.F.3 Nomenclature

A	constant in the weld joint fatigue curve equation.
B	exponent in the weld joint fatigue curve equation.
$C_1 \rightarrow C_{11}$	equation constants used to represent the smooth bar fatigue curves.
C_{us}	conversion factor, $C_{us} = 1.0$ for units of stress in ksi and $C_{us} = 6.894757$ for units of stress in MPa.
E_{ACS}	modulus of elasticity of carbon steel at ambient temperature or 21°C (70°F).
E_{FC}	modulus of elasticity used to establish the design fatigue curve
E_T	modulus of elasticity of the material under evaluation at the average temperature of the cycle being evaluated.
f_E	environmental correction factor to the welded joint fatigue curve.
f_I	fatigue improvement method correction factor to the welded joint fatigue curve.
f_{MT}	material and temperature correction factor to the welded joint fatigue curve.
q	parameter used to determine the effect equivalent structural stress range on the fatigue improvement factor.
N	number of allowable design cycles.
S_a	computed stress amplitude from Part 5.
$\Delta S_{ess,k}$	computed equivalent structural stress range parameter from Part 5.
σ_{uts}	minimum specified ultimate tensile strength.
X	exponent used to compute the permissible number of cycles.

3.F.4 Tables

Table 3.F.1 – Coefficients for Fatigue Curve 110.1 – Carbon, Low Alloy, Series 4XX, High Alloy Steels, And High Tensile Strength Steels For Temperatures not Exceeding 371 °C (700 °F) – $\sigma_{uts} \leq 552\ MPA\ (80\ ksi)$

Coefficients C_i	$48 \leq S_a < 214 (MPa)$ $7 \leq S_a < 31 (ksi)$	$214 \leq S_a \leq 3999 (MPa)$ $31 \leq S_a \leq 580 (ksi)$
1	2.254510E+00	7.999502E+00
2	-4.642236E-01	5.832491E-02
3	-8.312745E-01	1.500851E-01
4	8.634660E-02	1.273659E-04
5	2.020834E-01	-5.263661E-05
6	-6.940535E-03	0.0
7	-2.079726E-02	0.0
8	2.010235E-04	0.0
9	7.137717E-04	0.0
10	0.0	0.0
11	0.0	0.0
Note: $E_{FC} = 195E3\ MPa\ (28.3E3\ ksi)$		

3-112

Appendix E : Extract of CSA Standard W59-03 Welded Steel Construction, 2003

Table 12.3
Fatigue Constants and F_{srt} for Various Detail Categories
(See Clause 12.3.6.6)

Detail category	Fatigue life constant				Constant amplitude threshold stress range, F_{srt}		Fatigue resistances, F_{sr} [1,2]									
	γ		γ'				N-cycles									
							For 10 000 cycles		For 100 000 cycles		For 500 000 cycles		For 1 000 000 cycles		For 2 000 000 cycles	
	Metric	(Imperial)	Metric	(Imperial)	MPa	(ksi)	MPa	(ksi)	MPa	(ksi)	MPa	(ksi)	MPa	(ksi)	MPa	(ksi)
A	8.19E+12	2.5E+10	2.23E+17	1.4E+13	165	24.0	936	136	434	63	254	37	202	29	165[3]	24[3]
B	3.93E+12	1.2E+10	4.76E+16	3.1E+12	110	16.0	732	106	340	49	199	29	158	23	125	18
B1	2.00E+12	6.1E+09	1.38E+16	8.8E+11	83	12.0	585	85	271	39	159	23	126	18	100	15
C	1.44E+12	4.4E+09	6.86E+15	4.4E+11	69	10.0	524	76	243	35	142	21	113	16	90	13
C1	1.44E+12	4.4E+09	9.92E+15	6.4E+11	83	12.0	524	76	243	35	142	21	113	16	90	13
D	7.21E+11	2.2E+09	1.66E+15	1.1E+11	48	7.0	416	60	193	28	113	16	90	13	71	10
E	3.61E+11	1.1E+09	3.47E+14	2.2E+10	31	4.5	330	48	153	22	90	13	71	10	57	8
E1	1.28E+11	3.9E+08	4.15E+13	2.6E+9	18	2.6	234	34	109	16	63	9	50	7	40	6

Notes:
(1) *Fatigue resistances are independent of the strength of the material.*
(2) *The conditions of Clause 12.3.6 shall also be satisfied.*
(3) *Limited by F_{srt}*

Table 12.4 (Continued)

General condition	Situation	Detail category	Illustrative example see Figure 12.1
Longitudinally loaded members with fillet-welded attachments	Base metal at details attached by fillet welds:		
	• when the detail length in the direction of applied stress is		
	• less than 50 mm (2 in) or stud-type shear connectors	C	13, 14, 15, 18, 20
	• between 50 mm (2 in) and 12 times the detail thickness, but less than 100 mm (4 in)	D	13, 14, 18, 20
	• greater than either 12 times the detail thickness or 100 mm (4 in)		7, 13, 14, 16, 18, 20
	• detail thickness < 25 mm (1 in)	E	
	• detail thickness ≥ 25 mm (1 in)	E1	
	• with a transition radius, R, with the end of welds ground smooth, regardless of detail length		
	• R ≥ 50 mm (2 in)	D	12
	• R < 50 mm (2 in)	E	
	• with a transition radius with end of welds not ground smooth	E	12
Transversely loaded fillet-welded attachments with welds parallel to the direction of primary stress	Base metal at details attached by fillet welds:		12
	• with a transition radius, R, with end of welds ground smooth:		
	• R ≥ 50 mm (2 in)	D	
	• R < 50 mm (2 in)	E	
	• with any transition radius with end of welds not ground smooth	E	
Fillet-welded HSS to base plate	Shear stress on fillet weld	E1	21
Tee and cruciform joints, welded both sides, in tension	• Fillet weld at toe	C (see Note(a))	19
	• Fillet weld at root	C (see Note(b))	
	• PJP groove weld at toe	C	
	• PJP groove weld at root	C	
	• CJP groove weld at toe, GTSM or backing removed		
Butt joints with backing	Transverse to load:		17
	• Tack welds inside groove	D	
	• Tack welds outside the groove	E	
	Longitudinal to load:		
	• Tack welds inside groove	B1	
	• Tack welds outside groove	E	
Plug and slot welds loaded in shear	Base metal	E	
	Weld metal	E1	

(Continued)

Nalcor Doc. Rev.	Andritz Doc. Rev.	Modification	Date	Prepared / Préparé	Appr.
C1	04	Issued for construction. Table 13, SNC input values added. Table 15, values updated. Tables 16, 17 & 18 updated. "Surge" replaced by "load rejection". Conclusion revised.	06-09-2013	Y.M.	RHLM
A1	03	Contract number and front page changed	29-10-2012	Y.M.	RHLM
---	02	Part of bottom ring weight added in load Q1. Concrete mass, center of gravity and pressure area changed from analytical calculation to 3D model values. Stay vanes numbering corrected and tables updated.	07-09-2012	Y.M.	RHLM
---	01	Design pressure corrected, general revision and clarifications added.	18-07-2012	Y.M.	RHLM
---	00	Initial release	11-06-2012	Y.M.	RHLM

PROVINCE OF NEWFOUNDLAND AND LABRADOR
PEGNL
PERMIT HOLDER
This Permit Allows
ANDRITZ HYDRO LTD
To practice Professional Engineering in Newfoundland and Labrador.
Permit No. as issued by PEGNL N0602
which is valid for the year 2013

Title / Titre

STAY VANES AND ANCHORS CALCULATION

HCM	Date	Name / Nom
Prepared by:	Sept 6, 2013	Yves Mercier, Eng.
Approved by:	Sept 6, 2013	Ricardo Libreros, Eng.

Contract / Contrat No.: 0200-183001 to 0200-183004

Part Bill / Nomenclature No.: 030

Andritz Doc. No.	Rev.	Sheet / Feuille	1
CAL0200500030	04	of / de	38

ANDRITZ Hydro

Professional Engineer's Stamp

REGISTERED PROFESSIONAL ENGINEER
PEGNL
YVES MERCIER
SIGNATURE
6 Sept 2013
DATE
NEWFOUNDLAND & LABRADOR

Client

nalcor energy
LOWER CHURCHILL PROJECT

Project

LOWER CHURCHILL PROJECT

MUSKRAT FALLS HYDROELECTRIC DEVELOPMENT

SNC·LAVALIN

NE Doc. No.	Rev.
MFA-AH-SD-3410-ME-H27-0001-01	C1

TABLE OF CONTENTS

Page

TABLE OF APPENDIXES

TABLES LIST

FIGURES LIST

1. INTRODUCTION

The tension and compression stress in the stay vanes will be calculated with the superimposed loads of the concrete, the generator and turbine weight and the hydraulic force for each of the condition considered. This calculation report will present the result of the calculation in each stay vanes and anchors.

2. STAY RING AND ANCHORS MATERIAL AND MECHANICAL PROPERTIES

Table 1 - ASTM A516M Grade 485

Material	Yield Strength Sy [MPa]	Tensile Strength Su [MPa]
ASTM A516M Grade 485	**260**	**485**

3. ALLOWABLE STRESSES

3.1 STAY VANES

3.1.1 TENSION:

In pure tension, the allowable stress used is as per the latest version of ASME Section VIII, Division 1.

$S_{allowable}$= min [2/3 Sy; 1/3.5 Su] = 138.225MPa

3.1.2 BUCKLING

The criteria for buckling is based on the buckling ratio as found by using the Euler or Johnson formula depending on the column being short or long. For Muskrat Falls, only the stay vane #4 is considered as a short column, all the others are long columns. Formulas is shown in section 4.6

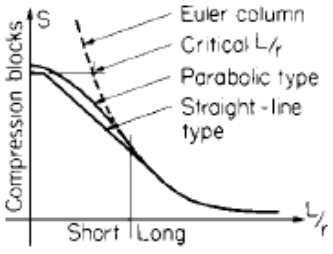

Figure 1 – Euler-Johnson buckling curve

4. LOADS

Schematic loads are shown on figure 2 with a description of it in section 4.2 and 4.3.

4.1 LOADS FOR ANCHORS

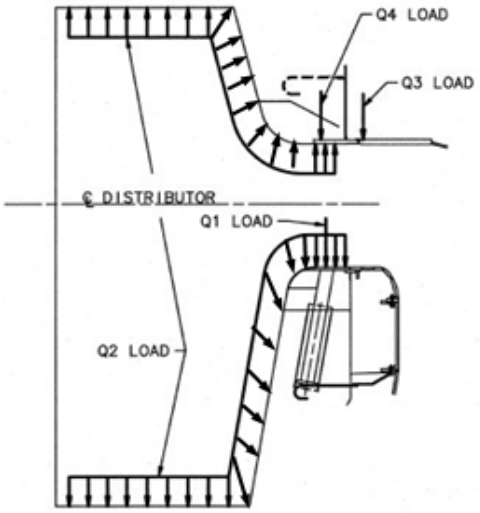

Figure 2 – Schematic Load Diagram

4.2 LOADS APPLIED ON CONCRETE

4.2.1 LOAD Q1:

The load Q1 is considered in the calculation of the lower anchors. The load Q1 is the sum of the masses of all components supported by the stay ring bottom flange. Contributing loads considered are the stay ring itself, the wicket gates, the levers and half of the links.

- Stay ring weight (preliminary estimation of finished mass)	165 000 kg
- Wicket gates weight	79 000 kg
- Part of bottom ring supported by stay ring[1]	20 200 kg
- Levers weight and half of the links	12 760 kg
Total load Q1 (applied at bottom of the stay ring)	**276 960 kg**

[1] Bottom ring weight supported by stay ring is estimated from the reaction force on the center of gravity of the bottom ring section. Estimated mass of the bottom ring is m=53525 kg. Estimated center of gravity of section is xcg=4996.14mm, bolting circle with stay ring is d1=11960mm and inner diameter is d2=8800mm. Equivalent mass of bottom ring on stay ring is m*(d1/2-xcg)/(d1/2-d2/2)≈ 20 200kg.

Wicket gates supported by the bottom ring:

Wicket gates are supported by the bottom ring. On the bottom of the wicket gate there is an autolubricant surface that will rest over an adjustable stud. After adjustment, the stud is locked in place to keep the wicket gate elevation setting. The adjustment of the wicket gates is done in a similar manner as the adjustment made when it is supported on the top by turning the adjusting bolt till the proper gap is reached. Avestaforsen (1 Kaplan unit of 23.48 MW for Fortum Generation AB in Sweden commissioned in 2007), Hunsfoss Øst (1 Kaplan unit of 14.92 MW for Agder Energi Produksjon AS in Norway, commissioned in 2007), Cheongsong (2 Francis pump-turbine units of 306.1 MW for Kowepo in Korea, commissioned in 2006) and Wuskwatim (3 Fixed blades propeller units of 69.7 MW for Manitoba Hydro in Canada, commissioned in 2012), are some of our reference projects using this configuration.

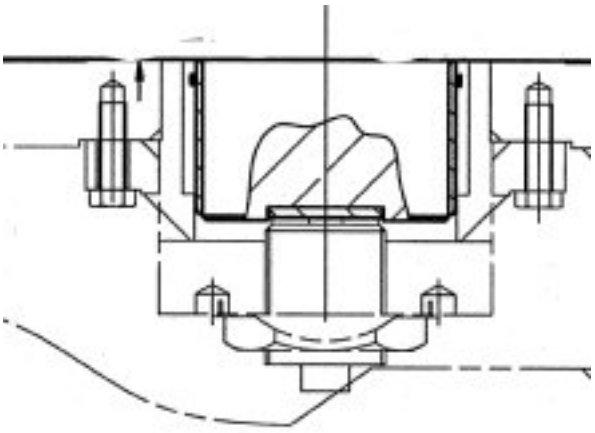

Figure 3 – Wicket gates supported by the bottom ring (Example of the Wuskwatim design)

Therefore, the weight of the wicket gates, attached levers and half of the links will be transmitted through the bottom ring to the stay ring.

4.3 LOADS APPLIED ON STAY RING

4.3.1 LOAD Q2:

Load from load rejection pressure in casing (Design pressure) Pd = 504 kPa
(15% pressure rise of maximum static head of 39-(-5.7)=44.7m at centerline of distributor)

In dewatered condition, the load Q2 is 0 kPa since there is no pressure in the casing.

4.3.2 LOAD Q3:
Load from components masses (estimation of finished mass)

Turbine[2]

- Outer head cover	70 000 kg
- Inner and intermediate head cover	86 200 kg
- Regulating mechanism (half of the links weight, stop blocks and links pins)	2 510 kg
- Guide bearing	14 000 kg
- Gate operating ring	20 600 kg
- Servomotors	21 000 kg
- Shaft seal	7 800 kg
- Thrust bearing support	32 100 kg
Total load for turbine stationary parts (W_{TS})	254 210 kg
- Turbine shaft	67 500 kg
- Kaplan Runner, mechanism and cone	260 000 kg
Total load for turbine rotating parts (W_{TR})	327 500 kg
Total load for turbine applied to head cover	**581 710 kg**

Generator

- Generator shaft	70 000 kg
- Rotor	630 000 kg
- Generator thrust bearing + thrust ring + half of Lower bracket	82 500 kg
Total load for generator applied to head cover (W_{GR})	**782 500 kg**
Total load Q3 (applied at the head cover connexion with the stay ring)	**1 364 210 kg**

[2] The wicket gates and levers load is not included here because their weights are supported by the bottom ring, it is therefore considered in the load Q1.

4.3.3 LOAD Q4:

Load through concrete and pit liner

- Pit liner	45 700 kg
- Concrete	(See details in section 4.3.4)
- Half of lower bracket and soleplates	48 250 kg
- Generator stator (frame, core, windings, coolers & piping)	249 230 kg
- Upper bracket	40 000 kg
- Generator covers	24 000 kg
Total load Q4 (applied to stay ring through concrete) (W_{GS})	**407 180 kg**

Table 2 - Summary of the loads

Variable	Definition	Load(s)	Value	Unit
W_{SR}	Weight of the stay ring and parts supported on the bottom of the stay ring.	(Q1)	276 960	kg
Pd	Load rejection pressure load	(Q2)	504	kPa
W_{HC}	Total weight through thrust bearing support and head cover (W_{TS}+W_{TR}+W_{GR})	(Q3)	1 364 210	kg
W_{GS}	Total weight through concrete and pit liner (concrete blocks W_C to be added)	(Q4 -Wc)	407 180	kg
Ww	Total weight of parts (= W_{GS} + Whc= W_{GS}+W_{TS}+W_{TR}+W_{GR})	(Q3+Q4 - Wc)	1 764 430	kg

4.3.4 CONCRETE LOAD DETAILS

The concrete load is calculated as per the concrete mass of the blocks as shown below (See Figure 4):

- Block 1 is the concrete trapped between the pit liner and the casing void
- Block 2 is the concrete between the pit liner and the casing wall
- Block 3 is the concrete between the generator lower bracket pit diameter and the casing wall
- Block 4 is the concrete between the generator pit wall and the casing wall;

Concrete blocks having complicated shapes are calculated directly by the 3D model. See figure 4 for a sectional view representation of each block.

The blocks located upstream are considered ending at the nose of the concrete entry piers. See figure 5 for more details.

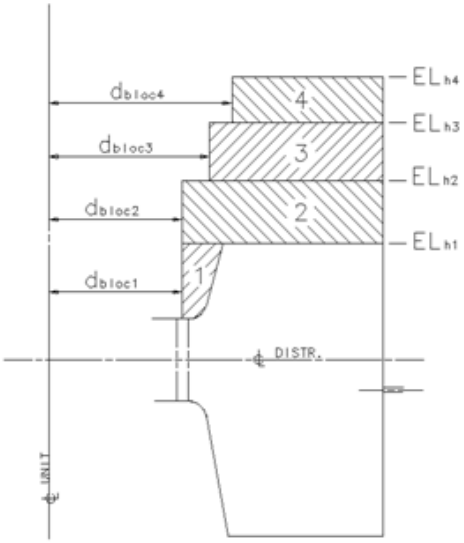

Figure 4 – Concrete blocks elevations

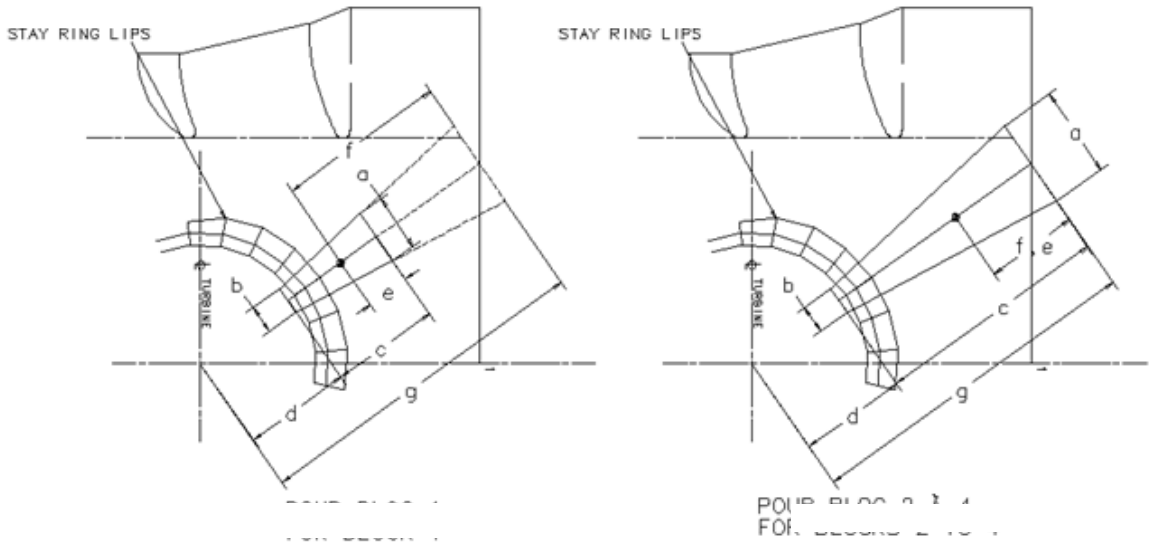

Figure 5 – Concrete blocks at entry sections[3]

[3] On blocks 2 to 4, e=f. "f" is the distance from casing wall to center of gravity and "e" is the distance between the block outer radius and the center of gravity (which is the same except for the first block).

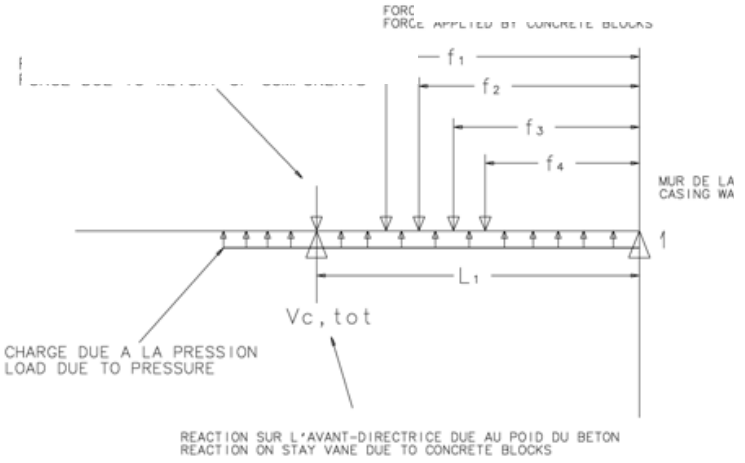

NOTE: THE LOAD REJECTION PRESSURE IS APPLIED FROM THE CASING WALL TO THE WICKET GATE CIRCLE.

Figure 6 – Reaction force on stay vanes due to concrete blocks

As shown on figure 4, the elevations and diameters are as per follow:

Table 3 - Elevations and radius of concrete blocks

EL_{h1}	Elevation of block 1 top	See table 4 for height of blocks[4]	
EL_{h2}	Elevation of block 2 top	4.75	m
EL_{h3}	Elevation of block 3 top	6.5	m
EL_{h4}	Elevation of block 4 top	15.5	m
d_{block1}	Distance from center of turbine to block 1 (pit liner)	6162.5	mm
d_{block2}	Distance from center of turbine to block 2 (pit liner)	6162.5	mm
d_{block3}	Distance from center of turbine to block 3 (lower bracket pit)	7970	mm
d_{block4}	Distance from center of turbine to block 4 (generator pit)	9000[5]	mm

To calculate the properties of each spiral casing section we used the formulas shown on page 14. For the upstream sections, some adjustments are required to some of the formulas (calculation of the first block) and for simplicity they will not be shown here as they have been directly measured on the 3D model.

[4] The elevation of block 1 is defined by the hydraulic drawing HDS0-4304 of the spiral case outline by the variable "L" for the 14 sections of the casing, where L= H-K. the height of the block will be the mean height between 2 section.

[5] Since the generator pit is square, the radius taken will vary for each of the section; 4 values will be used, with the smallest one on the axis of the unit and the biggest one on the corner of the generator pit (9077.7, 9409.6, 10542.875 & 11344.25 mm).

Table 4 - Casing dimensions

Casing section #	Height of block 1 [6] (mm)	H (Casing height) $H_{hyd,k}$ (mm)	K (Distance of casing bottom to distributor centerline) $K_{hyd,k}$ (mm)	R (Casing outside radius) $R_{hyd,k}$ (mm)	A (Casing inner top radius) $A_{hyd,k}$ (mm)
1	1325.5	N/A	N/A	12711.48	7074.13
2	2719	N/A	N/A	15730.27	7074.13
3	4668.5	N/A	N/A	13580.25	7074.13
4	5694	N/A	N/A	12693.54	7074.13
5	5521.5	N/A	N/A	12693.54	7074.13
6	5079.5	N/A	N/A	13580.25	7074.13
7	4533	N/A	N/A	15730.27	7074.13
8	4037.5	N/A	N/A	19771.8	7074.13
9	3695	N/A	N/A	16937.45	7074.13
10	3549	13900	8500	15510/15716.07[7]	8572.90
11	3527	13784	8384	15372.5	8552.45
12	3527	13512	8112	15060.8	8504.49
13	3527	13200	7800	14720.7	8449.48
14	3452	12717	7467	14376.8	8390.76
15	3302.7	12243.5	7142	14035.4	8333.45
16	3137.2	11675	6756	13616.4	8265.39
17	2941.5	11040	6330	13136.9	8190.28
18	2727.7	10393.5	5902	12635.4	8114.81
19	2512.5	9782.5	5503	12148.3	8044.45
20	2274.7	9046	5030	11544.8	7961.05
21	1968	8099	4433	10740.1	7855.78
22	1593	7063.5	3797.5	9822.6	7743.73
23	1129	5764	3026	8610	7607.69
24	669.5	5117.7	2598.2	8108.5	7532.26

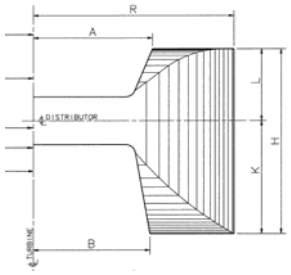

Figure 7 – Casing variables

[6] Height of block 1 is the mean height of the section as measured on the 3D model
[7] 15510mm is measured at the axis, the end of the section radius is at 15716.07mm. See figure 8 for details.

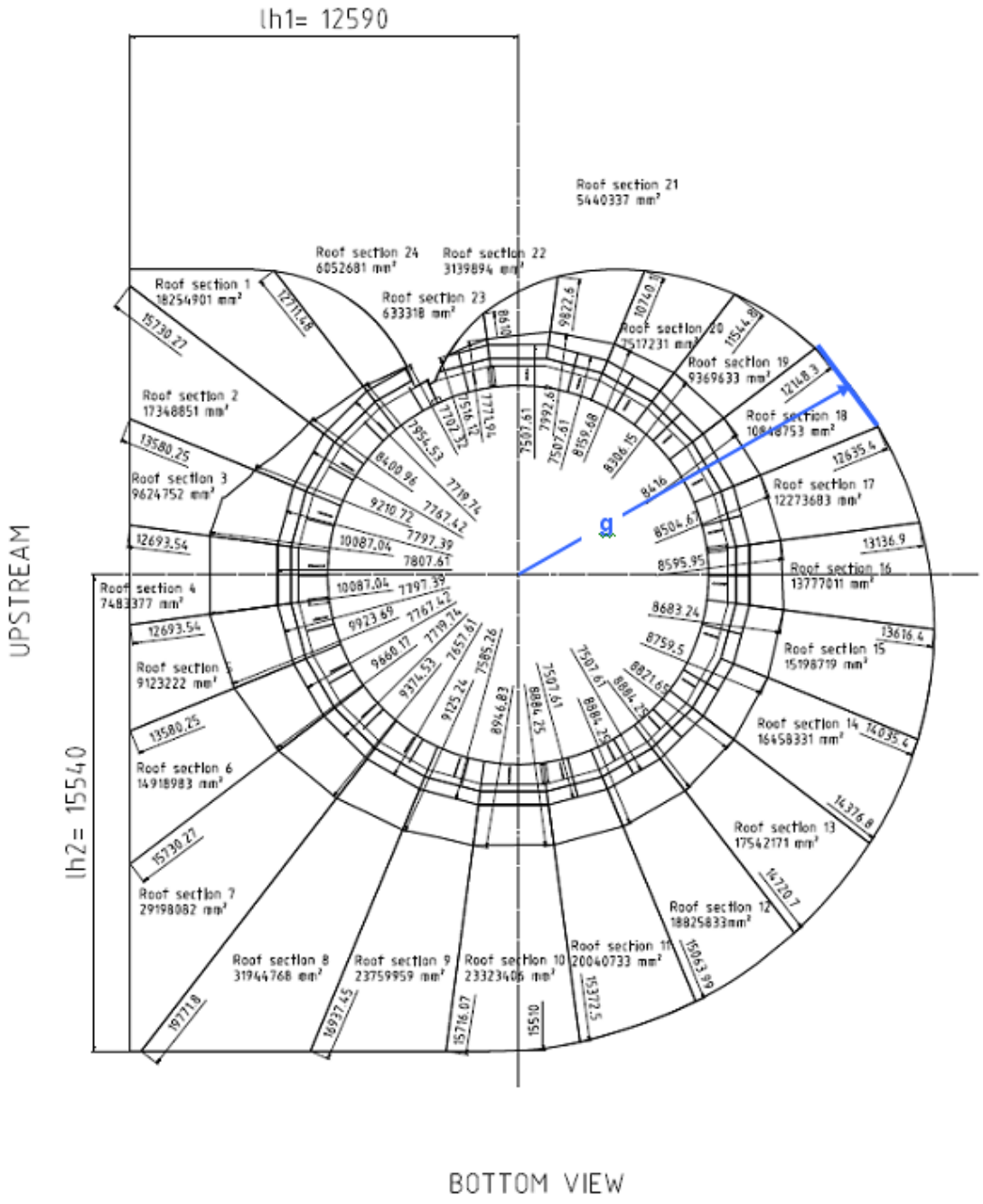

Figure 8 – Casing dimensions and areas (concrete sections)

θ_{h2}	Angle of a sector	15°
d_{wgc}	Wicket gates circle	10 682 mm
E	Distributor height	3 581 mm
t_{11}	Distributor shroud plate thickness	82.55 mm
i or No.section	Section number	(1 to 24)
l_{h1}	Distance between entry piers and units centerline (See figure 8)	12 590 mm
l_{h2}	Distance from turbine centerline and entry wall of casing (See figure 8)	15540 mm
g_i	Outer radius of concrete block (see table 4 for R values and figure 8 for details)[8] $g_i=(R_{HYD,k}+R_{HYD,k+1})/2$	(see table 6)
a_i[9]	Concrete block outer width=$2*g_i*\tan(\theta_{h2}/2)$	(see table 6)
b_i	Concrete block inner width =$2*d_i*\tan(\theta_{h2}/2)$	(see table 6)
c_i	Concrete block length - for block 1: $c_i= A_{hyd,k} -d_i$ - for block 2, 3 & 4 : $c_i= g_i - d_i$	(see table 6) (See table 4 for $A_{hyd,k}$)
d_i	Inner radius of each blocks (to flat) - for block 1 to 3 = d_{block} - for block 4 see footnote 5	(see table 6) (See table 3)
e_i	Centroïd of Section (**from outer concrete wall**) =$1/3* c_i *(a_i+2*b_i)/(a_i+b_i)$ For verification and more simple calculation, the centroid is taken directly from the 3D model. Due to the 300mm offset of upstream casing section, analytical calculations are not exact. Using real values from model is more conservative and will give slightly higher stay vanes constraints. These will be use for final values.	(see table 6)
f_i	Distance from outer concrete radius to block centroïd - for block 1: $fi=g_i-d_i-c_i+e_i$ - for block 2 to 4: fi=ei	(see table 6) (See figure 5)

[8] "g" values will be taken as the mean value between each section due to the change of radius at each of the section.

[9] Note that dimensions c,d and g are from center of the turbine perpendicular to "a" and "b". They are not the hypotenuse of the pressure surface. Thus the values of a and b are related to the tangent of the sector angle as shown.

h_i	Height of concrete blocks - For block 1: h1=((($H_{HYD,k}$ - $K_{HYD,k}$) + ($H_{HYD,k+1}$ - $K_{HYD,k+1}$))/2 –E/2- t11 - For block 2 = EL_{h2}*1000-EL_0*1000-h1 - For block 3 = EL_{h3}*1000- EL_{h2}*1000 - For block 4 = EL_{h4}*1000- EL_{h3}*1000	(See table 4 for $H_{hyd,k}$ & $K_{hyd,k}$)
$L_{1,i}$	Distance between casing wall and centroïd of stay vane = g_i- $r_{82,i}$	(See table 5 for $r_{82,i}$)
Ws	Concrete density	2.357E-5 N/mm^3
Vc_i	Concrete load on each stay vane for each block - for blocks 1 to 3 =(a_i+b_i) *c_i/2*h_i*Ws*f_i /$L_{1,i}$ - for block 4 = Vol_{block4}*Ws *f_i /$L_{1,i}$	
V_{ctot}	Total concrete load on stay vane $\sum Vc_i$	
$V_{c,tot,\ 3D}$	Total concrete load on stay vane from 3D model input = $Vol_{block1-3}$*Ws *(g_i-$centroid_{1-3}$) /$L_{1,i}$ +Vol_{block4}*Ws *(g_i-$centroid_4$) /$L_{1,i}$	

4.4 PRESSURE LOAD

$A_{p,i}$	Pressure area for a stay vane section (on concrete roof)[10] = π * ($R_{hyd,k}^2$ –(d_{wgc}/2)^2)* (θ_{h2}/360) with 3D model input: $A_{p1,I}$ (projected area of concrete roof) $A_{p2,I}$ (projected area of concrete ramp) $A_{p3,I}$ (projected area of stay ring shroud)
$f_{p,i}$	center of pressure surface to casing wall = $R_{hyd,k}$-2/3* sin(θ)/θ *($R_{hyd,k}^3$ –(d_{wgc}/2)^3)/ ($R_{hyd,k}^2$ –(d_{wgc}/2)^2) with 3D model input: $f_{p1,i}$ =gi- $centroid_1$ of area $f_{p2,i}$ =gi- $centroid_2$ of area $f_{p3,i}$ =gi- $centroid_3$ of area
pd	Design pressure at centerline of distributor (Max static pressure) = 504 kPa
p_{up}	pd - E/2 * ρ * g/1e6 = 486 kPa
g	gravitational acceleration = 9.81 m/s^2
ρ	water density = 999 kg/m^3
$p_{1,i}$	Pressure applied to the casing roof at load rejection[11] =pd-($H_{hyd,i}$-$K_{hyd,i}$)*g/1000000

[10] In order to be more precise on the roof pressure, the area calculated correspond to the radius arc on the outer part of the roof and also an arc at the wicket gates circle. The usual conservative method is to use both as flat surface leading to a bit more surface. Real projected area is taken from the 3D model and is presented in tables 10, 11 and 12.

$p_{2,i}$ $= (p_{1,i} + p_{up})/2$

$p_{3,i}$ $= p_{up}$

$F_{v,i}$ Resulting force on stay vane at load rejection (Actual calculated value, not averaged)

$$= \frac{A_{p,i} \cdot p_{1,i} \cdot f_{p,i}}{L_{1,i}}$$

$F_{v1,i}$ Resulting force on stay vane at load rejection from roof casing section

$= A_{p1,i} * p_{1,i} * f_{p1,i}/L_{1,i}$

$F_{v2,i}$ Resulting force on stay vane at load rejection from ramp casing section

$= A_{p2,i} * p_{1,i} * f_{p1,i}/L_{1,i}$

$F_{v3,i}$ Resulting force on stay vane at load rejection from stay ring shroud plate

$= A_{p1,i} * p_{1,i} * f_{p1,i}/L_{1,i}$

$F_{v\_tot,i}$ Resulting force on stay vane at load rejection (Actual calculated value, not averaged)

$F_{v\_tot,i} = F_{v1,i} + F_{v2,i} + F_{v3,i}$

4.5 FORCE IN STAY VANES

$F_{n81,ad,i}$ Force in stay vane in dewatered condition

$$= \frac{W_w \cdot 9.81}{N_v} - V_{c,tot,i}$$

$F_{n,81,ad,mean,i}$ Average force in stay vane in dewatered condition[12]

$$= \frac{F_{n81,ad,i-2} + F_{n81,ad,i-1} + F_{n81,ad,i} + F_{n81,ad,i+1} + F_{n81,ad,i+2}}{5}$$

$\sigma_{n,81,ad,i}$ Compressive stress in dewatered condition = $F_{n81,ad,mean,i}/A_{81,i}$

$F_{n81,s,i}$ Force in stay vane at load rejection

$$= F_{n81,ad,i} + F_{v,i}$$

$F_{n,81,s,mean,i}$ Average force in stay vane at load rejection

$$= \frac{F_{n81,s,i-2} + F_{n81,s,i-1} + F_{n81,s,i} + F_{n81,s,i+1} + F_{n81,s,i+2}}{5}$$

The design of the stay ring include a barrel that will rigidify the stay ring upper shroud significantly. However, the average value is based on the concrete rigidity, implying smooth transfer of load through the whole structure and not as independent blocks of concrete.

$\sigma_{n,81,s}$ Stress in stay vane at load rejection (tension) = $F_{n,81,s,mean,i}/A_{81,i}$

---

[11] Pressure on roof is corrected by the height difference between the roof and the centerline for each section. Pressure will be different on concrete casing roof section, inclined section and upper stay ring shroud.

[12] Concrete rigidity equilibrates loading between several stay vanes. This is why an average force on 5 stay vanes is calculated.

4.6 ALLOWABLE STRESSES IN STAY VANES

4.6.1 TENSION

Allowable stress in tension (As described in section 3.1.1)

$\sigma_{n,81,ad,all} = S_{allowable} = 138.225MPa$

4.6.2 BUCKLING

$Ea_{,80}$	Young modulus of steel (210 GPa)
$I_{82,i}$	Inertia of stay vane (see table 5)
$A_{81,i}$	Area of stay vane (see table 5)
Sy_{80}	Yield strength = 260 MPa
sRatio	Buckling ratio sRatio = $Ea_{80}/\sqrt{(I_{82,i}/A_{81,i})}$ (See table 10)
Cc	Delimitation between long and short column = $/\sqrt{(2*\pi^2*Ea_{80}/Sy_{80})}$= 126.27
$\sigma_{critical}$	Critical buckling stress

For sRatio < Cc (Johnson)

$$\sigma_{critical} = Sy_{80} \cdot \left[1 - \frac{sRatio^2}{2 \cdot Cc^2}\right]$$

For sRatio > Cc (Euler)

$$\sigma_{critical} = \frac{\pi^2 Ea_{80}}{sRatio^2}$$

$\sigma_{n,81,ad,all}$ Allowable stress in stay vane to avoid buckling

For sRatio < Cc

$$\sigma_{n,81,ad,all} = \frac{\sigma_{critique}}{\left[\frac{5}{3} + \frac{3}{8} \cdot \frac{sRatio}{Cc} - \frac{1}{8} \cdot \left(\frac{sRatio}{Cc}\right)^3\right]}$$

For sRatio > Cc

$\sigma_{n,81,ad,all} = \sigma_{critical}/1.92$

5. LOAD CASES

Two load cases will be examined for the calculation of the stay ring:

- Load rejection pressure (Q1+Q2+Q3+Q4)

- Dewatered condition (Q1+Q3+Q4)

The maximum pressure that can occur is used to determine the maximum force that will act upon the stay vanes.

In dewatered condition, the loads are transferred through the stay vanes producing compression stresses. The allowable buckling constraint will be the criteria of design in that condition.

We will calculate first the stay vanes stresses. Then we will do it for the upper anchors and finally for the lower anchors.

6. CALCULATIONS

6.1 STRESSES IN STAY VANES

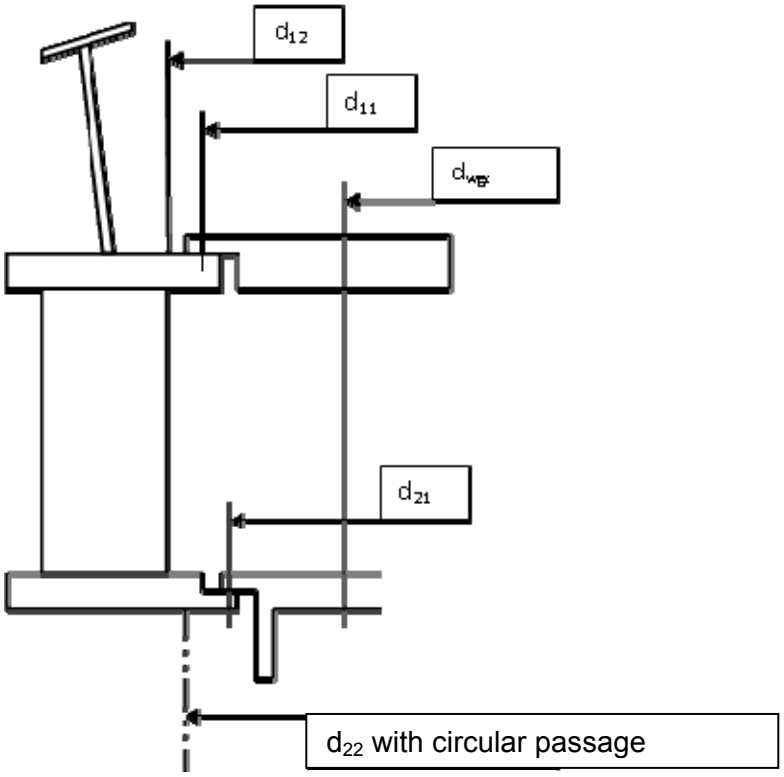

Figure 9 – Schematic of variables

Table 5 - Stay vanes properties

Stay vane #	$A_{81,i}$ Area of the stay vane cross section mm^2	$r_{82,i}$ Radius between center of the unit to stay vane center of gravity mm	$I_{82,i}$ Inertia mm^4
1	101 757	6 655.35	3.37E+08
2	93 886	6 599.81	2.07E+08
3	81 732	6 514.69	1.14E+08
4	70 324	6 462.08	5.51E+07
5	67 771	6 434.84	5.18E+07
6	78 992	6 477.86	4.35E+07
7	67 771	6 419.53	5.18E+07
8	67 771	6 419.53	5.18E+07
9	67 771	6 419.53	5.18E+07
10	67 771	6 419.53	5.18E+07
11	67 771	6 419.53	5.18E+07
12	67 771	6 419.53	5.18E+07
13	67 771	6 419.53	5.18E+07
14	67 771	6 419.53	5.18E+07
15	67 771	6 419.53	5.18E+07
16	67 771	6 419.53	5.18E+07
17	67 771	6 419.53	5.18E+07
18	67 771	6 419.53	5.18E+07
19	67 771	6 419.53	5.18E+07
20	67 771	6 419.53	5.18E+07
21	67 771	6 419.53	5.18E+07
22	67 771	6 419.53	5.18E+07
23	67 771	6 419.53	5.18E+07

An example of calculation is presented in the following pages for the first 8 vanes located in the spiral section, corresponding to stay vanes number 10 to 17.

Table 6 - Casing geometric values[13]

Casing section	Block #	Stay vane #	g	a	b	c	d	e	f
			mm	mm	mm	mm	mm	mm	mm
1	1	10	15544.3	2355.5	1622.6	2783.5	6162.5	1306.3	7904.5
	2		15544.3	4092.9	1622.6	9381.8	6162.5	4015.1	4015.1
	3		15544.3	4092.9	2098.5	7574.3	7970.0	3380.5	3380.5
	4		15544.3	4092.9	2390.2	6466.6	9077.7	2950.2	2950.2
2	1	11	15218.2	2339.3	1622.6	2721.8	6162.5	1278.8	7612.8
	2		15218.2	4007.0	1622.6	9055.7	6162.5	3888.6	3888.6
	3		15218.2	4007.0	2098.5	7248.2	7970.0	3246.5	3246.5
	4		15218.2	4007.0	2477.6	5808.6	9409.6	2676.0	2676.0
3	1	12	14892.3	2339.3	1622.6	2721.8	6162.5	1278.8	7286.9
	2		14892.3	3921.2	1622.6	8729.8	6162.5	3761.7	3761.7
	3		14892.3	3921.2	2098.5	6922.3	7970.0	3111.8	3111.8
	4		14892.3	3921.2	2776.0	4349.5	10542.9	2050.8	2050.8
4	1	13	14548.8	2339.3	1622.6	2721.8	6162.5	1278.8	6943.3
	2		14548.8	3830.8	1622.6	8386.3	6162.5	3627.2	3627.2
	3		14548.8	3830.8	2098.5	6578.8	7970.0	2969.0	2969.0
	4		14548.8	3830.8	2987.0	3204.5	11344.3	1536.2	1536.2
5	1	14	14206.1	2322.8	1622.6	2659.2	6162.5	1250.9	6635.4
	2		14206.1	3740.5	1622.6	8043.6	6162.5	3492.4	3492.4
	3		14206.1	3740.5	2098.5	6236.1	7970.0	2825.8	2825.8
	4		14206.1	3740.5	2776.0	3663.2	10542.9	1741.2	1741.2
6	1	15	13825.9	2306.4	1622.6	2597.0	6162.5	1223.2	6289.6
	2		13825.9	3640.4	1622.6	7663.4	6162.5	3342.0	3342.0
	3		13825.9	3640.4	2098.5	5855.9	7970.0	2665.7	2665.7
	4		13825.9	3640.4	2477.6	4416.3	9409.6	2068.3	2068.3
7	1	16	13376.7	2286.3	1622.6	2520.7	6162.5	1189.0	5882.4
	2		13376.7	3522.1	1622.6	7214.2	6162.5	3163.1	3163.1
	3		13376.7	3522.1	2098.5	5406.7	7970.0	2475.1	2475.1
	4		13376.7	3522.1	2390.2	4299.0	9077.7	2012.3	2012.3
8	1	17	12886.2	2263.4	1622.6	2433.5	6162.5	1149.9	5440.1
	2		12886.2	3393.0	1622.6	6723.7	6162.5	2966.3	2966.3
	3		12886.2	3393.0	2098.5	4916.2	7970.0	2264.9	2264.9
	4		12886.2	3393.0	2477.6	3476.6	9409.6	1647.9	1647.9

[13] This table is not use with 3D input values, except “g” value.

Table 7 - Concrete load (3D model input values)

Casing section	$Vol_{block1-3}$ Volume of the blocks 1 to 3	$centroid_{1-3}$ of the concrete blocks 1 to 3 (from center of the unit)	Vol_{block4} Volume of the blocks 4	$centroid_4$ of the concrete blocks 4 (from center of the unit)
	mm^3	mm	mm^3	mm
1	1.77231E+11	10706.0	8320048591	13464.9
2	1.39068E+11	10353.9	6.622E+10	12567.7
3	98275295120	9423.2	1.1681E+11	11274.6
4	91623197478	9191.7	9.3472E+10	10897.3
5	97773096640	9421.3	8.7102E+10	11274.6
6	1.23063E+11	10249.7	9.3472E+10	12567.7
7	1.90264E+11	12183.0	1.1681E+11	15415.6
8	2.26592E+11	12645.1	1.6586E+11	15115.7
9	1.99185E+11	11702.7	6.0585E+10	11352.8
10	2.07489E+11	11268.0	2.8732E+10	10816.1
11	1.7867E+11	11148.6	2.951E+10	10919.5
12	1.70696E+11	10965.6	2.5505E+10	11497.3
13	1.63385E+11	10771.6	2.5188E+10	12642.5
14	1.56893E+11	10580.6	2.7691E+10	11317.6
15	1.49042E+11	10366.3	2.6033E+10	10408.8
16	1.38845E+11	10130.4	2.1761E+10	10044.9
17	1.29471E+11	9853.3	2.1761E+10	10126.1
18	1.20346E+11	9590.8	2.1266E+10	10942.8
19	1.10903E+11	9293.4	2.2351E+10	11771.9
20	94574341272	8909.2	3281654531	10667.5
21	94574341272	8909.2	1.6026E+10	9707.9
22	75691188340	8419.2	2.2114E+10	9285.2
23	23675140166	7685.5	502318082	0.0
24	23320151550	7100.4	0	11498.2

Table 8 - Concrete load

Casing section	Block #	H Height of the block	L1 Distance from the casing wall to stay vane center	V_{ci} Concrete load per block applied on the stay vane	$V_{c,tot}$ Concrete load (total analytical)	$V_{c,tot,\ 3D}$ Concrete load (total 3D input)
		mm	mm	N	N	N
1	1	3527.0	9125	401.20E+3	2.38E+6	2.65E+6
	2	5050.0		1.40E+6		
	3	1750.0		358.31E+3		
	4	9000.0		218.96E+3		
2	1	3527.0	8799	387.80E+3	2.25E+6	2.24E+6
	2	5050.0		1.34E+6		
	3	1750.0		336.76E+3		
	4	9000.0		211.54E+3		
3	1	3527.0	8473	385.47E+3	2.12E+6	2.10E+6
	2	5050.0		1.28E+6		
	3	1750.0		315.64E+3		
	4	9000.0		145.50E+3		
4	1	3527.0	8129	382.82E+3	2.01E+6	1.94E+6
	2	5050.0		1.21E+6		
	3	1750.0		293.82E+3		
	4	9000.0		112.18E+3		
5	1	3377.0	7787	363.70E+3	1.94E+6	1.94E+6
	2	5200.0		1.17E+6		
	3	1750.0		272.53E+3		
	4	9000.0		145.95E+3		
6	1	3228.5	7406	337.27E+3	1.87E+6	1.89E+6
	2	5348.5		1.13E+6		
	3	1750.0		249.46E+3		
	4	9000.0		171.35E+3		
7	1	3046.0	6957	308.03E+3	1.76E+6	1.77E+6
	2	5531.0		1.08E+6		
	3	1750.0		222.97E+3		
	4	9000.0		148.36E+3		
8	1	2837.0	6467	275.76E+3	1.63E+6	1.65E+6
	2	5740.0		1.03E+6		
	3	1750.0		195.01E+3		
	4	9000.0		130.71E+3		

Table 9 - Force at load rejection pressure (Analytical calculations and comparison with 3D model input and calculation results)

Casing section	Load rejection pressure				
	Area on concrete roof sector (15°) (concrete roof)	center of pressure surface to casing wall	pressure @ concrete roof	Maximum Force on stay vane at load rejection from analytical calculation (Actual calculated value)	Maximum Force on stay vane at load rejection from 3D input
	A_p	f_p	p1	Fv (analytical)	Fv (3D)
	mm2	mm	Mpa	N	N
1	27 755 162	4386	0.451	6 040 299	6 895 820
2	27 199 317	4333	0.451	5 937 809	5 849 443
3	25 957 595	4213	0.451	5 708 378	5 615 143
4	24 631 752	4081	0.451	5 462 659	5 372 038
5	23 321 888	3948	0.452	5 236 138	5 143 388
6	22 052 170	3815	0.454	5 014 594	4 892 221
7	20 535 553	3650	0.456	4 747 434	4 601 863
8	18 856 344	3461	0.458	4 448 274	4 293 134

Table 10 - Force at load rejection pressure on roof (3D model input and calculations)

Casing section	Load rejection pressure			
	Area on concrete roof sector (15°) (concrete roof)	center of pressure surface to casing wall	pressure @ concrete roof	Maximum Force on stay vane at load rejection (Actual calculated value)
	A_{p1}	f_{p1}	p1	Fv1
	mm2	mm	Mpa	N
1	23323406	3118.119166	0.451026	3594719.824
2	20040733	2953.638064	0.451026	3034262.891
3	18825833	2801.120219	0.451026	2807112.411
4	17542171	2671.51428	0.451026	2600120.894
5	16458331	2541.953451	0.4524975	2431215.062
6	15198719	2406.986341	0.453954285	2242267.009
7	13777011	2245.9731	0.45574461	2026989.982
8	12273683	2070.956493	0.4577949	1799448.769

Table 11 - Force at load rejection pressure on casing ramp (3D model input and calculations)

Casing section	Load rejection pressure			
	Area on concrete ramp sector (15°) (concrete roof)	center of pressure surface to casing wall	pressure @ concrete ramp	Maximum Force on stay vane at load rejection (Actual calculated value)
	A_{p2}	f_{p2}	p2	Fv2
	mm2	mm	Mpa	N
1	4174588	0.468730598	7576.400955	1624720.507
2	3640601	0.468730598	7250.111203	1406118.122
3	3650396	0.468730598	6921.952895	1397861.68
4	3577695	0.468730598	6595.016699	1360484.633
5	3427878	0.469466348	6287.083236	1299370.017
6	3274906	0.47019474	5942.447317	1235482.338
7	3089307	0.471089903	5536.6345	1158193.769
8	2888840	0.472115048	5093.418866	1074245.104

Table 12 - Force at load rejection pressure between wicket gates and casing ramp on stay ring shrouds (3D model input and calculations)

Casing section	Load rejection pressure			
	Area on concrete roof sector (15°) (concrete roof)	center of pressure surface to casing wall	pressure @ concrete roof	Maximum Force on stay vane at load rejection (Actual calculated value)
	A_{p3}	f_{p3}	pup	Fv3
	mm2	mm	Mpa	N
1	2837552	0.486435195	9316.977631	1676379.818
2	2837552	0.486435195	8982.157842	1409062.48
3	2837552	0.486435195	8656.257842	1410169.376
4	2837552	0.486435195	8312.662842	1411432.482
5	2837552	0.486435195	7970.012842	1412803.128
6	2837552	0.486435195	7589.812842	1414472.412
7	2837552	0.486435195	7140.562842	1416680.024
8	2837552	0.486435195	6650.062842	1419440.613

Table 13 - Stresses in stay vanes at load rejection pressure (with Fv (3D) & concrete load from 3D model)

Stay vane number	Casing section	Max casing pressure condition (Load rejection) (Tension verification)			
		$F_{n,81,s}$ (Force in stay vanes)	**$F_{n,81.s.mean}$[14] (averaged forces)**	$\sigma_{n,81,s}$ (Stay vanes)	**$F_{n,FEA,SNC}$[15]**
		N	**N**	Mpa	**N**
1		2.21E+6	**1.66E+6**	34.87E+0	-0.85E+6
2		2.17E+6	**1.72E+6**	32.46E+0	-0.69 E+6
3		1.71E+6	**1.86E+6**	32.46E+0	-0.46 E+6
4		1.52E+6	**1.94E+6**	27.51E+0	-0.30 E+6
5		1.69E+6	**2.20E+6**	32.46E+0	-0.27 E+6
6		2.32E+6	**2.76E+6**	34.87E+0	-0.41 E+6
7		3.78E+6	**3.13E+6**	46.05E+0	-0.36 E+6
8		4.48E+6	**3.49E+6**	51.45E+0	-0.37 E+6
9		3.36E+6	**3.61E+6**	53.12E+0	-0.30 E+6
10	1	3.52E+6	**3.41E+6**	50.21E+0	-0.12 E+6
11	2	2.89E+6	**3.05E+6**	44.99E+0	0.13 E+6
12	3	2.79E+6	**2.88E+6**	42.40E+0	0.43 E+6
13	4	2.71E+6	**2.63E+6**	38.75E+0	0.72 E+6
14	5	2.48E+6	**2.47E+6**	36.45E+0	0.97 E+6
15	6	2.28E+6	**2.30E+6**	33.91E+0	1.15 E+6
16	7	2.11E+6	**2.16E+6**	31.87E+0	1.22 E+6
17	8	1.93E+6	**2.05E+6**	30.23E+0	1.19 E+6
18	9	2.02E+6	**1.94E+6**	28.52E+0	1.08 E+6
19	10	1.92E+6	**1.81E+6**	26.69E+0	0.88 E+6
20	11	1.70E+6	**1.68E+6**	24.76E+0	0.60 E+6
21	12	1.49E+6	**1.52E+6**	22.34E+0	0.27 E+6
22	13	1.27E+6	**1.33E+6**	19.61E+0	-0.09 E+6
23	14	1.20E+6	**1.43E+6**	21.11E+0	-0.45 E+6

Stresses in all stay vanes are below the allowable stress of 138.6 MPa.

[14] The averaged stay vane load is the value used for the FEA analysis averaged with the SNC concrete analysis results to obtain the final values of anchor load.
[15] SNC concrete analysis for stay vanes load values (Input value).

Table 14 - Force and stresses in stay vanes at dewatered condition (with concrete load from 3D model)

Stay vane number	Casing section	Dewatered condition (Buckling verification)						
		$F_{n,81,ad}$	$F_{n,81,ad,mean}$	S_{ratio}	Cc	$\sigma_{critical}$	$\sigma_{n,81,ad}$	$\sigma_{n,81,ad,all}$
		N	N	(L/r)		Mpa	Mpa	Mpa
1		-2.82E+6	-2.12E+6	62.26	126.27	88.88	39.24	46.29
2		-3.19E+6	-2.45E+6	76.26	126.27	123.37	42.71	64.26
3		-2.64E+6	-2.76E+6	96.00	126.27	123.37	42.71	64.26
4		-2.53E+6	-2.79E+6	128.02	126.27	126.46	39.61	65.86
5		-2.61E+6	-2.90E+6	129.61	126.27	123.37	42.71	64.26
6		-2.99E+6	-3.10E+6	152.70	126.27	88.88	39.24	46.29
7		-3.73E+6	-3.25E+6	129.61	126.27	123.37	47.86	64.26
8		-3.66E+6	-3.40E+6	129.61	126.27	123.37	50.11	64.26
9		-3.25E+6	-3.40E+6	129.61	126.27	123.37	50.04	64.26
10	1	-3.37E+6	-3.22E+6	129.61	126.27	123.37	47.37	64.26
11	2	-2.96E+6	-3.02E+6	129.61	126.27	123.37	44.42	64.26
12	3	-2.82E+6	-2.90E+6	129.61	126.27	123.37	42.68	64.26
13	4	-2.66E+6	-2.74E+6	129.61	126.27	123.37	40.43	64.26
14	5	-2.66E+6	-2.65E+6	129.61	126.27	123.37	39.05	64.26
15	6	-2.61E+6	-2.56E+6	129.61	126.27	123.37	37.70	64.26
16	7	-2.49E+6	-2.46E+6	129.61	126.27	123.37	36.28	64.26
17	8	-2.37E+6	-2.32E+6	129.61	126.27	123.37	34.18	64.26
18	9	-2.18E+6	-2.16E+6	129.61	126.27	123.37	31.84	64.26
19	10	-1.95E+6	-1.98E+6	129.61	126.27	123.37	29.12	64.26
20	11	-1.81E+6	-1.75E+6	129.61	126.27	123.37	25.76	64.26
21	12	-1.57E+6	-1.48E+6	129.61	126.27	123.37	21.84	64.26
22	13	-1.23E+6	-1.31E+6	129.61	126.27	123.37	19.34	64.26
23	14	-849.4E+3	-1.51E+6	129.61	126.27	123.37	22.31	64.26

Compression stresses in all stay vanes are below the allowable stress values as shown on last column of table 14.

6.2 BEARING PRESSURE ON CONCRETE UNDER ANCHORS RETAINING PLATES

Table 15 - Anchors calculation data

variable name	value	units	variable name in section 4.3	Input data, for reference
N_v	24			Number of vanes
t_{11}	82.55	mm		Stay ring plate thickness
E	3590	mm		Distributor height[16]
d_{11}	11 960	mm		Headcover to stay ring bolt circle diameter
d_{21}	11 650	mm		Bottom ring to stay ring bolt circle diameter
Ws	23 570	N/m^3		Concrete density
fc	30	MPa		Concrete resistance
g	9.81	m/s^2		gravity
				Input data, required for calculation of anchor loads
pd	504	kPa	Q2	Load rejection pressure (design pressure) at centerline distributor
p_{up}	504/ 487	kPa		Pressure on upper stay ring shroud [17]
p_{down}	504/ 522	kPa		Pressure on lower stay ring shroud[18]
d_{wgc}	10 682	mm		Diameter of wicket gate circle
d_{12}	12 376	mm		Outer diameter of pit liner
d_{22}	12 139	mm		Outer diameter of passage liner
d_{HC}	12 121	mm		Seal diameter of head cover with stay ring.
d_{br}	11 726	mm		Seal diameter of bottom ring with stay ring.
W_{SR}	276 960	kg	Q1	Weight of stay ring, wicket gates, levers and half of the links
W_{TS}	254 210	kg		Weight of stationary turbine components resting on the stay ring (head covers, mechanism, servomotors, thrust bearing support.)
W_{TR}	327 500	kg		Weight of rotating parts of turbine (Runner, shaft, rotating oil sump)
W_{GR}	782 500	kg		Weight of rotating parts of generator (rotor, poles)
W_{HC}	1 364 210	kg	Q3	$W_{TS}+W_{TR}+W_{GR}$

[16] 3581mm is the height at the distributor (guide vane); at the stay vanes, the height is 3590mm.
[17] The difference due to the elevation was neglected in FEA analysis the difference is not significative. However, to calculate as it was done by SNC, this difference is considered and the pressure is 487 kPa for the upper shroud.
[18] The difference due to the elevation was neglected in FEA analysis the difference is not significative. However, to calculate as it was done by SNC, this difference is considered and the pressure is 522 kPa for the lower shroud.

W_{GS}	407 180	kg	Q4 -Wc	Weight of stationary parts of generator, load through concrete (stator, soleplates, core, windings, pit liner)
Vc,tot	See table 8			Weight of concrete resting on the vane
$F_{n,81,s}$	See table 13			Water load at load rejection pressure
$P_{p12,wgc}$	644.2/ 666.7	kN		Pressure load per vane from area between d_{12} & d_{wgc} = $p_{up}.(\pi/4).(d_{12}^2 - d_{wgc}^2)/N_V$ (upper flange)
$P_{p22,wgc}$	394.1	kN		Pressure load per vane from area between d_{22} & d_{wgc} = $p_{down}.(\pi/4).((d_{22}^2 - d_{br}^2)+0.6*(d_{br}^2 - d_{wgc}^2))/N_V$ (lower flange)[19]

$F_{n,81,s,moy}$	Load on stay vane = water load - concrete - machinery weights except stay ring and wicket gates (See table 8) (= $F_{n,81,s}$ - Vc,tot $-(W_{GS} + W_{TS} + W_{GR} + W_{TR})*g/N_v$)
P_{AU}	Load on upper anchor, (with thrust bearing support on headcover) = water load - concrete - machinery weights transmitted through concrete - pressure load from pit liner to d_{WGC} = $F_{n,81,s,moy}$ + P_{HC}- $P_{p12,dwgc}$ (with P_{HC}= $(W_{TS} + W_{GR} + W_{TR})*g/N_v$) = $F_{n,81,s,moy}$ + $(W_{TS} + W_{GR} + W_{TR})*g/N_v$ - $P_{p12,dwgc}$
$P_{AU,SNC}$	Load on upper anchors, considering the load case used by SNC (with pressure difference on top and bottom) = $F_{n,FEA,SNC}$ - $P_{HC,SNC}$- $P_{p,up,SNC}$ (with $P_{HC,SNC}$= -6164kN/N_v= -257kN & $P_{p,up,SNC}$ =3692kN/Nv= 154kN) = $F_{n,FEA,SNC}$ +103kN
$P_{AU,AVE}$	Load on upper anchors is then the average of both values. That value is used for the anchors capacity. = $(P_{AU} + P_{AU,SNC})/2$
$F_{n,81,s,AVE}$	Load on stay vane derived form the averaged value considered = $P_{AU,AVE}$- P_{HC}+ $P_{p12,dwgc}$
P_{AL}	Load on lower anchor (with circular passage) = $F_{n,81,s,AVE}$ - $P_{p22,dwgc}$ -$W_{SR}*g/N_v$ = $F_{n,81,s,AVE}$ – 394.1 kN – 113.2 kN

[19] Note that load on the bottom ring is partially taken by the stay ring and the other part is taken by the discharge ring. 60% is used as ratio of load sharing on stay ring from bottom ring.

Anchors dimensions are listed in the following tables:

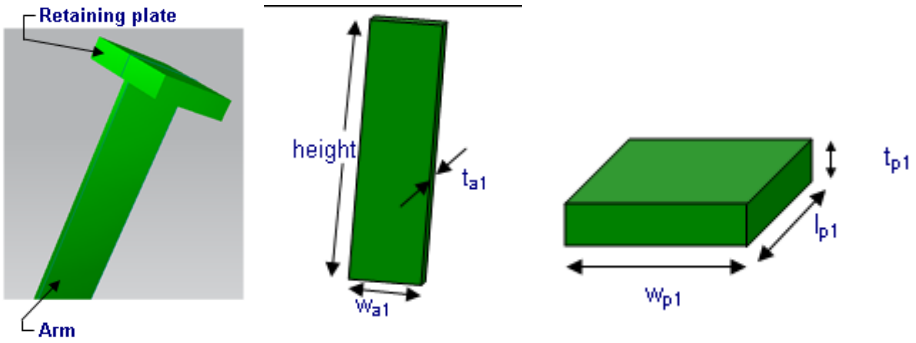

Figure 10 – Upper anchors variables

Table 16 - Upper anchors dimensions

Anchor arm				Upper anchor retaining plate			
capacity	thickness	width	arm cross section area (t_{a1}* w_{a1})	width	length	Area in contact with concrete (w_{p1}* l_{p1})- (t_{a1}* w_{a1})	thickness
kN	(t_{a1})mm	(w_{a1})mm	(a_{a1}) mm^2	(w_{p1}) mm	(l_{p1})mm	(a_{p1}) mm^2	(t_{p1}) mm
1734	60	300	18000	640	540	327600	100
1160	60	200	12000	340	490	154600	100

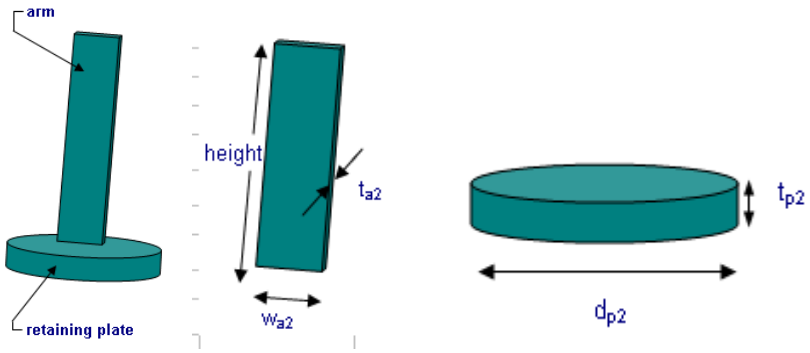

Figure 11 – Lower anchors variables

Table 17 - Lower anchors dimensions

Anchor arm				Lower anchor retaining plate		
capacity	thickness	width	arm cross section area (t_{a2}* w_{a2})	diameter	Area in contact with concrete (π*d_{p2}^2)/4- (t_{a2}* w_{a2})	thickness
kN	(t_{a2})mm	(w_{a2})mm	(a_{a2}) mm^2	(d_{p2})mm	(a_{p2}) mm^2	(t_p2) mm
1314	60	225	13500	490	175 074	100

Stress in the anchor arm is the average load on anchor divided by the area of the anchor arm.

The mean bearing pressure under the anchor retaining plate is the load on the anchor divided by the area in contact with the concrete. The concrete resistance is 30 MPa on the Muskrat Falls foundations. Therefore, the average concrete bearing pressure allowed is 7.5MPa, based on the CSA A23.3-70 standard[20]. As indicated below, all anchors have a bearing pressure below the allowable values given by the CSA standard.

[20] CSA A23.3-70 standard allows to use 0.25 times the concrete resistance for average bearing pressure and 0.375 for local bearing pressure.

Table 18 - Mean forces on anchors

Anchor #	Upper anchors				lower anchors			
	Mean force P_{AU}	Anchor capacity	Stress in anchor	Pressure under the plate (concrete bearing pressure)	Mean force P_{AL}	Anchor capacity	Stress in anchor	Pressure under the plate (concrete bearing pressure)
	kN	kN	MPa	MPa	kN	kN	MPa	MPa
1	412	1160	21.9	2.79	-9	1314	-1.0	-0.05
2	524	1160	27.8	3.55	104	1314	12.3	0.59
3	709	1160	37.6	4.80	288	1314	34.3	1.64
4	827	1160	43.9	5.60	406	1314	48.4	2.32
5	975	1160	51.8	3.07	554	1314	66.0	3.17
6	1182	1734	42.9	3.72	762	1314	56.4	4.35
7	1391	1734	50.4	4.37	971	1314	71.9	5.54
8	1569	1734	56.9	4.94	1149	1314	85.1	6.56
9	1661	1734	60.2	5.22	1241	1314	91.9	7.09
10	1652	1734	59.9	5.20	1232	1314	91.2	7.04
11	1601	1734	58.1	5.03	1181	1314	87.4	6.74
12	1662	1734	60.3	5.23	1242	1314	92.0	7.09
13	1683	1734	61.0	5.29	1263	1314	93.5	7.21
14	1730	1734	62.7	5.44	1310	1314	97.0	7.48
15	**1733**	1734	62.9	5.45	**1314**	1314	97.3	7.50
16	1700	1734	61.6	5.35	1279	1314	94.8	7.31
17	1629	1734	59.1	5.12	1208	1314	89.5	6.90
18	1516	1734	55.0	4.77	1095	1314	81.1	6.26
19	1354	1734	49.1	4.26	933	1314	69.1	5.33
20	1148	1734	41.6	3.61	728	1314	53.9	4.16
21	901	1160	47.8	6.10	481	1314	57.2	2.75
22	629	1160	33.4	4.25	208	1314	24.8	1.19
23	500	1160	26.5	3.38	79	1314	9.4	0.45

7. STAY RING SHROUDS BEARING PRESSURE

The allowable average bearing pressure under the upper and lower shrouds of the stay ring is, as per the specification of section 1.2.6.1.1 , 4 MPa.

In the calculation of the stay ring area, the anchors and ribs will be removed. The values are taken from the 3D model, as shown below in figures 12 and 13.

- Upper shroud area: 28 510 769mm^2
- Lower shroud area : 35 008 057mm^2

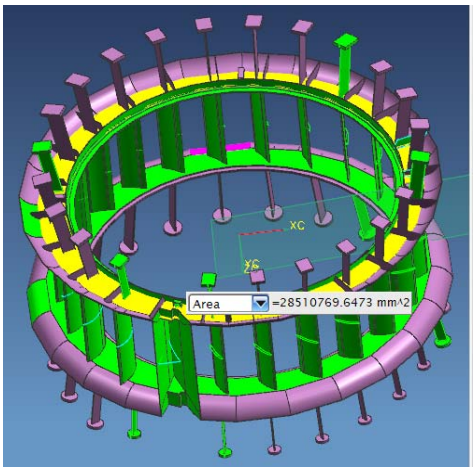

Figure 12 – Upper shroud area

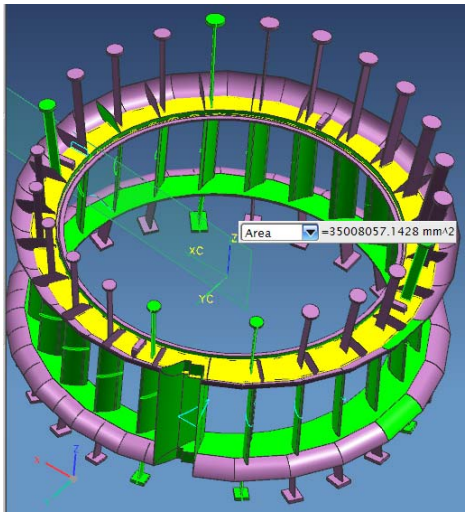

Figure 13 – Lower shroud area (upside down view)

For simplification, the total force will be distributed over these areas and average pressure is calculated as follow:

The upper shroud force: Σ Fn,81,ad,moy = -60 066 673N (compression)
The average bearing pressure: Σ Fn,81,ad,moy/Area= -60 066 673/28 510 769= -2.11MPa

The lower shroud force: Σ Fn,81,ad,moy – WSR = -60 066 673 - 2716977.6= -62 783 651N (compression)
The average bearing pressure: Σ Fn,81,ad,moy/Area= -62 783 651/35 008 057= -1.79MPa

The average bearing pressure is therefore well below the allowable 4MPa.

8. CONCLUSION

The allowable tension and buckling stresses are met on all stay vanes.

The upper anchors will be of 2 different sizes and only one size for all lower anchors. The upper anchors will have capacities of 1734 kN for vanes numbers 6 to 20 and 1160kN for the remaining. The lower anchors will have all the same capacity of 1314kN. Introduction of civil analysis, for concrete behaviour influence on the anchors loads, show the possibility of reducing the anchor size. To remain conservative, the value used for the final anchor load is the mean value between the two methodologies.

Average bearing pressure under the anchors plate is below the allowable 7.5MPa (0.25*30MPa) as per CSA A23.3-70.

Stay ring average bearing pressure is lower than the allowable 4 MPa as per specification section 1.2.6.1.1.

APPENDIX A Semi-spiral casing concrete load

Table 19 - Muskrat falls concrete blocks over casing

Section	Mass [kg] wide casing	Bloc #4 (top bloc) of wide casing
1	584 939	159 107
2	614 802	280 663
3	460 712	224 586
4	429 424	209 281
5	459 506	224 586
6	576 347	280 663
7	855 656	398 507
8	689 999	145 567
9	547 616	69 035
10	569 438	70 905
11	490 570	61 280
12	470 651	60 519
13	459 098	66 533
14	437 018	60 053
15	412 886	54 784
16	385 889	52 286
17	362 174	51 095
18	342 858	53 702
19	274 351	7 885
20	265 739	38 505
21	267 106	39 872
22	196 331	14 468
23	56 884	0
24	76 022	19 991
Total	**9 701 077**	**2 484 765**

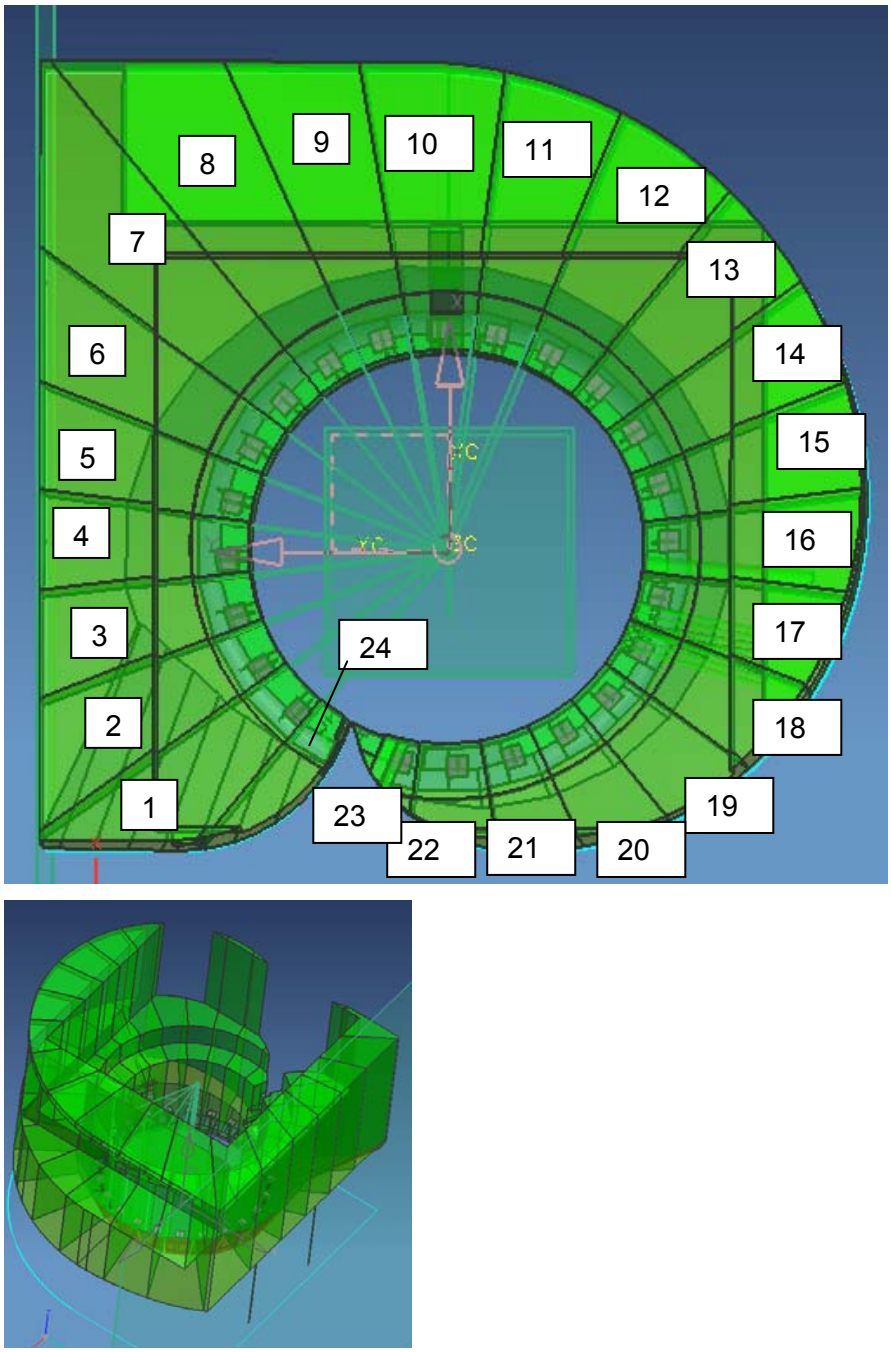

Figure 14 – Concrete blocks on 3D model

PROVINCE OF NEWFOUNDLAND AND LABRADOR
PEGNL Newfoundland and Labrador PROFESSIONAL ENGINEERS AND GEOSCIENTISTS
PERMIT HOLDER
This Permit Allows
ANDRITZ HYDRO LTD
To practice Professional Engineering in Newfoundland and Labrador.
Permit No. as issued by PEGNL N0602
which is valid for the year 2013

Nalcor Doc. Rev.	Andritz Doc. Rev.	Modification	Date	Prepared / Préparé	Appr.
C1	01	Updated according to client comments and AH replies	13-Sept-2013	RQ	AH/14
A1	00	Initial release	26-Oct-2012	RQ	AH/14

Title / Titre

STAY VANE VON KARMAN VORTEX ANALYSIS REPORT

HCM	Date	Name / Nom
Prepared by:	26-Oct-2012	Ruixia Qian, Eng. jr.
Approved by:	26-Oct-2012	Caroline Marchand, Eng.

Contract / Contrat No.: 0200-183001 to 0200-183004

Part Bill / Nomenclature No.: 060

Andritz Doc. No.	Rev.	Sheet / Feuille	1
AHCM-2012-0026	00	of / de	16

ANDRITZ Hydro

Professional Engineer's Stamp

REGISTERED PROFESSIONAL ENGINEER
PEGNL Newfoundland and Labrador PROFESSIONAL ENGINEERS AND GEOSCIENTISTS
CAROLINE MARCHAND
SIGNATURE
2013-08-19
DATE
NEWFOUNDLAND & LABRADOR

Client

nalcor energy
LOWER CHURCHILL PROJECT

Project

LOWER CHURCHILL PROJECT

MUSKRAT FALLS HYDROELECTRIC DEVELOPMENT

SNC·LAVALIN

NE Doc. No.	Rev.
MFA-AH-SD-3410-ME-H27-0001-01	C1

TABLE OF CONTENTS

TABLE OF APPENDICES

TABLES LIST

FIGURES LIST

1. INTRODUCTION

Von Karman vortices can excite vibrations on hydraulic profiles in hydraulic turbines such as stay vanes, guide vanes and runner blades. Significant vibration amplitudes can occur if von Karman frequencies come within a lock-in range of some natural frequencies of the components. In the past this has happened to stay vanes [1, 2]. In order to ensure that such vibrations are not going to occur on the Muskrat Falls stay vanes, a von Karman analysis has been performed with modern in-house calculation methods.

At Andritz Hydro, well established computational approaches exist to predict von Karman vortex frequencies [1] and amplitudes by means of unsteady 2D CFD. Using eigen-mode shapes in water and their modal parameters [2] (natural frequency, modal mass, modal stiffness) the CFD results can be used to compute vibration amplitudes. These values are compared with allowable vibration amplitudes that are calculated with FEA and fatigue analysis in order to accept the designs. A flow chart of von Karman calculation procedure is shown in Appendix A.

2. BASIC DATA

2.1 STAY VANE PROFILES

The stay vane profiles of Muskrat Falls are shown in Appendix B. There are a total of 24 sets of stay vanes and guide vanes. Seven (7) different stay vane profiles are analyzed: Stay vane No.1, No.2, No.3, No.4, No.5, No.6 and No.7 to No. 23. Please note that stay vane No. 7 to stay vane No. 23 have an identical hydraulic profile.

2.2 OPERATING POINTS

The operating points are chosen based on Model Test results to cover the complete operating range. Two operating points are analyzed: full load and low load. The prototype discharges and the corresponding guide vane openings are shown in Table 2-1.

Table 2-1 Operating points used for Muskrat Falls von Karman vortex analysis

OP	Q [m^3/s]	GV [°]
Full Load	674	39
Low Load	340	23

2.3 INFLOW ANGLES AT STAY VANE INLET

The inflow angles at the stay vane inlets are important inputs for von Karman analysis and defined as α=atan(Vr/Vt), as shown in Figure 2-1. They are obtained from 3D steady CFD casing calculation results: circumferentially averaged angles of a mid-span section with the stay vane centered. The inflow angles at the stay vane inlets used in our von Karman analysis are shown in Table 2-2. For stay vane No. 7 to No. 23, the angle varies in the range of 33° to 44°. Here we only do von Karman analysis for the two extreme inlet angles: inflow angle of 44° for stay vane No.7 and inflow angle of 33° for stay vane No.11.

Table 2-2 Inflow angles at stay vane inlets used for Muskrat Falls von Karman vortex analysis

STV #	Inflow angle [°]
1	98
2	91
3	79
4	67
5	59
6	51
7	44
11	33

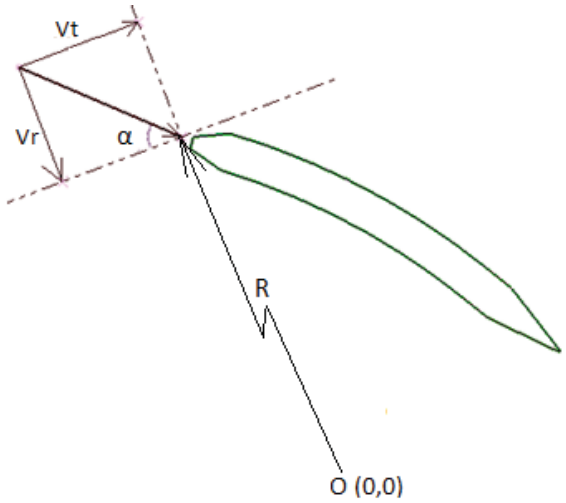

Figure 2-1 Inflow angle at the stay vane inlet

3. VIBRATION MODE SHAPES

Generally first order modes such as the first bending and the first torsion modes can be excited more easily than higher order modes. This is due to the higher stiffness of higher order modes and the fact that they have more nodes where excitation forces have no effect. Furthermore, at the nodes the shed vortices have to change phase by 180° resulting in less coherence along the height of the vane. Also higher load operating points are more typically critical because of the higher amount of energy available from the flow for excitation. According to previous investigations, torsion modes have lower hydrodynamic damping than corresponding order bending modes.

In this analysis, 1st bending, 1st torsion and 2nd bending mode shapes have been checked for the above reasons. Figure 3-1 shows the three mode shapes of the Muskrat Falls stay vanes. The natural frequencies in water and the allowable vibration amplitudes in water of the modes have been calculated with 3D FEA method and fatigue analysis and are given in Table 4-1 and Table 4-2 for comparison purpose. The allowable vibration amplitudes are calculated considering that each stay vane is continuously vibrating at its natural frequency for 75 years and considering that the material is unprotected carbon steel.

1st Bending Mode shape 1st torsion Mode shape 2nd Bending Mode shape

Figure 3-1 Different mode shapes of the Muskrat Falls stay vanes

4. VON KARMAN ANALYSIS RESULTS

In Table 4-1, the unsteady von Karman analysis results are given in terms of frequencies and deviations of von Karman shedding frequencies from natural frequencies. For some stay vanes, two excitation frequencies are present (No.1, No. 2 and No.11); in these cases, two lines are given. After validation with existing projects, the accuracy of the von Karman shedding frequency prediction is believed to be in the range of ±15% including lock-in effect, and therefore the risk of resonance exists for all von Karman vortex shedding frequencies that come within this range of the natural frequency. Based on this, we consider that the separation of the frequencies by 15 % or more is sufficient to avoid the frequency lock-in, resonance and any significant amplification. As the contract requires a 20% margin between natural and von Karman frequencies, maximum vibration amplitudes, assuming lock-in and resonance, are calculated for all stay vanes which are within this range. The cases where the von Karman frequency is within 20% of the natural frequency are highlighted in Table 4-1 and the corresponding vibration amplitudes at resonance are given in Table 4-2. It is shown that for all those cases, von Karman vibration amplitudes at resonance are lower than mechanical allowable vibration amplitudes.

Figures in Appendix C show the charts with the results from our standard 2D unsteady von Karman predictions as well as the relevant natural frequencies and vorticity contours around the stay vanes.

Table 4-1 Muskrat Falls von Karman analysis results - Frequencies

ST V No.	Low load at GV 23°				Full load at GV 39°				Natural frequencies in water [Hz]		
	vK freq [Hz]	vK freq. deviation from natural freq. $(f_n-f_{vK})/f_n$ [%]			vK freq [Hz]	vK freq. deviation from natural freq. $(f_n-f_{vK})/f_n$ [%]					
		1st Bending	1st Torsion	2nd Bending		1st Bending	1st Torsion	2nd Bending	1st Bending	1st Torsion	2nd Bending
1	6.8	84	NA[1]	93	14.6	65	87	86	41.5	NA[1]	103.9
1	65.8	-59	NA[1]	37	69.2	-67	37	33	41.5	NA[1]	103.9
2	10.6	68	81	88					32.9	54.5	90.9
2	62.1	-89	-14 [2]	32	70.2	-113	-29	23	32.9	54.5	90.9
3	62.3	-110	1 [2]	25	70.7	-138	-13 [2]	15 [2]	29.7	62.8	83.3
4	63.0	-137	18 [2]	16 [2]	71.0	-167	8 [2]	5 [2]	26.6	77.1	75.1
5	63.9	-148	15 [2]	12 [2]	71.1	-175	5 [2]	2 [2]	25.8	75.0	72.8
6	63.2	-192	3 [2]	-1 [2]	70.7	-227	-9 [2]	-13 [2]	21.6	64.9	62.6
7	62.9	-143	16 [2]	14 [2]	70.3	-171	6 [2]	4 [2]	25.9	75.1	73.1
11	15.5	40	79	79					25.9	75.1	73.1
11	61.8	-139	18 [2]	15 [2]	69.0	-166	8 [2]	6 [2]	25.9	75.1	73.1

[1] No obvious 1st torsion mode is observed on stay vane No.1 by FEA

[2] ▭ von Karman frequency is within ±20% of the natural frequency and resonance may occur; however the amplitudes are lower than allowable values

Table 4-2 Muskrat Falls von Karman analysis results overview – Vibration amplitudes at resonance where the von Karman frequency is within 20% of the natural frequency

STV No.	Low load at GV 23°				Full load at GV 39°				Allowable amplitudes in water [mm]		
	vK freq [Hz]	vK amplitudes u [mm]			vK freq [Hz]	vK amplitudes u [mm]					
		1st Bending	1st Torsion	2nd Bending		1st Bending	1st Torsion	2nd Bending	1st Bending	1st Torsion	2nd Bending
2	62.1		0.019		70.2				0.093	0.111	0.041
3	62.3		0.017		70.7		0.057	0.021	0.119	0.113	0.046
4	63.0		0.014	0.009	71.0		0.055	0.036	0.182	0.118	0.063
5	63.9		0.013	0.009	71.1		0.051	0.036	0.169	0.118	0.056
6	63.2		0.013	0.009	70.7		0.057	0.039	0.224	0.119	0.067
7	62.9		0.009	0.006	70.3		0.029	0.020	0.142	0.103	0.047
11	61.8		0.009	0.006	69.0		0.030	0.021	0.142	0.103	0.047

5. CONCLUSION

Experience shows that von Karman vortices can excite stay vanes in hydraulic turbines with high distributor heights if excitation frequencies are near natural frequencies. The vibration amplitude depends on mechanical (structural) and hydraulic elements. With an unsteady CFD method, von Karman vortex analysis has been performed for the Muskrat Falls project. With this method, von Karman shedding frequency and resonant amplitudes at different modes are predicted with good accuracy. The von Karman analysis presented in this report shows that no risk of detrimental vibration exists with the Muskrat Falls stay vanes.

6. REFERENCES

[1] Vu,T.C., Nennemann, B., Ausoni, P., Farhat, M., and Avellan, F., “Unsteady CFD prediction of von Karman vortex shedding in hydraulic turbine stay vanes”, Proceedings Hydro 2007, Granada, Spain, October 2007

[2] Coutu A., Proulx, D., Coulson S., “Dynamic Assessment of Hydraulic Turbines”, Waterpower XIII, Buffalo, NY, July 28-31, 2003.

Appendix A: Flow chart of von Karman calculation procedure

ANDRITZ Hydro

STAY VANE VON KARMAN VORTEX ANALYSIS REPORT

Client: Nalcor Energy	Project: Muskrat Falls	Contract: 0200-183001 to 04

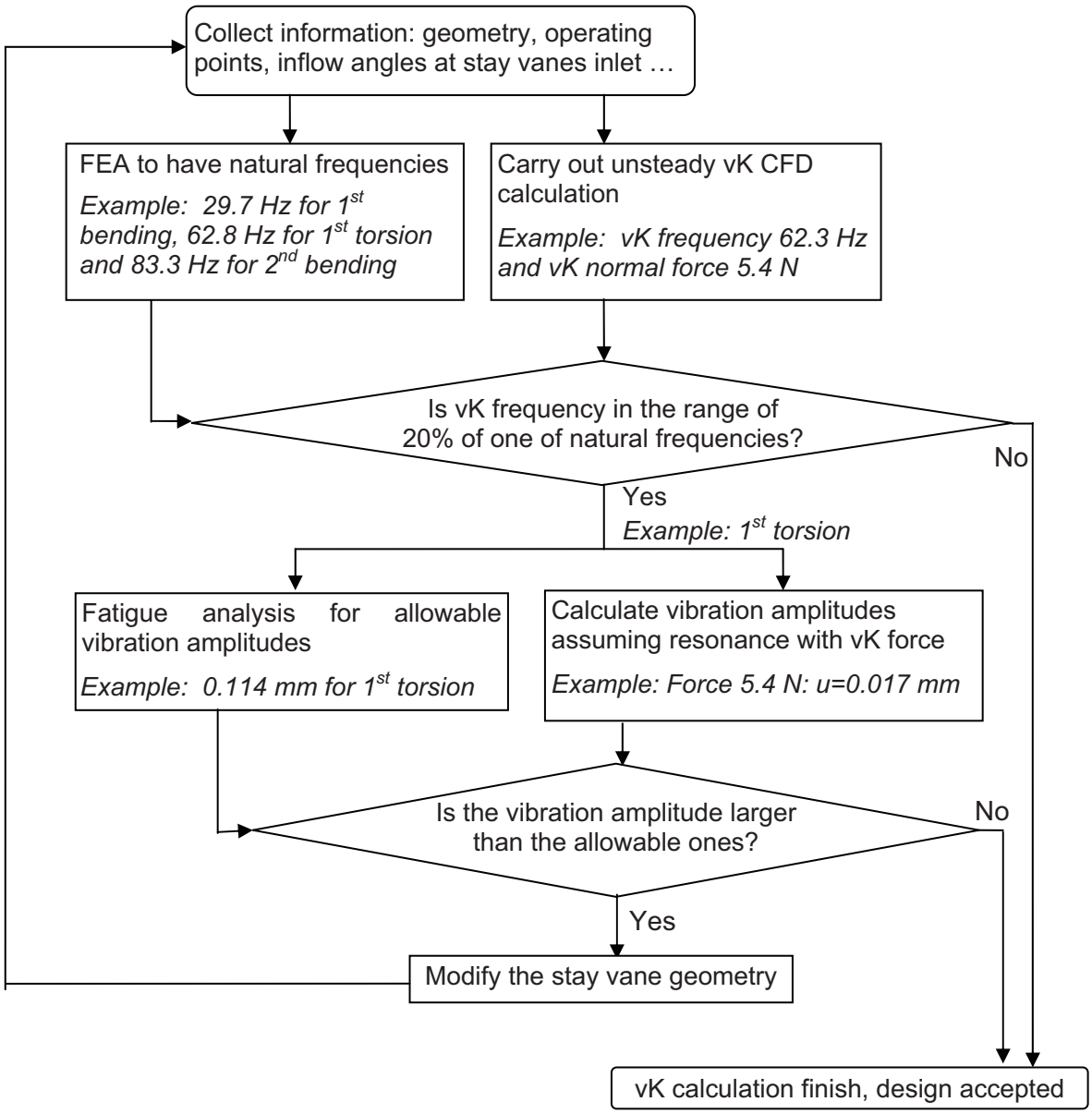

Appendix B: Drawing of Stay Vanes and Guide Vanes HDSO-4303

CALCULATION REPORT

ANDRITZ Hydro

STAY VANE VON KARMAN VORTEX ANALYSIS REPORT

Client: Nalcor Energy	Project: Muskrat Falls	Contract: 0200-183001 to 04

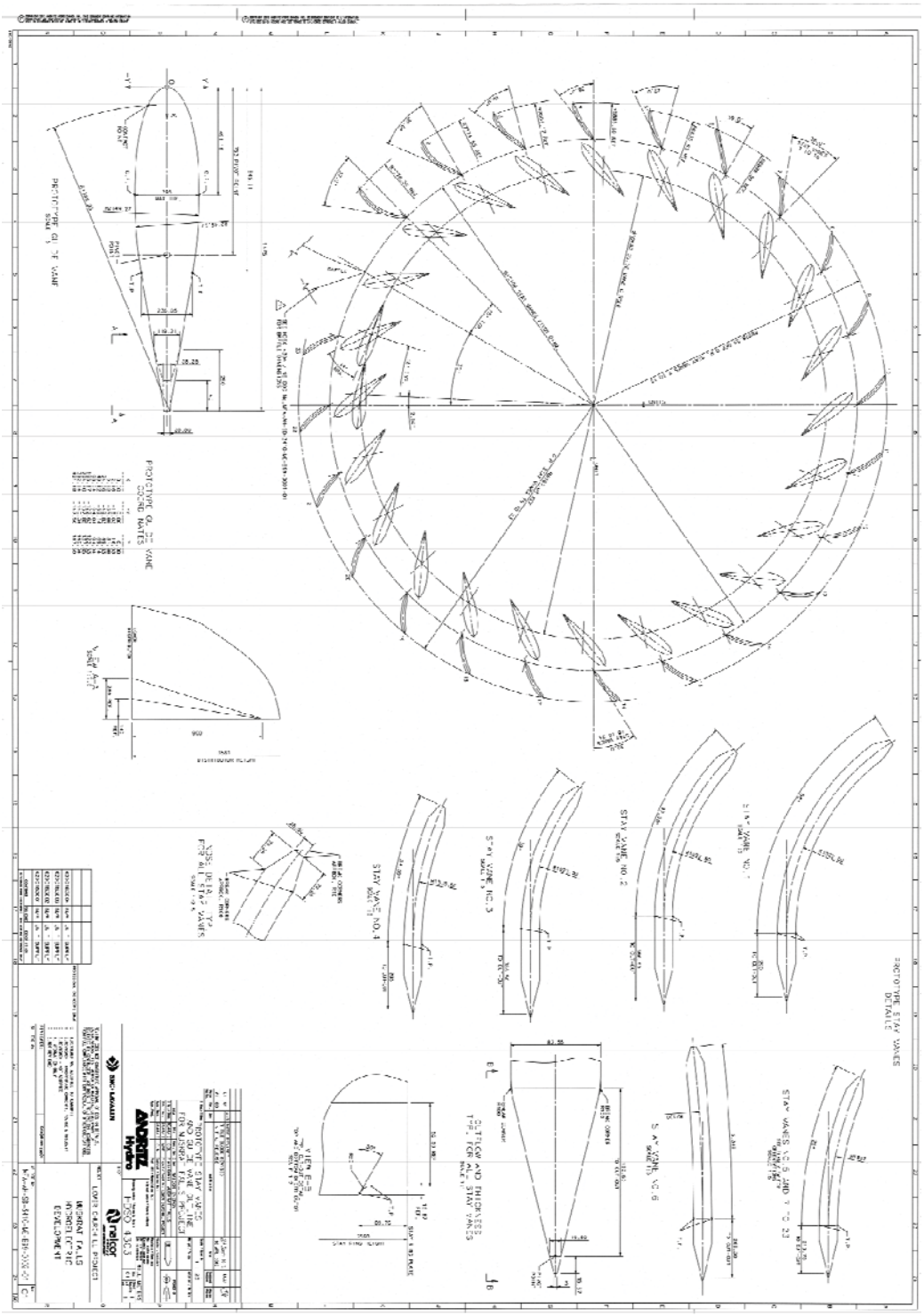

Prepared by: Ruxia Qian, Eng. jr,	Date: 26-oct-2012	Page 11 of 16
Approved by: Caroline Marchand, Eng.	Date: 26-oct-2012	Report No. AHCM-2012-0026

NALCOR ENERGY DOC. NO.:	Rev
MFA-AH-SD-3410-ME-H27-0001-01	C1

Appendix C: Von Karman Analysis Figures

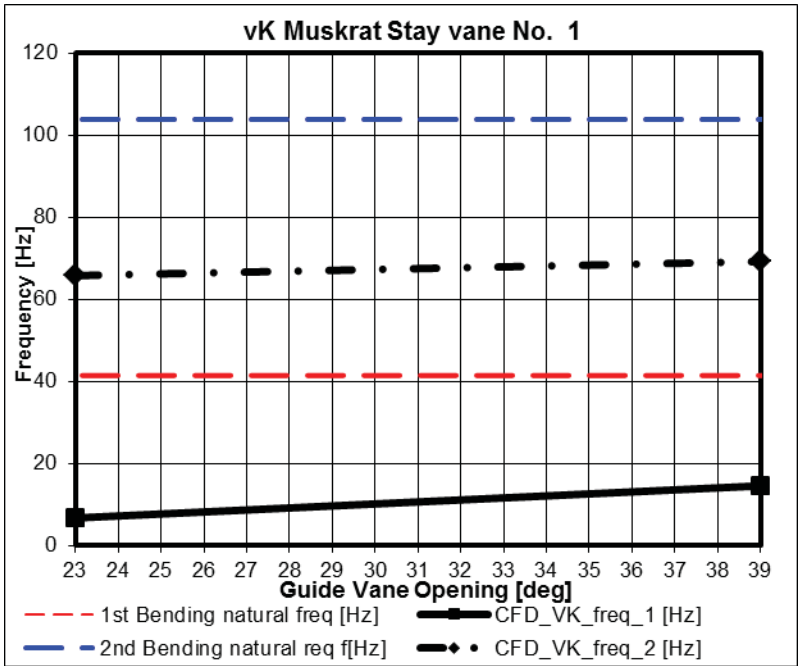

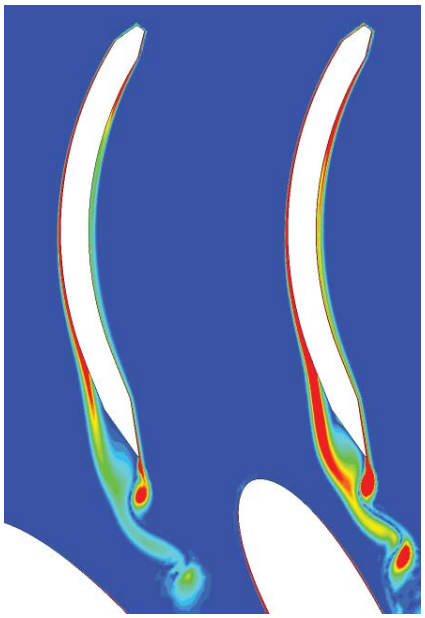

Vorticity at gv23 Vorticity at gv39

Figure C 1 Unsteady von Karman analysis results on stay vane No.1

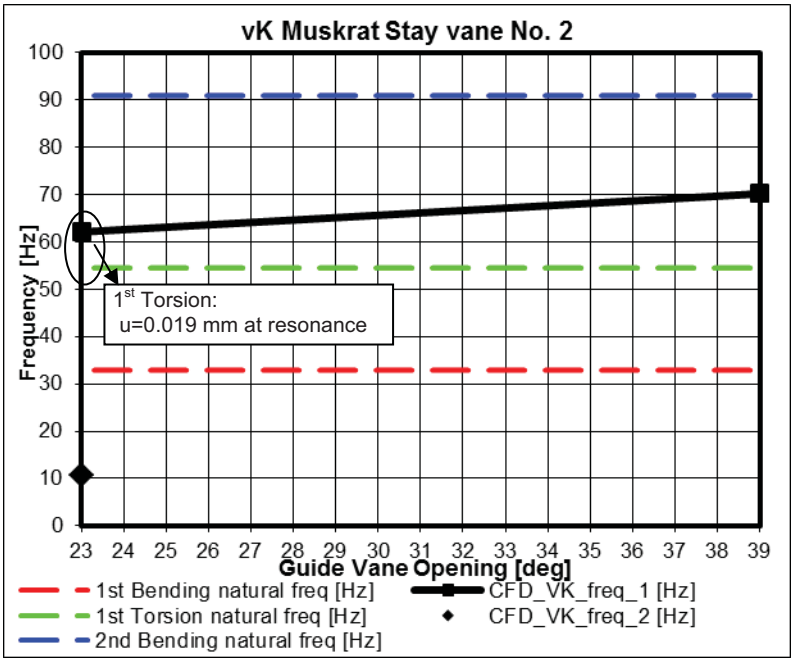

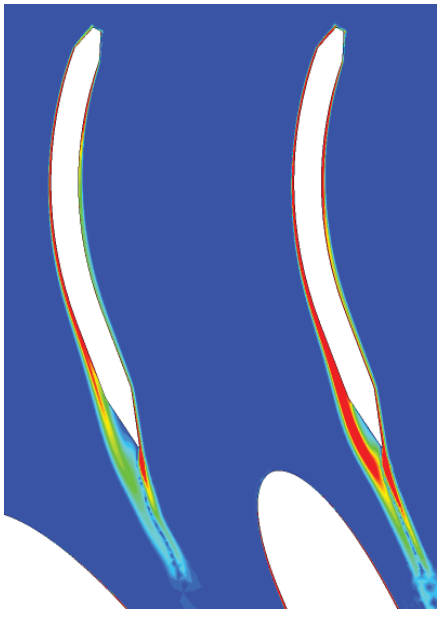

Vorticity at gv23 Vorticity at gv39

Figure C 2 Unsteady von Karman analysis results on stay vane No.2

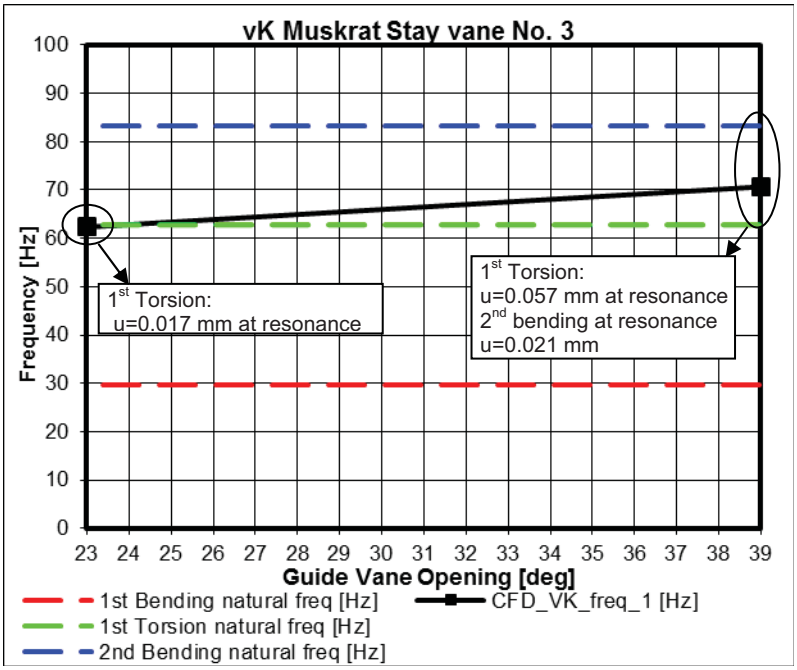

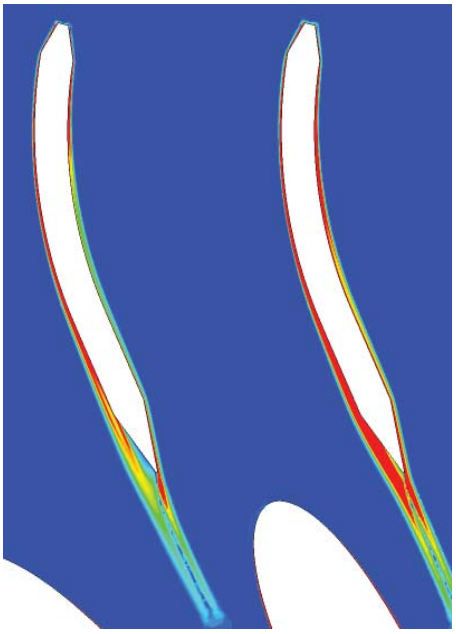

Vorticity at gv23 Vorticity at gv39

Figure C 3 Unsteady von Karman analysis results on stay vane No.3

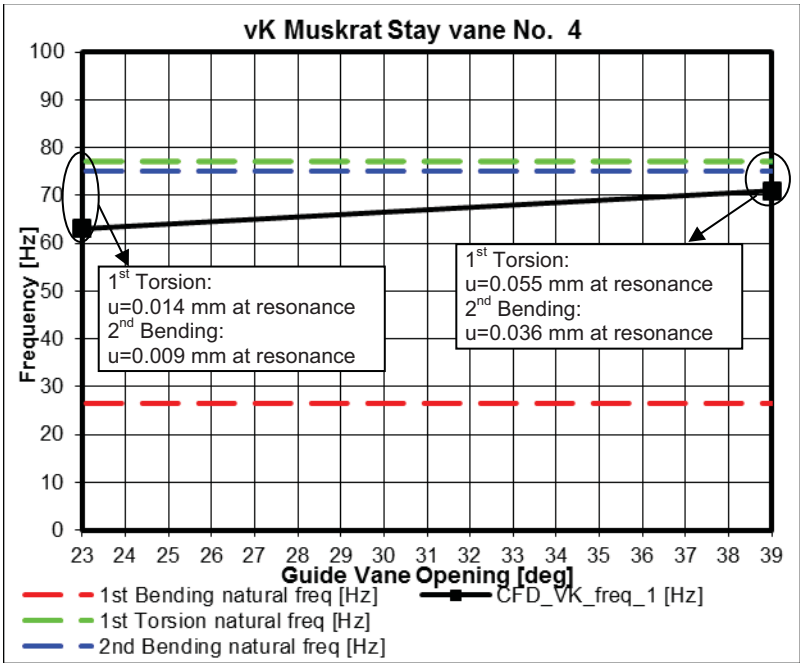

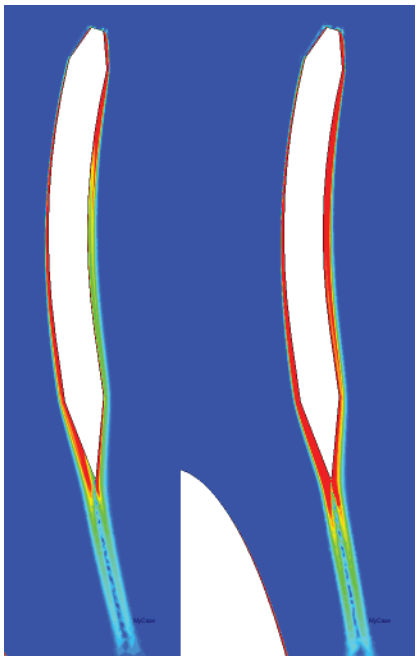

Vorticity at gv23 Vorticity at gv39

Figure C 4 Unsteady von Karman analysis results on stay vane No.4

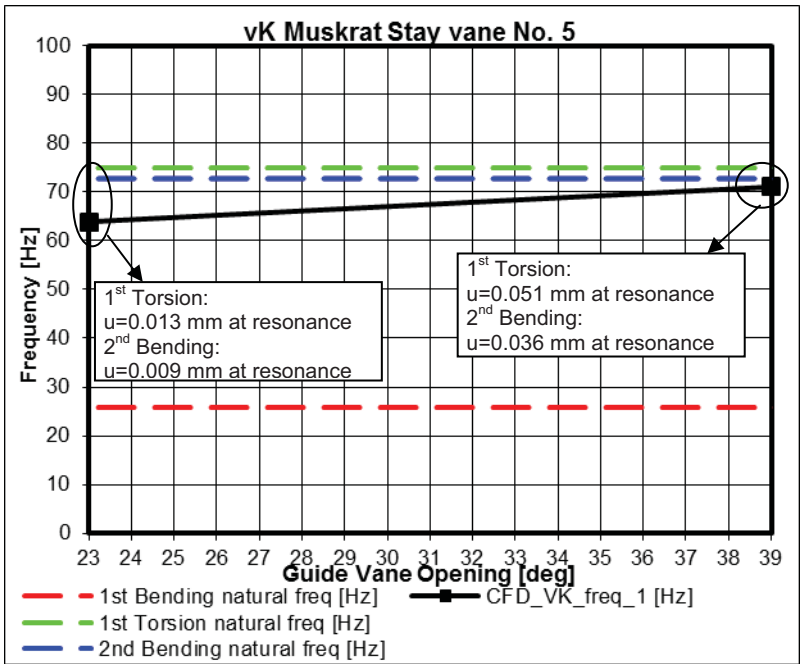

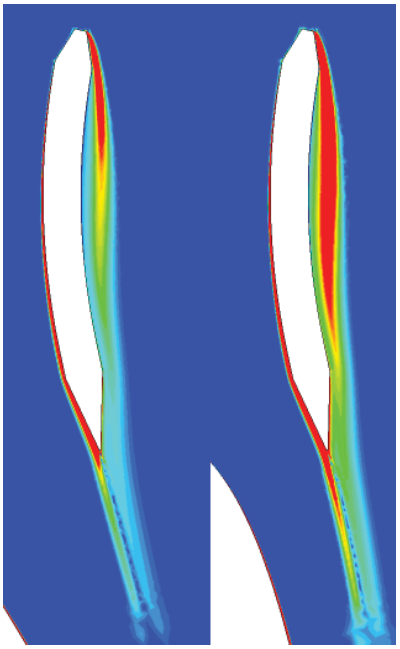

Vorticity at gv23 Vorticity at gv39

Figure C 5 Unsteady von Karman analysis results on stay vane No.5

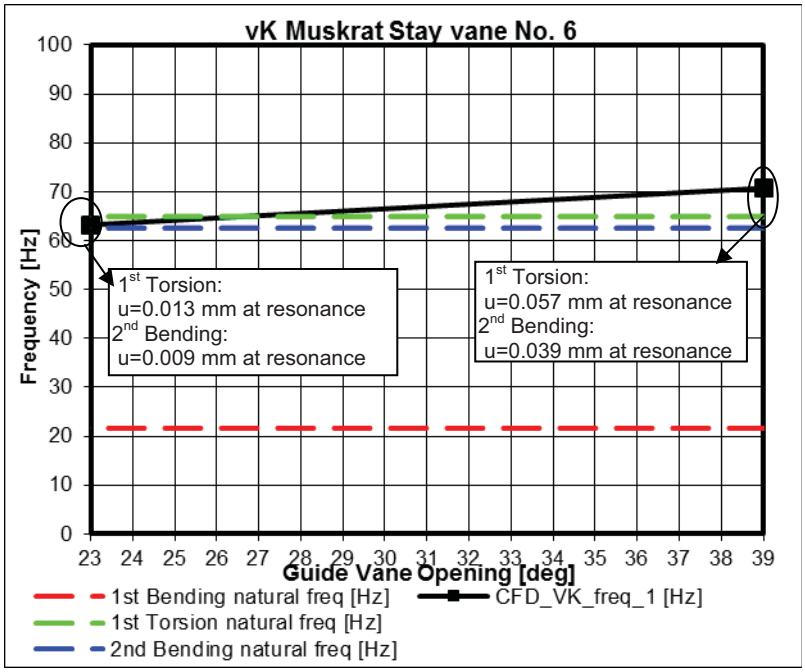

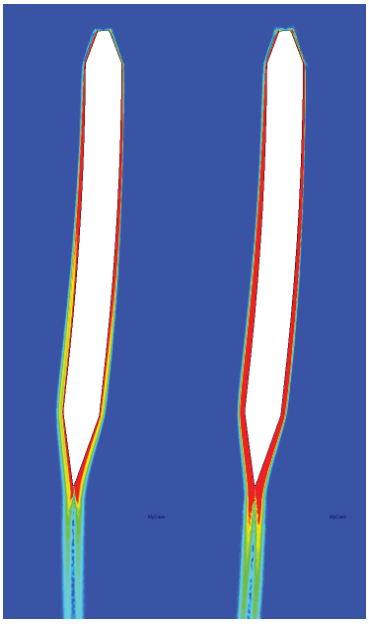

Vorticity at gv23 Vorticity at gv39

Figure C 6 Unsteady von Karman analysis results on stay vane No.6

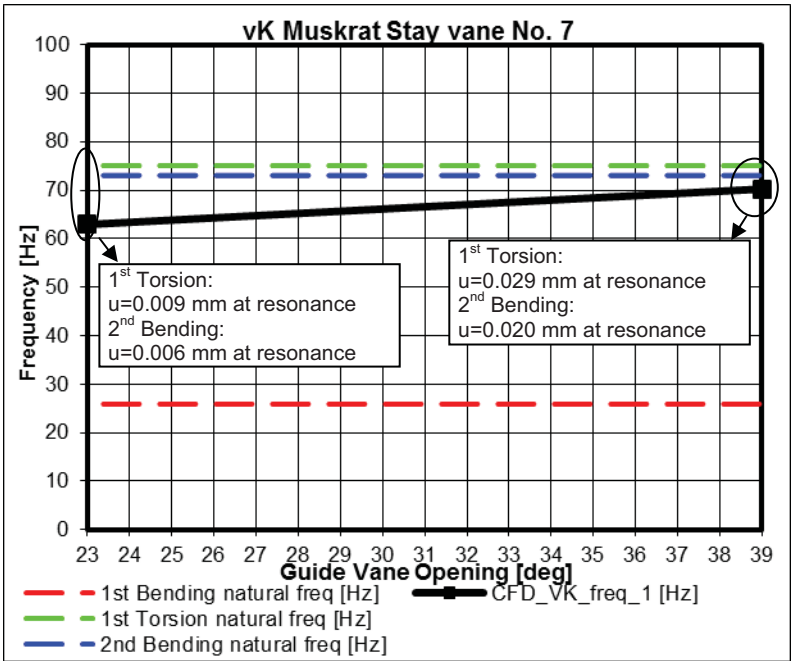

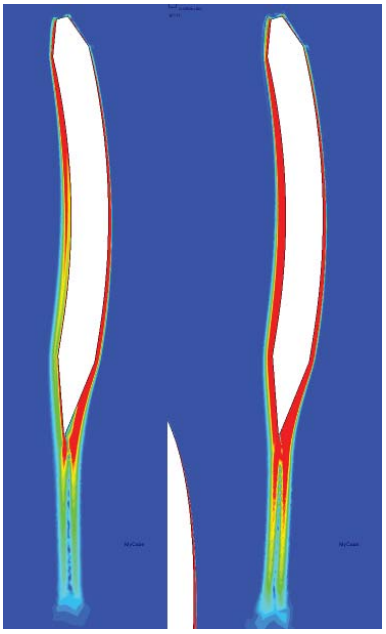

Vorticity at gv23 Vorticity at gv39

Figure C 7 Unsteady von Karman analysis results on stay vane No.7

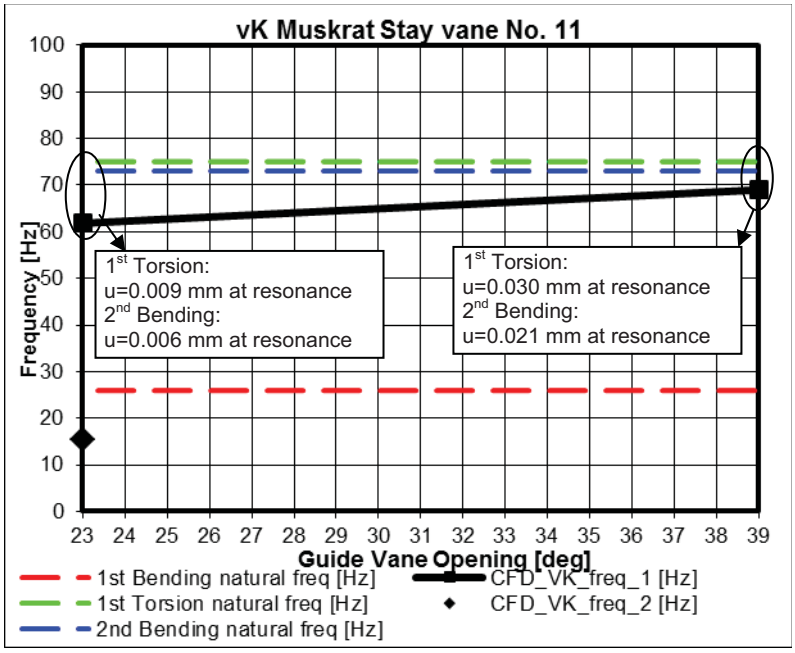

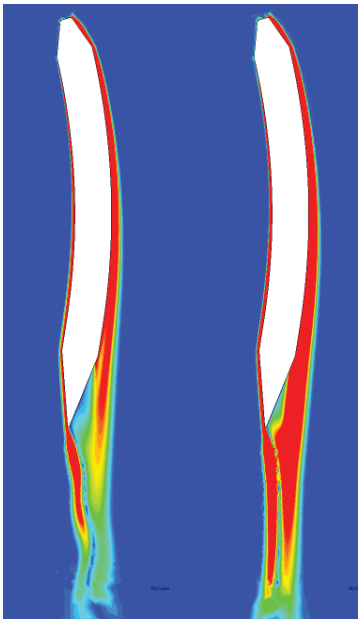

Vorticity at gv23 Vorticity at gv39

Figure C 8 Unsteady von Karman analysis results on stay vane No.11

CH0030 Turbines and Generators

Response to Independent Engineer's Questions

Question 1:

Cleaning of ferritic contamination of stainless steel surfaces: It is normal practice when using or working with stainless steel/ martensitic components care should be taken to avoid contamination with ferritic materials as this can cause corrosion pitting later on during operation. A water test (using copper sulfate solution) is normally recommended to establish any possibility of contamination. Any such contamination should be removed either by grinding/polishing with uncontaminated stone or sand belts. Ideally if there is severe contamination, stainless steel should be cleaned by passivating gels. These gels should not be used on the martensitic 410 Grades. It is recommended these to be cleaned with citric acid fluids.

Answer:

The Muskrat Falls specification does not require passivation of the stainless components. This was discussed at the start of manufacturing and Andritz advised that they do not normally acid wash the stainless parts. The guide vanes and blades are machined after they leave the foundry or fabrication hall so the risk of contamination is low.

During the recent visit to Tianbao it was noted that grinding of the runner levers was occurring due to a clearance problem. The levers, which are carbon steel, and stainless steel blades were installed in the runner at the time and grinding particles were collecting on some of the blade. Andritz will be asked to check the parts for contamination prior to packaging and the clean them if necessary.

Question 2:

Runner blades to hub gaps: It was observed that some of the runner blades are rubbing tight against the hub surface (scratched marks on the paint). The IE recognizes that this is not the final assembly however it is important to point out that the proper gap dimensions should be achieved and gaps should measure within the allowable design tolerances. Those should be verified at FAT.

Answer:

The design gap is between 2 and 3 mm as shown on the clip from the runner assembly drawing below. The gaps will be checked and recorded during the final stages of the FAT. We will advise the results when they are available.

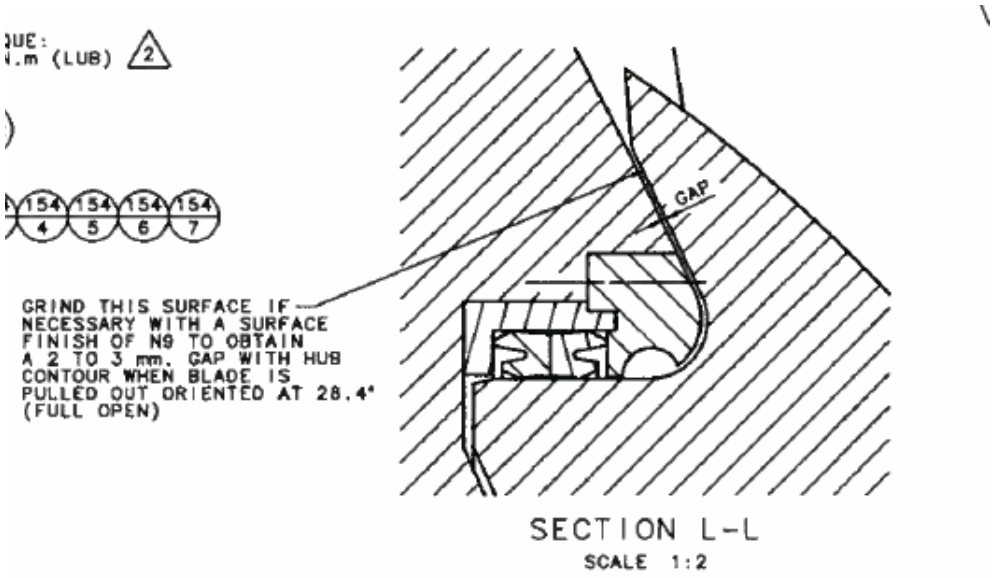

Question 3:

Runner blades to discharge ring gaps. Verification of the gap between the runner blades and the discharge ring surface should be considered in light of blades deflection due to operating pressures on the blades and the resulting potential bridging of the gap in closed or open position of the blades.

Answer:

The design clearance between the runner and discharge ring is 6 mm.

In 2013 Andritz had a problem during commissioning of a project where the runner rubbed the discharge ring during over speed testing. LCP was given a presentation on the issue and Andritz rechecked their calculations for defection during operation for Muskrat Falls and confirmed the clearances are sufficient.

Question 4:

IE requested a design report on Von Karman vortices at stave vane locations, indicating the natural frequencies of the vane and the effect of these vortices on the vanes. The concern is related to possible resonance oscillation of the vanes induced by vortex frequencies closed to the natural frequencies of the stay vanes. Apparently such a report exist and Andritz is to make it (if not already) available to NALCOR.

Answer:

The stay vane calculation report numbered MFA-AH-SD-3410-ME-H27-0001-01 is attached. The Von Karman results are in the last section of the report.

Question 5:

IE requested also a verification of the discharge ring operational fatigue stresses and potential fracture issues particularly at the junction of the vertical ribs at top and bottom flanges of the ring.

Answer:

The discharge ring calculation report numbered MFA-AH-SD-3410-ME-H12-0001-01 is attached.

Question 6:

IE inquired if the unit will be able to start in case there is no oil film between the trust bearing contact surface, e.g. high pressure oil pumps malfunctioning concurrently with no compressed air availability for activation of generator brakes.

Answer:

The thrust bearing is a babbitt bearing and is provided with a high pressure oil injection system consisting of a pump to inject oil into the thrust pads providing an oil film prior to starting the unit. The pump is powered from the unit control board which is connected to the essential board when black starting. The specification requires the bearings to be able to withstand a restart within 24 hours of shutdown without the high pressure oil injection system. If the unit has been shut down for an extended period the high pressure oil system is required to prevent bearing damage during restart.

RS
7-April-2015